Technische Universität München
TUM School of Natural Sciences

Reduced Molecular Flavins as Single Electron Transfer Catalysts: Cyclization of Barbituric Acid Derivatives

Richard Foja

Vollständiger Abdruck der von der TUM School of Natural Sciences der Technischen Universität München zur Erlangung eines

Doktors der Naturwissenschaften (Dr. rer. nat.)

genehmigten Dissertation.

Vorsitz: Priv.-Doz. Dr. Alexander Pöthig

Prüfende der Dissertation:

1. TUM Junior Fellow Dr. Golo T. B. Storch
2. Prof. Dr. Cathleen Zeymer

Die Dissertation wurde am 26.06.2024 bei der Technischen Universität München eingereicht und durch die TUM School of Natural Sciences am 16.07.2024 angenommen.

Das Leben kann sehr kurz sein,

wenn man sich auf zu wenige Dinge konzentriert.

F.L.

This thesis was conducted under the direction of Dr. Golo Storch at the Technical University of Munich from February 2021 until July 2024.

Parts of this thesis have been published:

Foja, R.; Walter, A.; Jandl, C.; Thyrhaug, E.; Hauer, J.; Storch, G., Reduced Molecular Flavins as Single-Electron Reductants after Photoexcitation, *J. Am. Chem. Soc.* **2022**, *144*, 11, 4721 – 4726.

Foja, R.; Walter, A.; Storch, G., Chemoselective Reduction of Barbiturates by Photochemically Excited Flavin Catalysts, *Synlett* **2023**, *35,* 09, 952 – 956.

Acknowledgments

Für die Aufnahme in seinen Arbeitskreis und dafür, mich dem Thema der zuvor nicht erkundeten, reduzierten Flavine anvertraut zu haben, danke ich **Dr. Golo Storch** vielmals. Meine Entscheidung, mich in der organischen Synthesechemie zu betätigen und diese als meinen langfristigen Weg während meiner akademischen Laufbahn zu wählen, wurde durch seine herausragende und persönliche Betreuung manifestiert. Die Forschung auf dem Gebiet reduzierter Flavine war durch die Neuheit des Themas eine Herausforderung, aber bot gleichzeitig die Möglichkeit, meine Kreativität in einem freien Umfeld nutzen zu können. Im gleichen Zuge möchte ich auch Prof. Dr. Thorsten Bach danken, der den Lehrstuhl Organische Chemie I betreut, zu welchem unser Arbeitskreis gehört. Auch **Dr. Alexandra Walter**, **Dr. Andreas Rehpenn** und **Tim Langschwager** als meinen direkten Labornachbarn und allen Mitgliedern des AK Storch, insb. der Sauna-Subgroup, möchte ich danken. Die persönliche Atmosphäre, die ihr erschaffen habt, hat die schlechten Tage abgefedert und die guten Tage unvergesslich gemacht. Wegen wissenschaftlicher Beteiligung herauszustellen sind **Dr. Alexandra Walter** für viele CV-Messungen, **Miriam Jänchen** und **Yi Xu** für (transiente) Spektroskopie und **Olaf Ackermann** für HPLC-Analytik. Außerdem danke ich **Kerstin Voigt** für ihre organisatorische Unterstützung, sowie **Prof. Dr. Zeymer** und **Dr. Pöthig** für die Prüfung und natürlich meinen Praktikanten. **Tim Langschwager** und **Maxi** Schuibuam **Iglhaut** danke ich fürs Korrekturlesen und für unnormal rare und intellektuelle Diskussionen.

Als nächstes möchte ich **meiner Familie** danken. Ohne die fortlaufende Unterstützung vor und während des Studiums, wäre ich heute nicht dort, wo ich bin. Die Motivation und den Rückhalt, welche ich durch euch erfahren habe, lassen sich mit Worten nur bedingt würdigen. Без вашей поддержки я бы не смог стать тем, кем сегодня стал. Знаю, что вы мной гордитесь, и я рад, что вы дали мне такую возможность. Gleichzeitig möchte ich auch meiner Freundin **Daniela Brandt** danken. Du trägst durch deine Unterstützung mehr Anteil an diesem Titel, als ich es in Worten ausdrücken kann. Ohne deine geduldige und liebevolle Art, hätte ich es nicht geschafft.

Meinen Uni-Freunden **Anton**, **Michaela**, **Patrick, Raphi**, **Sarah** und **Zausi** danke ich für die Hilfe im Studium. Einige Prüfungen konnte ich nur durch euch wahrnehmen und ich erteile euch allen Inselverbot. Gleichzeitig danke ich auch allen Freunden in der **Königinstraße**, die einen wesentlichen Anteil zu meiner Entwicklung erbracht haben und für mich wie eine zweite Familie sind. **Philipp Steudle**, für seine Weisheiten und **Valentin Langer**, **Matthias Manthey** und **Fabrizzio Manthey** für ihre maßgeblichen Einflüsse auf meine Person, danke ich für dieses Band, das uns verbindet. Den Freunden, die mich schon am längsten begleiten **Dennis Rudenko** und **Julien Gossen**, danke ich für ihre Kontinuität. Bleibt, wie ihr seid, denn durch euch werde ich nie vergessen, wer ich bin. Zahlreichen Freunden aus beiderlei Heimat, die mich auf diesem Weg unterstützt haben, werde ich immer dankbar sein.

Zuletzt danke ich der Studienstiftung des deutschen Volkes für die Förderung im Studium und der Promotion, sowie dem CRC 325 für die Ermöglichung dieses Projekts. Die erbrachte Unterstützung ist einzigartig und ermöglichte mir die Durchführung dieses Vorhabens nach eigenen Wünschen.

Abstract

Flavins are a ubiquitous compound class found in a variety of enzymes with vastly different functions. While most flavoenzymes operate in ground-state oxidative reactions, the DNA photolyase uses reduced flavin in a photomediated process for the cleavage of thymine dimers to revert DNA damage. Additionally, it has been demonstrated that modified 'ene' reductases are capable of stereoselectively reducing substrates under photoirradiative conditions in synthetic transformations. Prior to this thesis, the use of reduced flavins outside of an enzymatic environment was scarce. Here, we report the application of reduced flavins in the photoreductive cyclization of barbituric acid derivatives using γ-terpinene as sacrificial reductant. Optimization of the reaction conditions was performed with a novel reduced flavin that evades oxidation under air through a conformational bias strategy. Oxidized flavins can be used as precatalysts and different electron acceptors (amides, haloalkanes, alkenes) were successfully employed. Furthermore, substrates with multiple possible sites of reduction were investigated to gain insight into reduced flavin reactivity in comparison to the rare-earth metal reductant samarium (II) iodide. Orthogonal conversion of barbituric acid derivatives and reduction of *O*-methyl oximes which were resistant to samarium (II) iodide reduction demonstrate the additional utility of the novel reduced flavin method.

Zusammenfassung

Flavine sind eine ubiquitäre Verbindungsklasse, die in verschiedenen Enzymen unterschiedlicher Reaktivität vorkommt. Während die meisten Flavoenzyme an Oxidationen im Grundzustand beteiligt sind, verwendet die DNA-Photolyase ein reduziertes Flavin in der photomediierten Spaltung von Thymin-Dimeren zur Reparatur von DNA-Schäden. Zusätzlich wurden modifizierte En-Reduktasen in der stereoselektiven Reduktion verschiedener Substrate unter Bestrahlung benutzt. Bis zu dieser Thesis mangelte es an einer Anwendung reduzierter Flavine außerhalb einer enzymatischen Umgebung. Wir berichten die Anwendung reduzierter Flavine in der photoreduktiven Cyclisierung von Barbitursäurederivaten mit γ-Terpinen als terminales Reduktionsmittel. Optimierung der Reaktionsbedingungen erfolgte anhand eines neuartigen reduzierten Flavins, welches aufgrund seiner Struktur durch eine sterisch bedingte Tendenz in der Konformation gegenüber Luft stabil ist. Oxidierte Flavine könne als Präkatalysatoren eingesetzt werden und verschiedene Elektronenakzeptoren

(Amide, Haloalkane, Alkene) wurden erfolgreich reduziert. Darüber hinaus wurden Substrate, die verschiedene reduzierbare Funktionalitäten beinhalten, untersucht, um Unterschiede zwischen reduzierten Flavinen und Samarium(II)iodid zu identifizieren. Orthogonale Reaktionen von Barbitursäurederivaten und Reduktion von *O*-Methyloximen, welche nicht mit Samarium(II)iodid reagieren, demonstrieren die Nützlichkeit der neuentwickelten Methode reduzierter Flavine.

Table of Contents

Abbreviations

FAD	Flavin adenine dinucleotide
FMN	Flavin mononucleotide
HAT	Hydrogen atom transfer
ISC	Intersystem Crossing
HOMO	Highest occupied molecular orbital
LUMO	Lowest unoccupied molecular orbital
MCAD	Medium-chain acyl-CoA dehydrogenase
NAD	Nicotinamide adenine dinucleotide
NMR	Nuclear magnetic resonance
OYE	Old yellow enzymes
PET	Photoinduced electron transfer
SCE	Saturated calomel electrode
SET	Single electron transfer
SOMO	Single occupied molecular orbital
TBADT	Tetrabutylammonium decatungstate
TDAE	Tetrakis(dimethylamino)ethylene
TICT	Twisted intramolecular charge-transfer

1. Introduction

The earliest definition of oxidation can be found in Lavoisiers *Traité Élémentaire de Chimie* in 1789, where the incorporation of oxygen into a substrate is defined as oxidation and the removal of oxygen from a substrate as reduction.[1] A more modern interpretation consists of the transfer of electrons or atoms from/to a substrate with an ultimate change of the oxidation state and does not necessarily rely on oxygen participating in the reaction. Formally, a redox reaction can be split into an oxidative and a reductive half-step.[2] The tendency of a substance to undergo oxidation/reduction can be quantified by measuring the redox potential against a known reference such as the standard hydrogen electrode. Reductants can be classified by their mechanism of action and while two-electron reductants such as sodium borohydride are crucial for selected reactions like the conversion of carbonyl compounds to alcohols, one-electron reduction gives rise to radical ion intermediates that substantially differ in reactivity and thus broaden the scope of reductive transformations. Redox reactions are vital to different enzyme reactivities and can be catalyzed by a multitude of cofactors.

Flavoenzymes constitute a class of non-metal enzymes that rely on the flavin cofactor and are involved in a plethora of secondary metabolite pathways.[3] Riboflavin (vitamin B_2) is essential for the biosynthesis of flavin adenine dinucleotide (FAD) and flavin mononucleotide (FMN) which are both derived from the heterocycle isoalloxazine (Scheme 1A).[4]

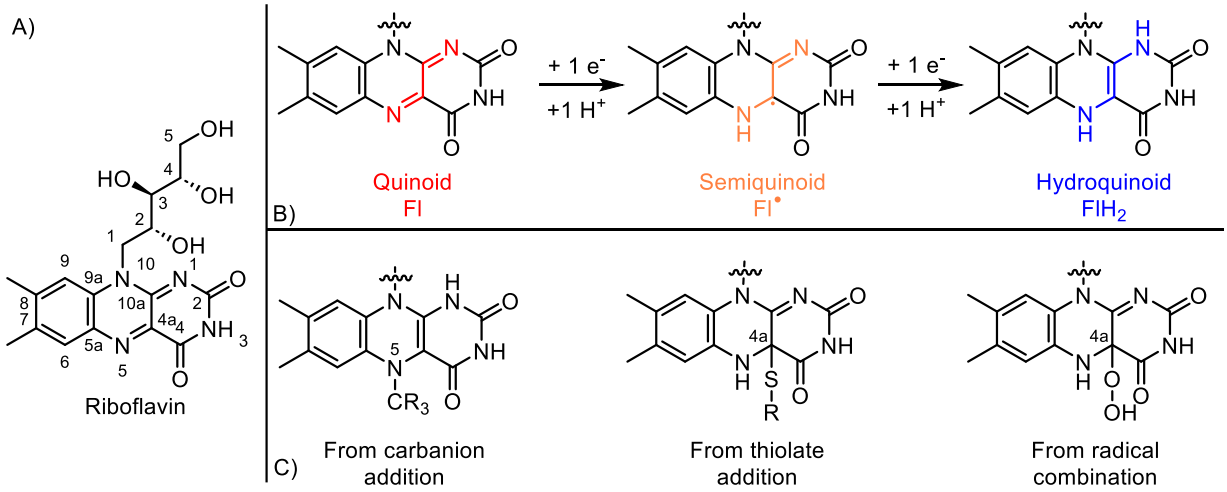

Scheme 1: A) The structure of flavin cofactors. B) The three redox states of flavins. C) Covalent flavin adducts involved in different enzymes.[3]

After the first observation of a fluorescent pigment in milk in 1872 by Alexander Blyth, growth enhancement in young rats that were given milk extracts eventually enabled isolation of old yellow enzyme (OYE).[5] Finally, independent characterization in 1939 by Paul Karrer and Richard Kuhn and recognition as an essential component for animal nutrition by Glatzle in 1968 established riboflavin as a subject of interest in the on-going research regarding metabolic pathways and the associated enzyme reactivities.[5]

In contrast to nicotinamide adenine dinucleotide (NAD), which is the most common cofactor involved in redox transformations in primary metabolic pathways (i.e. processes, that are essential for an organism's survival), flavin coenzymes are tightly, yet predominantly non-covalently, bound to their apoproteins.[3] Flavins adapt three redox states: the quinoid (fully oxidized) state, the semiquinoid (one electron reduced) state and the hydroquinoid (fully reduced) state (Scheme 1B), the latter of which is suspected to be the reason for the tight binding to the enzyme due to rapid oxidation outside the enzymatic scaffold. As a consequence of the redox versatility of the isoalloxazine core, flavins exhibit one-electron and two-electron reactivities (Scheme 1C) establishing them as the centerpiece in a multitude of biologically relevant processes.[6] This adaptability in regard to different mechanisms also enables flavins to function as linkers between reagents that necessitate a particular reactivity (e.g. the hydride donating nicotinamide adenine dinucleotide hydride (NADH) or one-electron transferring iron-sulfur clusters).[6]

2. Flavines in Enzymes

2.1. Flavoenzymes

At least 151 enzymes of the 3870 enzymes cataloged in the ENZYME database are known to use flavins as cofactors, making them one of the most common prosthetic groups.[7] Most flavin reactions in flavoenzymes can be divided into two half-reactions (Scheme 2A): a reductive half-step, where an oxidized flavin is converted to the hydroquinoid state by oxidation of a substrate (SH_2), and a reoxidation half-step leading to a quinoid flavin by reduction of an acceptor (S') either by hydride transfer (two-electrons at a time) or stepwise oxidation by molecular oxygen to a semiquinoid flavin.[3] The semiquinoid flavin combines with a superoxide radical anion to a flavin C_{4a}-hydroperoxide adduct from which hydroperoxide can be eliminated to liberate oxidized flavin. Many flavoenzymes operate by oxidizing a substrate with flavin as the electron acceptor, but some examples with hydroquinoid flavin as the catalytically active species such as 'ene' reductases[8] and DNA photolyases[9] are reported as well.

2.1.1. Acyl-CoA dehydrogenase

A prominent example of flavoenzymes that are essential to human metabolism is the family of acyl-CoA dehydrogenases.[10] Generally, they catalyze the α,β-oxidation of fatty acid thioesters **1** to the respective unsaturated compounds **2** (Scheme 2B).

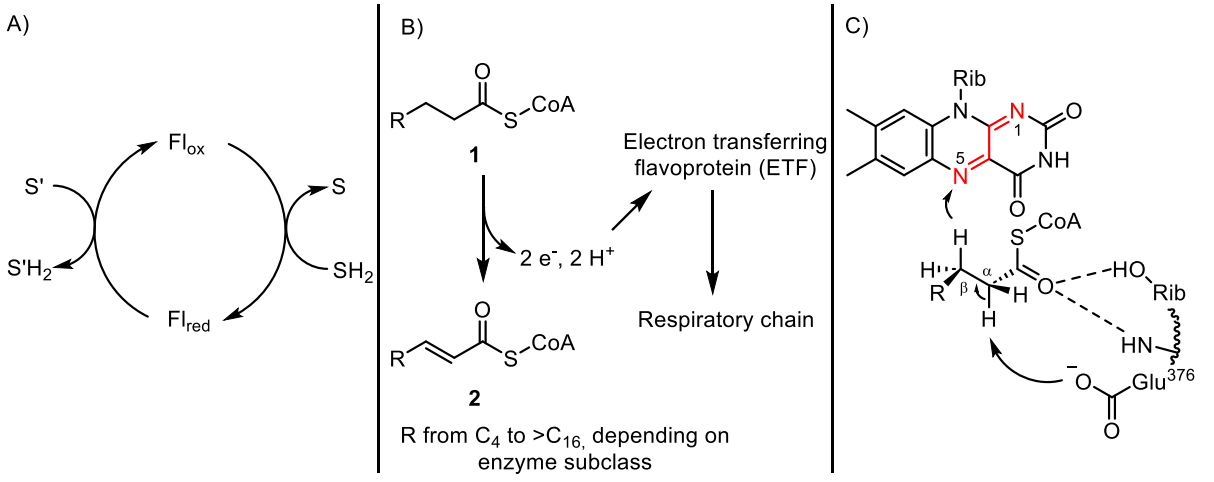

Scheme 2: A) General scheme of flavin mediated redox reactions. B) Simplified scheme of fatty acid oxidation. C) Key step of MCAD-catalyzed fatty acid oxidation and general scheme of flavin mediated redox reactions.[10]

Enzymes in this family are classified by the chain length of their substrates, however, they operate by similar mechanisms and the medium-chain acyl-CoA dehydrogenase (MCAD) which metabolizes fatty acid chains with 4 to 16 carbons is the best-studied member of this enzyme family.[10] A deficiency in MCAD is also a common genetic disorder with serious implications for patients, possibly resulting in coma or fatality if left untreated.[11]

In the first step, the enzyme and acyl-CoA substrate form a complex thus changing the protein conformation and the enzyme fluorescence.[12] Afterwards, α,β-dehydrogenation of the substrate yields reduced flavin and enzyme-bound enoyl-CoA.[10] The mechanism of this oxidation typically involves deprotonation by glutamic acid (Glu376) and concerted hydride transfer to oxidized flavin N^5 (Scheme 2C). An important mechanistic feature of this reaction is the pK_a decrease of the α-proton of the substrate from pK_a = 20 to pK_a = 8 by coordination of the carbonyl by secondary sites of the enzyme. After the reaction, another isomerization takes place before reduced flavin is reoxidized by electron-transferring flavoprotein which funnels the electrons into the respiratory chain. Interestingly, enoyl reductases performing the reverse reaction of fatty acid oxidation, mostly do not utilize reduced flavin in the reductive step except for FabK from *Streptococcus pneumoniae*, and instead, hydride transfer from NADH is the determining mode of action.[13]

2.1.2. Old yellow enzyme and reduced flavins in flavoenzymes

Old yellow enzymes constitute a family of flavoprotein oxidoreductases that rely on NADPH as a reductant and can catalyze the reduction of unsaturated substrates.[14] In their function as 'ene' reductases, OYEs are utilized in industry because of their broad substrate compatibility and good accessibility by conventional genetic methods. As the OYE family is rather diverse, no singular physiological role can be assigned to OYEs. Known functions range from detoxification of electrophilic compounds and a role in oxidative stress response to specific metabolic pathways. Across the OYE family, protein regions that are involved in catalysis and cofactor/substrate binding are very similar and flavin is noncovalently bound, as is the case for most flavoproteins. Another key feature in the active center is $tyrosin_{186}$, which acts as the proton donor during catalysis and is conserved throughout the OYE family. Interestingly, it was demonstrated that $tyrosin_{186}$ is not essential to catalysis by mutation of this residue.[15] The overall mechanism of OYEs as 'ene' reductases encompasses oxidation of NADPH by quinoid

flavin to form reduced flavin, which can transfer a hydride to activated alkenes, such as α,β-unsaturated ketones (Scheme 3).[14]

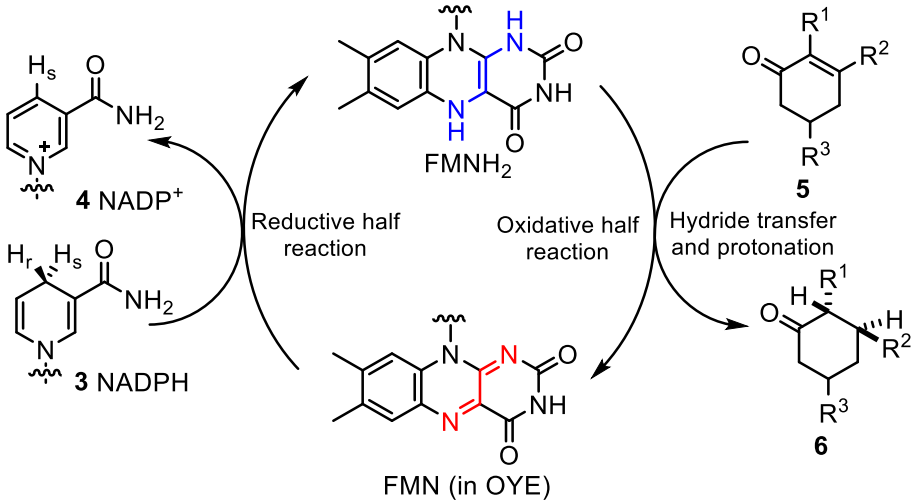

Scheme 3: Simplified mechanism of hydride transfer in OYE 'ene' reductases.[14]

The reductive half-reaction occurs by the formation of a Michaelis complex between enzyme-bound FMN and NADPH (**3**) as a cofactor before a charge transfer complex is formed, presumably due to π-π stacking between the pyridinium and isoalloxazine of the respective components.[14] From this complex, hydride transfer and subsequent $NADP^+$ (**4**) dissociation follow. The reoxidation half reaction proceeds by transfer of the flavin N^5 hydride to the β-carbon of the acceptor **5**, which is coordinated by histidine residues through the carbonyl oxygen to facilitate hydride acceptation. In a concerted manner, $tyrosine_{186}$ protonates the α-carbanion with absolute stereospecificity *trans* to the hydride from $FMNH_2$ to form the saturated product **6**. Regarding the application of OYEs on an industrial scale, using NADPH as a terminal reductant becomes a prohibiting factor due to instability and cost. Instead, several recycling systems to replenish NADPH by oxidation of glucose with a variety of glucose dehydrogenases are proposed.[14]

2.1.3. DNA Photolyase

Consisting of approximately 500 amino acids, photolyases are medium-sized monomeric proteins.[9] The task of enzymes in this class is the reversion of UV-induced damage to the DNA. This repair mechanism is mostly prevalent in simpler organisms like bacteria and archaea and was lost in higher organisms like placental mammals in the course of evolution which repair DNA by excision.[16] When *Escherichia coli* is exposed to far UV light, a large fraction of

the bacteria die due to DNA damage.[9] Subsequent subjection to blue light drastically increases the overall survival rate and marks the significance of DNA photolyases in these organisms.

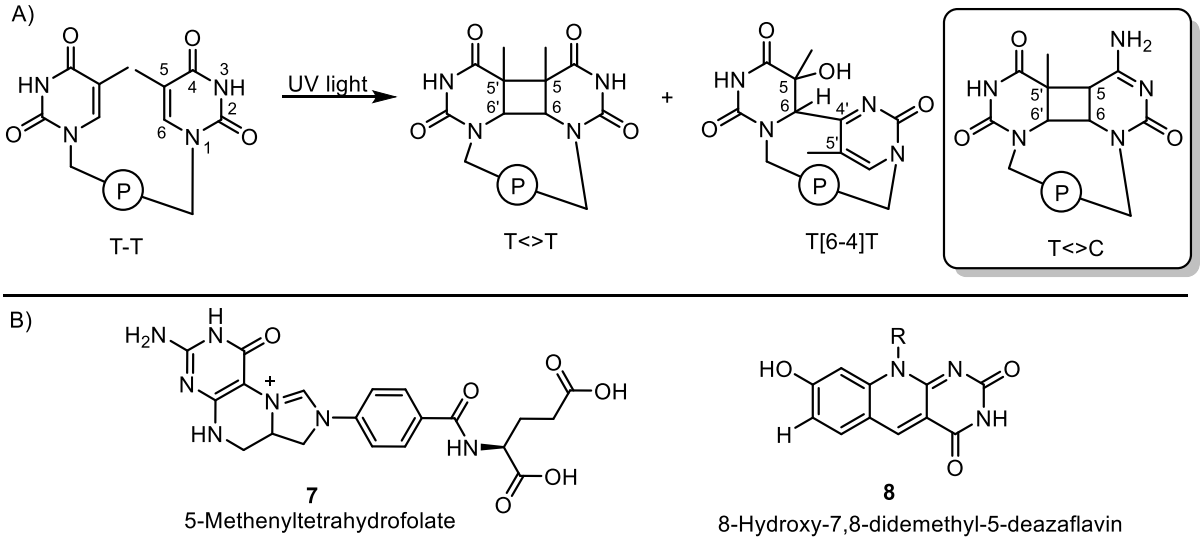

Scheme 4: A) Selected photodimerization products in DNA. T = thymine. C = cytosine. P = DNA backbone. B) Secondary cofactors (photoantennas) of photolyases.[9]

DNA photolyases can be further classified into two subgroups depending on the cleaved photodimer (Scheme 4A).[9] Cyclobutane pyrimidine dimers (T<>T) and the pyrimidine-pyrimidinone (6-4) photoproduct (T[6-4]T) are the two major lesions in DNA and, although the respective lyases are similar in structure and mechanism, no cross substrate compatibility is found and hence photolyases are separated into pyrimidine dimer (CPD) and (6-4) photolyases. Enzymes of both classes incorporate two noncovalently bound cofactors, one of which is FAD, while the second one is either methenyltetrahydrofolate (**7**) or 8-hydroxy-7,8-didemethyl-5-deazaflavin (**8**) (Scheme 4B). FAD is the catalytically active part of the enzyme and is essential for substrate binding and thus the more important chromophore, as reactivity was detected even in enzymes deficient in the secondary chromophore, while FAD omission shut down enzyme activity entirely. The second chromophore is mainly assisting FAD by energy transfer to ensure efficient DNA repair under limiting light conditions.[9] While oxidized FAD is a chromophore with intense absorption at λ_{max} ≈ 450 nm (depending on the environment),[17] the active species in DNA photolyase $FADH^-$ hardly absorbs in the blue light region, hence necessitating the second assisting chromophore.[9]

Regarding their structures, photolyases share a sequence of about 150 amino acids, which is responsible for FAD binding.[9] No structural relation to flavin oxidoreductases has been identified, presumably because of the photolyase operating with the ground state as well as the excited state of the cofactor, which requires fundamentally different structural features compared to a ground state reaction. In contrast to the flavin, which is bound very tightly to the enzyme and can only be extracted after mild denaturation, the photoantenna folate readily dissociates from the enzyme. Several photolyases have been crystallized and structurally resolved and despite comparatively low homology, the structures are highly similar with two well-defined domains. In a cleft between those domains the photoantenna is located and reaches outside of the enzyme, which is in stark difference to the FAD photocatalyst which is deeply buried within the enzyme. The flavin is bound tightly and cannot diffuse out of the pocket, while a small hole in the domain allows for a thymine dimer to enter the active site. A positively charged groove runs through the length of the enzyme and is hypothesized to bind to the DNA thus flipping out the thymine dimer into the active site. The distance and angular orientation between FAD and the photoantenna vary in different photolyases and enable rationalization of different efficiencies of energy transfer depending on the respective structure.[9]

Mechanistically, photolyases follow Michaelis-Menten kinetics with substrate binding, reaction, and product dissociation and absolutely require light for the catalytic transformation, which sets photolyases apart from most enzymes.[9] The association of the photolyase to DNA is structure-specific and not sequence-dependent. While the sequence which surrounds the binding site may influence overall enzyme-substrate complex formation, no significant difference in binding constants could be detected. After the formation of the enzyme-substrate complex, excitation of $FADH^-$ either by direct excitation or by energy transfer from the photoantenna occurs (Scheme 5).[9] Excitation of the cyclobutane dimers has been ruled out due to insufficient absorption at $\lambda > 250$ nm and no charge-transfer complex between enzyme and substrate could be detected. Then, photoexcited $FADH^-$ transfers an electron to the T<>T dimer **9** forming a dimer radical anion $\mathbf{9}^{\bullet-}$. Remarkably, this electron transfer demonstrates distinguished efficiency with a quantum yield of $\phi > 0.7$ for the overall photorepair. Likewise, energy transfer from the secondary chromophore deazaflavin occurs with a quantum yield of nearly one. Time-resolved fluorescence experiments were conducted by the group of Sancar to characterize the energy transfer of folate to $FADH^-$.[18] Efficient

quenching of the folate excited singlet state by $FADH^-$ in *E. coli* photolyase was detected and picosecond flash photolysis revealed accumulation of the flavin excited singlet state $^1(FADH^-)^*$ after (accelerated) decay of the folate singlet state. From the ratio of folate excited state decay time with and without flavin, an energy transfer quantum yield was calculated. Using the Förster equation, the chromophore distance was calculated to be R = 17.7 Å, which is in good agreement with the value determined by crystallography.[9]

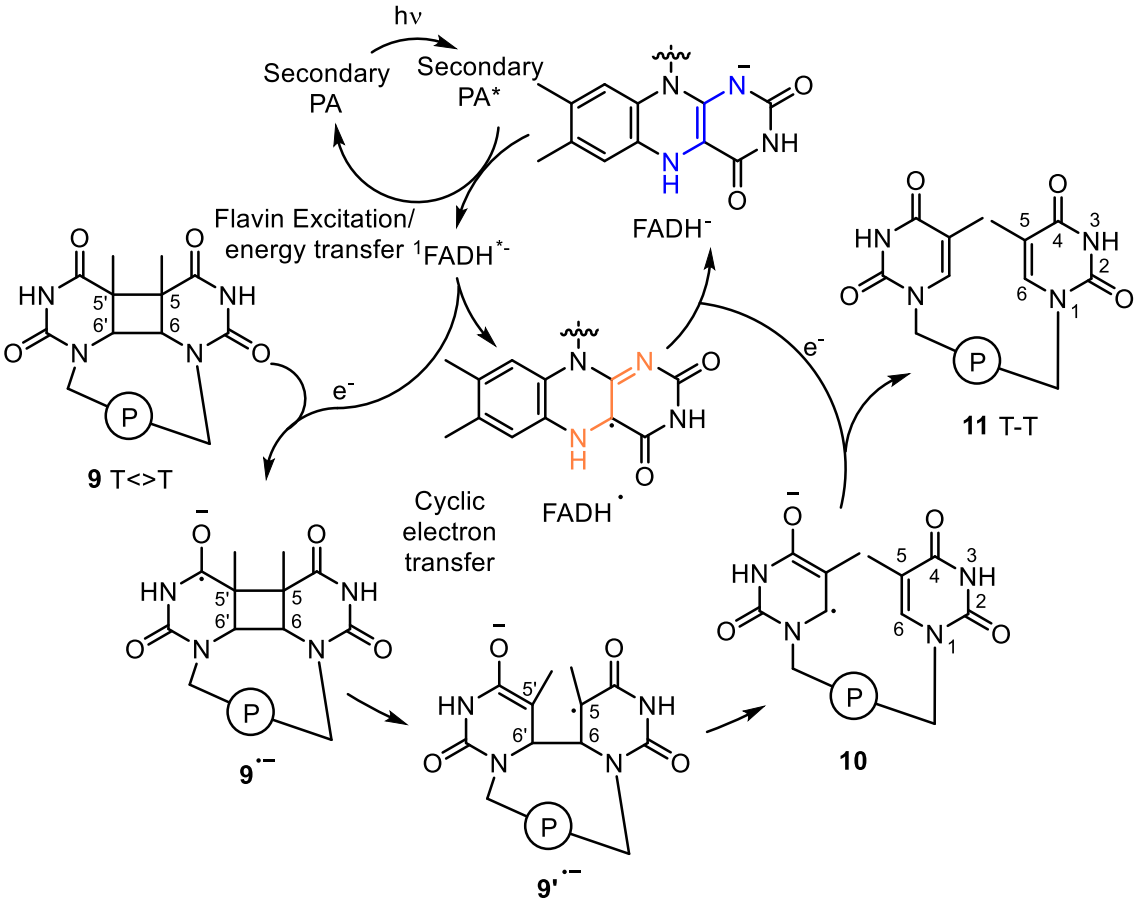

Scheme 5: A) Simplified mechanism of photolyase catalyzed cycloreversion of thymine dimers in damaged DNA.[9] PA: photoantenna.

Subsequent to electron transfer, the cyclobutane dimer splits into a pyrimidine and a pyrimidine radical anion **10**.[9] Single electron transfer (SET) from $FADH^-$ to the dimer has been confirmed by time-resolved fluorescence with efficient flavin excited state quenching by a thymine dimer.[19] The occurrence of $FADH^-$ rather than the neutral hydroquinoid $FADH_2$ in photolyases has been attributed to avoiding a zwitterionic $FADH_2^+$-$(T<>T)^-$ state, which could favor charge recombination rather than cycloreversion and thus decrease overall reaction efficiency.[20] Notably, electron transfer is not the single determining factor of successful dimer

splitting.[21] Transient absorption spectroscopy of the $^1(FADH^-)^*$ electron transfer to different dimers at low temperatures revealed inefficient dimer splitting below 200 K. This is attributed to a polypeptide chain introducing strain to the dimer thus providing the decisive amount of external energy in bond-breaking.[9] Cleavage of a dimer radical cation from flavin-mediated oxidation as an alternative pathway has been ruled out by comparison of isotope labeling effects of the respective dimer radical cation/anion splittings.[22] Photolyases are not capable of transferring enough energy to T<>T dimers to initiate an orbital symmetry-allowed concerted [2+2] cycloreversion.[9] The dimer radical anion undergoes symmetry-forbidden cycloreversion, the activation barrier of which has been lowered by electron transfer so that it can take place at ambient temperatures.[23] The catalytic cycle is closed by SET from the pyrimidine radical anion **10** to semiquinoid $FADH^{\cdot}$ forming product **11** which renders this process an overall redox-neutral reaction.[9]

2.1.4. Photochemical and redox properties of flavins

Oxidized flavins are bright yellow compounds in solution owing to the isoalloxazine core.[3] Characterization of the different oxidation states is crucial to develop a photochemical understanding of the processes that drive the DNA photolyase as well as synthetic applications of flavins and has been undertaken from an experimental[24] (Figure 1) and a theoretical perspective.[17] The absorption spectrum[24] of oxidized FAD in solution (aqueous phosphate buffer at pH = 7.4) shows two bands at $\lambda_{A,max}$ = 450 nm ($S_0 \rightarrow S_1$) and 375 nm ($S_0 \rightarrow S_2$), FMN in a flavodoxin protein shows a similar spectrum albeit with more distinct features ($\lambda_{A,max}$ = 476, 454, 432 nm ($S_0 \rightarrow S_1$) and 384 nm ($S_0 \rightarrow S_2$)). Maximal emission intensity is detected at $\lambda_{E,max}$ = 530 nm ($S_0 \rightarrow S_1$), in the enzyme flavodoxin a blue shift of the maximum of approximately 10 nm is observed for FMN due to the hydrophobic environment decreasing the solvation of the excited state.[25] For FAD in solution, a drastic difference in emission intensity compared to FMN has been determined.[26] The proposed reason is an intramolecular energy transfer from the FAD isoalloxazine to the adenine moiety in a stacked conformer in solution.[24] The biexponential decay dynamics for FAD in solution show a lifetime of τ = 2.5 ns which corresponds to the FAD open form, while a fast decay of τ = 9.2 ps has been ascribed to the aforementioned energy transfer. These two peculiarities highlight the difference of flavin spectroscopy in enzymatic environment and in solution. Apart from the special case of FAD in solution, oxidized flavins all exhibit excited state lifetimes of several nanoseconds. It was also demonstrated that oxidized flavins undergo intersystem crossing (ISC) to their respective

triplet states[27] which is verified by the conversion of triplet oxygen to singlet oxygen under flavin irradiation.[28]

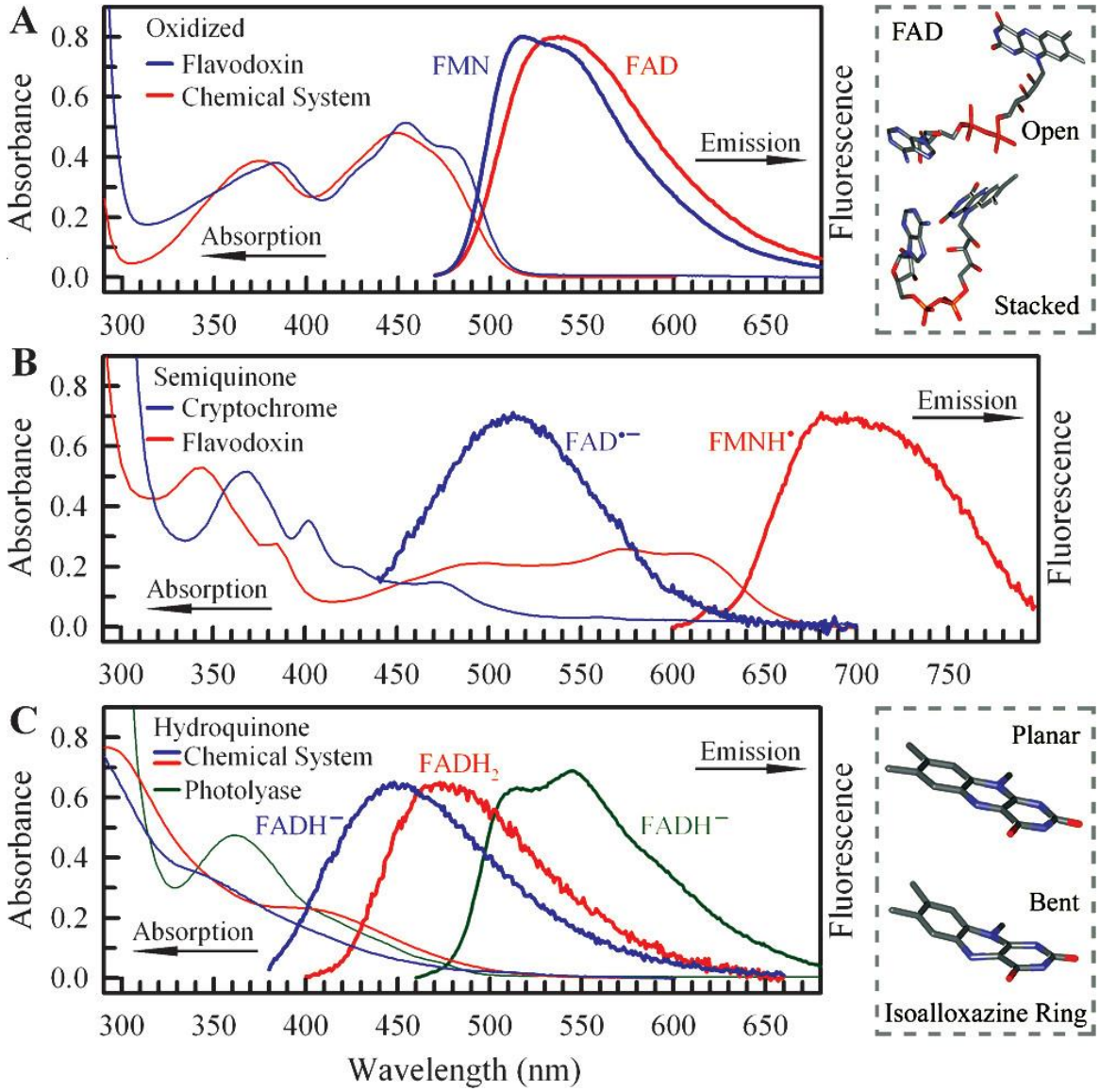

Figure 1: Absorption spectra of flavin in different oxidation states. (Reprinted with permission from *J. Am. Chem. Soc*. **2008**, 130, 39, 13132–13139. Copyright 2024 American Chemical Society).[24]

In comparison to the quinoid flavin, literature regarding spectroscopy of the semiquinoid state outside of the enzyme is rather scarce.[24] However, by using pulse radiolysis absorption spectra of semiquinoid flavin were recorded in an atmosphere of N_2O.[29] In an enzymatic environment, the semiquinoid flavin is more easily accessible and stabilized, thus facilitating spectroscopy of these species.[24] Neutral $FMNH^{\cdot}$ absorbs strongly at $\lambda_{A,max}$ = 340 nm, and also exhibits a very broad absorption band tailing until 700 nm. Comparatively, the absorption

maximum of deprotonated $FAD^{\bullet -}$ is shifted to $\lambda_{A,max}$ = 370 nm and there is tailing well beyond $\lambda_{A,max}$ = 550 nm.[24] Emission spectra of both semiquinoid species are weak in intensity and show broad maxima at $\lambda_{E,max}$ = 700 nm (neutral semiquinone) and $\lambda_{E,max}$ = 510 nm (deprotonated semiquinone), and for the latter, the maximum strongly depends on excitation wavelength. The excited state lifetime for $FMNH^{\bullet}$ was determined to τ = 230 ps.[24]

As DNA photolyases belong to the small group of enzymes requiring light, the spectroscopic properties of the active cofactor $FADH^-$ are particularly valuable for mechanistic understanding of this enzyme family.[9] $FADH^-$ in photolyase exhibits an absorption maximum at $\lambda_{A,max}$ = 360 nm which, compared to oxidized flavins in enzymatic/non-enzymatic environment, differs significantly from $FADH^-$ in a chemical system (aqueous phosphate buffer at pH = 8.5) with maxima at $\lambda_{A,max}$ = 300 nm and a broad feature at $\lambda_{A,max}$ = 400 nm.[24] The absorption spectrum of neutral $FADH_2$ in solution (aqueous phosphate buffer at pH = 5.0) has a similar shape as $FADH^-$, however the broad feature is shifted to $\lambda_{A,max}$ = 350 nm. Next, emission spectra for the reduced flavins are given with enzyme-bound $FADH^-$ emission peaking at $\lambda_{E,max}$ = 515 nm and 545 nm, and a lifetime of τ = 1.3 ns. For reduced flavins in solution, drastically decreased emission intensity at $\lambda_{E,max}$ = 455 nm ($FADH^-$) and $\lambda_{E,max}$ = 480 nm ($FADH_2$) is reported alongside rapid deactivation. Excitation wavelength influences the emission strongly, which is attributed to deactivating mechanisms by conical intersections of the ground state and excited state hypersurface.[24]

The decreased intensity is attributed to a bending mode of reduced flavin that dissipates excitation energy by a “butterfly” motion, while intramolecular energy transfer alike FAD in solution has been ruled out.[24] As opposed to oxidized flavins which are planar, reduced flavins are bent in their ground state in solution. According to quantum mechanical calculations,[17] in the enzymatic scaffold this bent geometry is much less pronounced due to the cofactor being constrained by its environment. This also serves as an explanation as to why reduced flavins’ absorption peak potentials are strongly dependent on whether they are embedded in an enzyme.[24] A low activation barrier (<20 kJ/mol)[30] bending motion along the N^5-N^{10} axis that facilitates radiationless decay from the excited state to the ground state by conical intersection of the respective potential energy surfaces is proposed.[24] This claim is supported by showing the dependency of the bending motion of solvent viscosity. In the enzyme, this motion is restricted hence resulting in an excited state lifetime of several

nanoseconds and ultimately higher emission intensity. Interestingly, in a recent report reduced riboflavin emission was investigated with samples using EDTA in a photoreduction in aqueous buffer.[31] No significant fluorescence at room temperature was observed and instead fluorescence at $\lambda_{E,max}$ = 450 nm was detected and attributed to lumichrome, a common flavin decomposition product. A previous study by Ghisla indicates that reduced flavoenzymes are non–fluorescent at room temperature, however emission at cryogenic conditions (77 K) occurs at $\lambda_{E,max} \approx$ 500 nm.[32]

To understand flavin reactivity, both in enzymes and in solution, apart from spectroscopic properties assessment of redox potentials is crucial.[33] Depending on the pH values, unbound flavins have redox potentials in the range of E_{red} (Fl/Fl$^{\bullet-}$) = −0.186 V – −0.219 V vs SCE (saturated calomel electrode). The diversity of flavoenzyme-catalyzed reactions is in part enabled by the ability of the enzyme to modulate the redox potential, a range of 500 mV (from +100 mV to −400 mV) has been reported.[34] Flavoenzyme redox potentials can be determined *via* potentiometric titration by determination of the measured potential dependent on the concentration of oxidized and reduced species. The concentration is determined by monitoring unique features like the UV-visible spectra of the oxidized and reduced species. Using the Nernst equation, the potential of the redox couple can be determined.[34]

A remarkable example of the potency of excited state reduced flavin as a SET reagent is found in DNA photolyases.[35] The redox potential of the dimers that are reduced in the flavin-mediated photorepair is E_{red} (thymine dimer/thymine dimer$^{\bullet-}$) = −2.20 V vs SCE. Using the ground state redox potential E_{red} (FlH$^{\bullet-}$/FlH^{-}) = −0.12 V vs SCE[36] and the emission band ($\lambda_{E,max}$ = 500 nm) of reduced flavin in DNA photolyases,[32] an excited state redox potential of E_{red} (FlH$^{\bullet-}$/FlH^{-}*) ≈ −2.6 V vs SCE can be estimated which is comparable to strong alkali metal reductant sodium (E_{red} (Na^{+}/Na) = −2.7 V vs SCE).[37]

3. Single Electron Reduction in Organic Synthesis

Alkali metals are considered among the strongest SET reagents[37] and provide a reaction mixture with solvated electrons which can be regarded as the smallest reagent.[38] A prominent example of this reactivity can be seen in the Birch reduction (Scheme 6).[39]

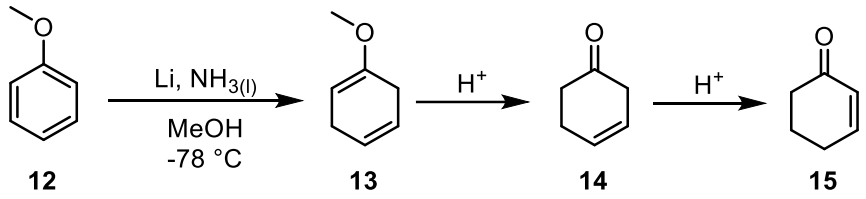

Scheme 6: Birch reduction of anisole (**12**) to 1-methoxy-1,4-cyclohexadiene (**15**).[39]

Elemental lithium can be dissolved at -78 °C in liquid ammonia resulting in the solvation of electrons indicated by a deep blue solution. Aromatic compounds such as anisole (**12**) serve as acceptors and the resulting carbanions are protonated by a protic solvent.[39] This reduction specifically results in 2,5-dihydro aromatic compound **13** and over acid-mediated hydrolysis and subsequent isomerization of intermediate **14** gives rise to α,β-unsaturated compound **15** which is a valuable building block as a Michael acceptor. While the Birch reduction enables an important transformation, its applicability is limited due to several factors. Cryogenic ammonia is inconvenient to work with, the solubility of substrates is rather limited, and alkali metals typically show limited functional group tolerance because of their strongly negative redox potentials, which lack tunability. This need for versatile and functional group tolerant reductants drives the development of new reagents. These are either metal based or organic and can act thermally or photochemically. Generally, reductive SET reactions operate by initial electron transfer of a donor (D) to an acceptor (A) resulting in a radical anion (Scheme 7).[40] In the case of alkyl halides (R-X), a commonly utilized substrate class for SET reactions, dissociation of a halide anion occurs, leaving a carbon-centered radical ($R^{\cdot}$). A second SET can occur to form the corresponding carbanion (R^{-}) which can react with an electrophile E (net conversion into a nucleophile). The carbon-centered radical can also combine with a donor radical cation ($D^{\cdot+}$) and subsequently react with a nucleophile Y. A common side reaction is hydrogen atom transfer (HAT) to the carbon-centered radical.[40]

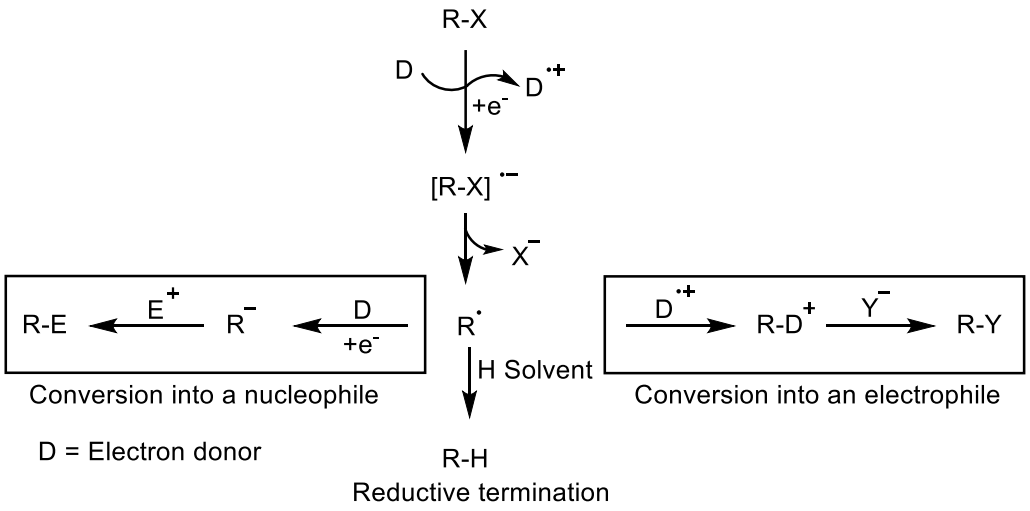

Scheme 7: General reaction scheme of SET processes.[40]

3.1. SET under thermal conditions

3.1.1. Samarium (II) iodide

Samarium (II) iodide (SmI_2) is a SET reagent that can be readily prepared from samarium and 1,2-diiodoethane in tetrahydrofuran and was first reported by the group of Kagan.[41] The storable dark blue solutions (in tetrahydrofuran) can be used at ambient temperature and under generally mild conditions. Tunability of the redox potential poses a crucial property enabling the application of SmI_2 in a wide range of different reactions.[42] Without any additives, SmI_2 has a redox potential of E_{red} (Sm^{3+}/ Sm^{2+}) = −0.9 V vs SCE in tetrahydrofuran. Coordination of Lewis bases to the Lewis acidic Sm^{2+} center can significantly alter the redox potential with SmI_2-HMPA reaching potentials of up to −1.8 V vs SCE and even non-toxic Lewis additives like water can enhance the reducing power (E_{red} = −1.0 V – −1.3 V, depending on the amount of water added).[42]

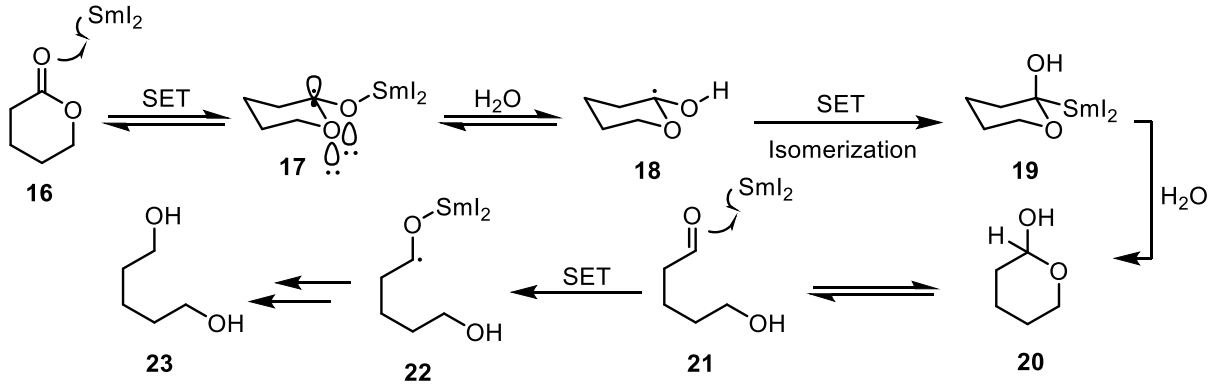

Scheme 8: Reductive cleavage of tetrahydro-2*H*-pyran-2-one with SmI_2-H_2O.[43]

Interestingly, the redox potentials do not necessarily depict the reactivity of samarium adducts accurately, as demonstrated by the selective reduction of 6-membered lactones to the corresponding diols (Scheme 8).[43] The reduction of lactone carbonyls (E_{red} = −3.0 V vs SCE)[42] by SmI_2 in tetrahydrofuran/water cannot be rationalized by comparison of the redox potentials.[43] Moreover, more strongly reducing SmI_2 adducts failed to show reactivity, and a critical role is assigned to water. The suggested mechanism includes lactone **16** carbonyl oxygen coordination to SmI_2 before a first SET occurs to form ketyl radical anion **17**. Protonation of the alkoxide to radical **18**, stereoinversion and reduction of the carbon-centered radical follows, yielding intermediate **19**. The resulting lactol **20** is in equilibrium with its open-chained form **21**, the aldehyde is efficiently reduced to ketyl radical **22** and ultimately to alcohol **23**. Control experiments showed efficient reduction of 5-membered lactols indicating that the chemoselectivity arises from initial reduction of the 6-membered lactone. Lone pair stabilization of radical anion **17** is significantly higher than in conformationally more labile rings and calculation revealed that the electron transfer to 6-membered lactones is approximately 25 kJ mol^{-1} more favorable than to 5-membered rings.[43]

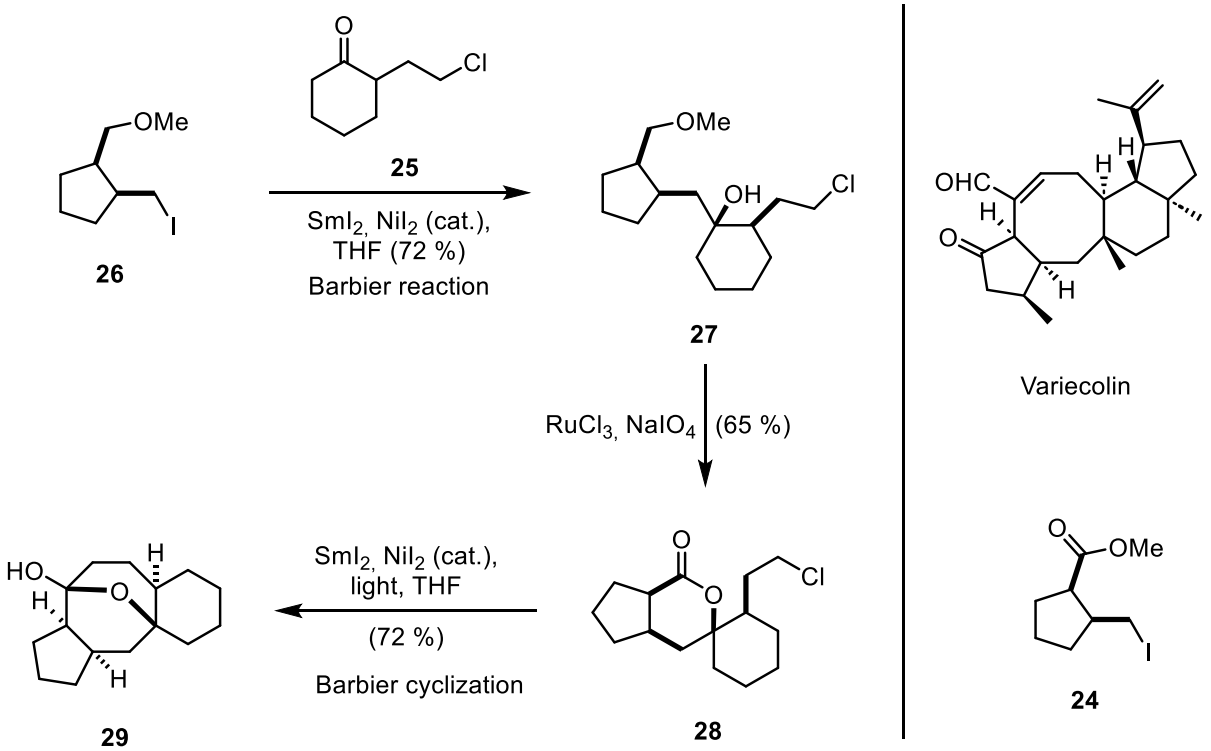

Scheme 9: SmI_2 mediated Barbier reactions in the synthesis of variecolin.[44]

While Birch-type reductions can also be performed with $SmI_2(H_2O)_n$,[42] reductions of alkyl halides and carbonyl compounds remain the most important transformations realized with

SmI_2, especially in the context of total synthesis.[45] The Barbier reaction of alkyl halides and a carbonyl compound can be carried out with SmI_2 and thus under homogenous and one-pot conditions, compared to the stepwise preparation of Grignard reagents. In the total synthesis of variecolin,[44] the group of Molander employed SmI_2 in two separate steps exploiting different reactivity of alkyl iodides and alkyl chlorides (Scheme 9).

Originally, coupling of 1,2-*cis* cyclopentane **24** with ketone **25** was planned.[44] Intramolecular cyclobutane formation was faster than intermolecular Barbier reaction and coupling of alkyliodide **26** with ketone **25** was carried out instead using SmI_2 under thermal conditions with catalytic NiI_2. The exact function of the latter is unknown, but enhanced reaction rates are typically observed.[45] The intermediate ether **27** is oxidized and cyclized to lactone **28**.[44] The second SmI_2-mediated reduction of the alkyl chloride to furnish hemiketal **29** proceeds under photoirradiative conditions.[46] Alkyl chlorides, in contrast to alkyl bromides and alkyl iodides, cannot be directly reduced using SmI_2 without additives. However, irradiation with light (λ > 400 nm) leads to efficient reduction yielding the radical that can be further reduced or intercepted by suitable reagents. This example highlights orthogonal reactivity with SmI_2 by choosing appropriate reaction conditions.[45]

Carbonyl-alkene couplings under SmI_2 conditions proceed by SET to form a ketyl radical which can then attack an alkene in a net umpolung approach as demonstrated by the group of Procter in their functionalization of barbituric acids (Scheme 10).[47] First, the monoreduction of barbituric acids **30** to hemiaminals **31** was investigated. SmI_2/H_2O proved to be suitable for this transformation and a range of barbituric acids including functional groups prone to reduction like arylbromide and trifluoromethyl were selectively reduced at the carbonyl amide with excellent diastereoselectivity. Notably, no over-reduction was observed and other additives (e.g. HMPA, amines) were unsuccessful despite lower redox potentials of the SmI_2 adducts. The introduction of linkers in the C^4 position that can intercept a radical by addition provided an array of substrates **32** which readily cyclized to the corresponding bicyclic products **33**. Unactivated alkenes and alkynes were tolerated in excellent diastereoselectivity. This is ascribed to stabilization of the ketyl radicals by anomeric effects, i. e. the half-life of the radical is increased by $n_N \rightarrow$ SOMO interactions resulting in the tether assuming the lowest energy conformer before cyclization. Mechanistic experiments suggest that proton transfer is not rate-determining, however H_2O concentration influences diastereoselectivity. This implies

that the ketyl radicals are not instantaneously reduced to carbanions, probably because of different SmI_2 complexations in dependence on water.[48] The key function of water is the stabilization of the radical anion after the initial SET. From here, either another SET or radical interception and a SET occur to furnish bicyclic barbituric acid derivatives.[47]

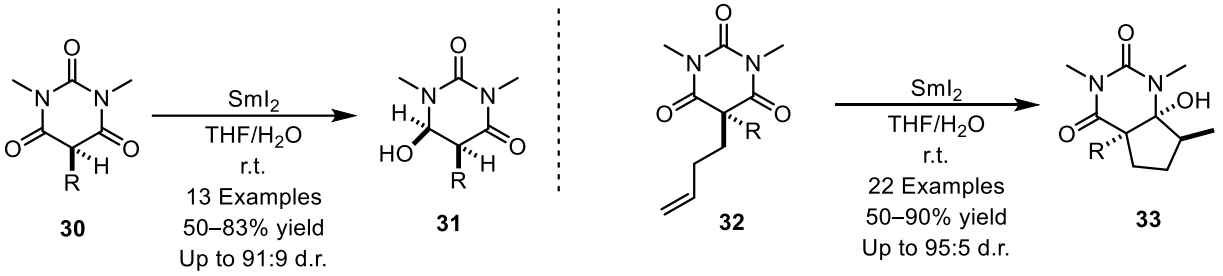

Scheme 10: SET reduction of barbituric acids with SmI_2.[47]

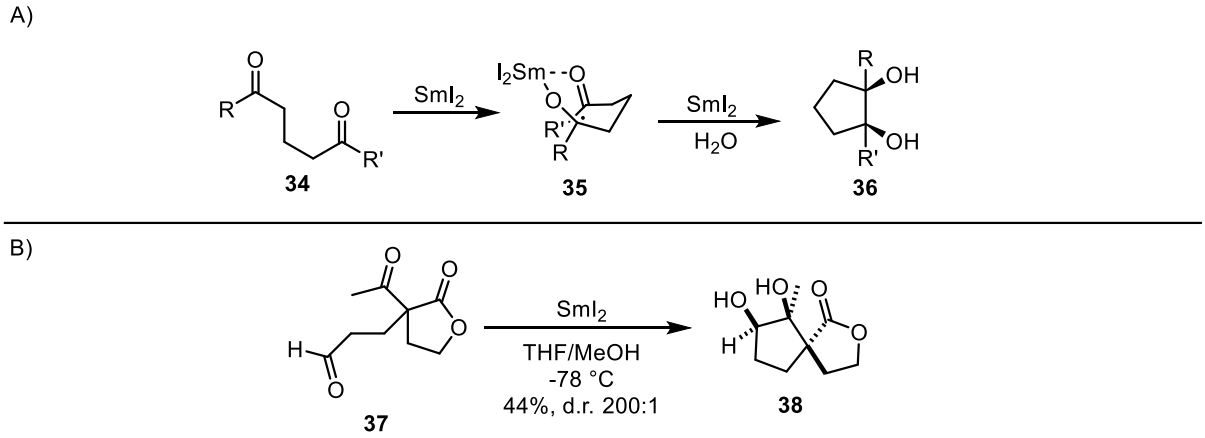

Scheme 11: A) Mechanism of SmI_2 mediated pinacol coupling.[45] B) Pinacol coupling of spirocyclic compound **37**.[49]

Due to its ability to coordinate carbonyl oxygen atoms, the application of SmI_2 in pinacol couplings has been reported in numerous total syntheses.[45] The general mechanism involves the reduction of one carbonyl moiety of a dicarbonyl compound **34** to form a ketyl radical **35** (Scheme 11A). For intermolecular reactions, radical addition to the second carbonyl occurs stereoselectively in *cis*-fashion because of oxygen coordination to the Lewis acidic samarium(III). After a second SET, the *cis*-diol is liberated by protonation to give 1,2-diol **36**. This reaction is not limited to carbonyl-carbonyl coupling and nitriles or methoximes are also suitable functional groups. One early example of SmI_2-mediated pinacol coupling involves diol formation in the spirocyclic compound **37** (Scheme 11B).[49] Reduction of the more electron-deficient aldehyde is proposed to initiate cyclization by ketyl radical addition to the ketone

carbonyl to ultimately form diol **38**. Notably, the appended lactone is orientated in an *anti*-configuration to the newly formed diol which is presumably caused by dipolar repulsion of the lactone and the Sm^{3+} chelate.[49]

3.1.2. Aromatic hydrocarbon anions

Radical anion intermediates, which result from the reduction of aromatic compounds can be used as powerful reductants if no further reaction pathway as described in the Birch reduction is possible.[50] The reaction of alkali metals and naphthalene in polar ethers results in radical anion species with strong reducing power, similar to elemental sodium. The choice of metal, substrate, and solvent affect the equilibrium of the reaction and also the nature of the mixture, i. e. whether the radical anion and metal cation form solvent-separated ions or contact ion pairs. The highest degree of radical anion formation is typically achieved by using lithium and ethylene glycol ethers due to their ability to form five-membered chelates with the metal cation. Larger aromatic compounds (e.g. anthracene) also favor solvent-separated ions due to better charge delocalization in comparison to naphthalene. However, a general rule cannot be postulated, and an individual assessment of each reaction system is necessary. Notably, free radical anions are not necessarily the most reactive species and ion pairing can increase reaction rates for selected reactions. Another factor to be considered is dianion formation. All arene-metal combinations tend to form the dianion in varying degrees, possibly by the disproportionation of two radical anions.[51] Because the dianion is a stronger base, this may be undesired and can be circumvented by the utilization of highly polar solvents to increase the amount of free radical anion formation which decreases the disproportionation rate.[50]

A common reaction for these arene radical anions is the protonation by compounds with $pK_a < 34$.[50] From that perspective, these reagents undergo Birch reductions under more versatile conditions because cryogenic temperatures and the limited solubility of substrates in ammonia are no longer limiting factors. This reactivity is of limited use and the application of arene radical anions over conventional bases is restricted to cases where exact stoichiometric addition is crucial because the amount of reagent can be monitored by its intense color. SET is the more common reaction type of arene radical anions, and due to the highly negative redox potential, a range of functional groups can be reduced.[50]

Aliphatic and aromatic halides are quickly converted to the corresponding radicals and halide anions.[50] A second reduction to form the corresponding carbanion rapidly follows, as demonstrated by the interception of the radical anion to form a Grignard reagent[52] and the debromohydrogenation of optically pure 1-bromo-1-methyl-2,2-diphenylcyclopropane with net stereo retention indicating electron transfer that is faster than C(sp^3) radical inversion.[53] A particularly interesting case is the efficient elimination of vicinal dihalides to the respective alkene (Scheme 12).[54] The reduction of enantioenriched linear dibromo alkanes **39** by two subsequent SET steps using sodium napthalenide was investigated to examine the stereoselectivity of one-electron reductants. Due to efficient second SET to C(sp^3) radical **40** forming the corresponding carbanion **41**, interconversion of the stereodetermining intermediates is suppressed and both enantiomers mostly retain their respective configuration after 1,2-dehalogenation, albeit to a varying extent due to thermodynamic preference for *(E)*-**42**. Another useful application of arene radical anions is found in deprotection chemistry.[55] Alcohols that are protected as activated ethers (benzyl ethers, allyl ethers, silyl ethers) can be deprotected with lithium powder in tetrahydrofuran using a catalytic amount of naphthalene. Moreover, sulfonyl amides and carboxamides allow for reductive cleavage under the same conditions establishing lithium napthalenide as important reagent for convenient deprotection chemistry.[55]

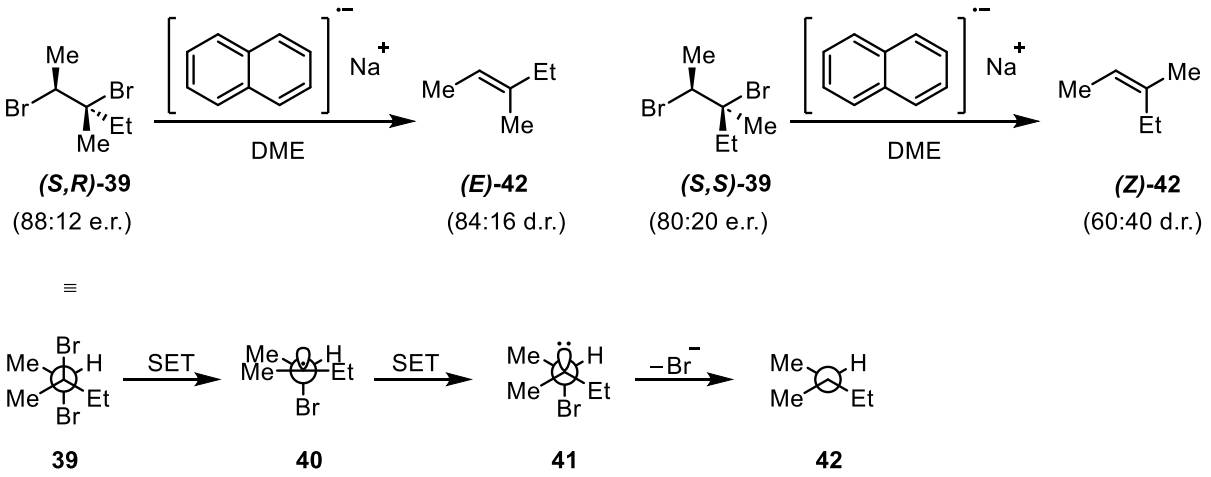

Scheme 12: Stereoretentive *trans*-elimination of 1,2-dibromo alkanes with sodium napthalenide.[54] Second SET occurs rapidly, thereby suppressing inversion of C-sp^3 centered radical **40**. *(S)*-**42** selectivity for *trans*-elimination is reduced due to *(E)*-**42** being the thermodynamically favored isomer.

Although sodium napthalenide is a comparatively harsh reagent due to its strong reducing potential, application in total synthesis is reported. In the total synthesis of cerorubenic acid-III[56], a precursor containing a carbon-halogen bond, a benzyl ether, and a conjugated diene is subjected to sodium napthalenide, which results in reduction of all three moieties in a one-pot procedure (Scheme 13). While the authors were able to carry out the reaction of precursor **43** in two subsequent steps in a traditional sodium napthalenide/tetrahydrofuran system by isolating the intermediate diene **44**, the reaction of **43** in tetrahydrofuran/water directly furnished product **45**. The overall yield of the one-pot procedure with water was better, however, the authors do not comment on the reason or possible problems due to sodium napthalenide protonation.[56]

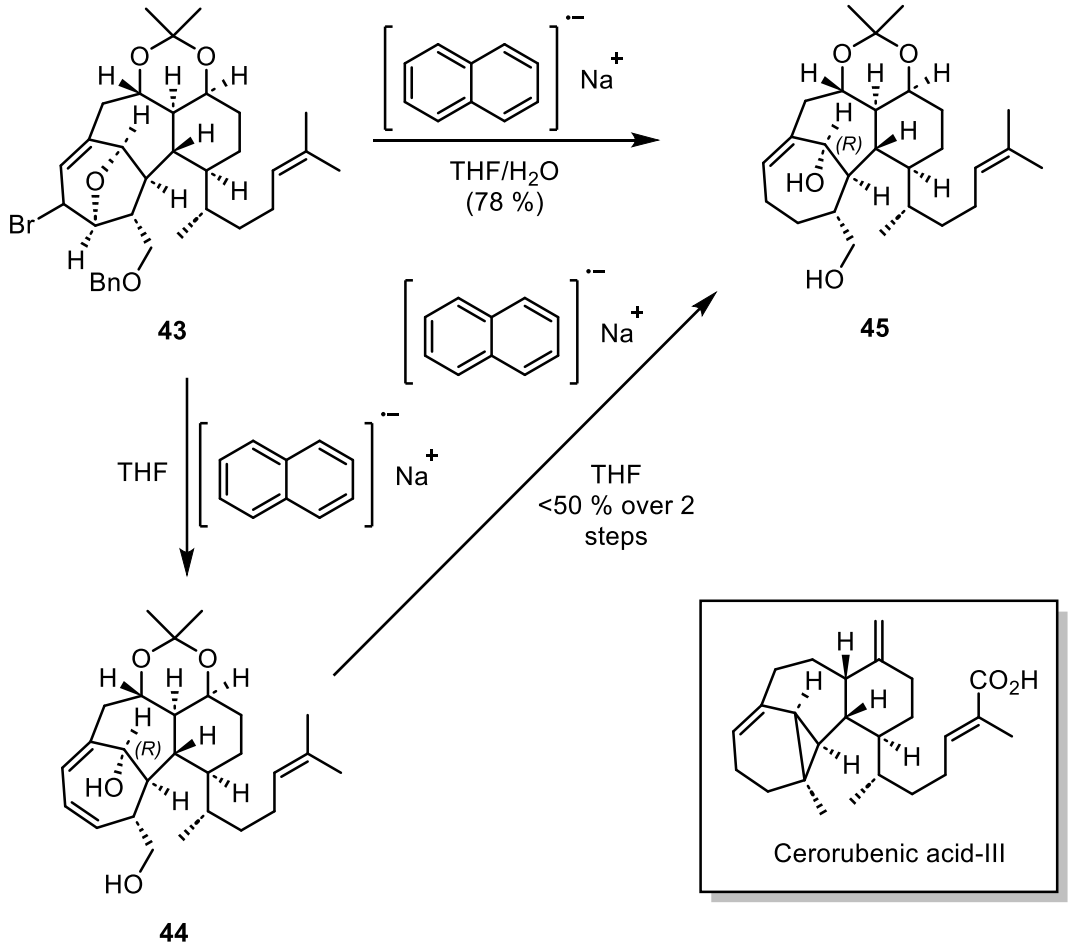

Scheme 13: Multiple site one-pot reduction of a precursor of cerorubenic acid-III by sodium napthalenide.[56]

The reduction of enantiopure 2-phenyl cyclohexanone **46** to the *trans*-alcohol **47** demonstrated the advantage of SET reagents over two-electron reductants in specific cases

(Scheme 14).[57] Sodium borohydride addition to the ketone yielded the undesired *cis*-compound **48** because of steric interaction with the adjacent phenyl group. Sodium napthalenide with acetamide as a proton donor selectively furnished the desired epimer, presumably because of carbanion isomerization to the thermodynamically favored intermediate.[57]

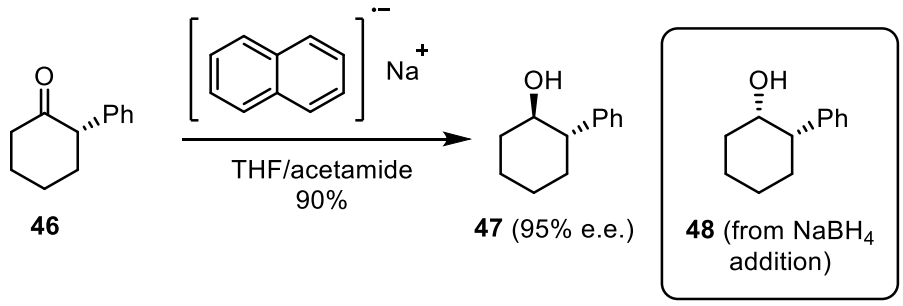

Scheme 14: Stereodivergent reduction of 2-phenyl cyclohexanone **46** with sodium napthalenide in contrast to sodium borohydride.[57]

The disadvantages of classical lithium napthalenide have led to the development of more refined reagents such as Freeman's reagent lithium di-*tert*-butylbiphenylide (LiDBB, Scheme 15) that have a more negative redox potential and do not suffer from side reactivity in the form of radical addition to napthalenide which is commonly observed in dehalogenation reactions and drastically diminishes reaction yields.[58] Radical addition to the arene radical anion is suppressed by introducing steric bulk. Pyrroles, such as derivative **49**, can be reduced to 2,5-dihydropyrroles **50** and alkylated under ammonia-free conditions using arene radical anions with LiDBB showing superior reactivity to lithium napthalenide (Scheme 15).[59] Interestingly, a disulfide is tolerated as electrophile when using LiDBB over napthalenide.

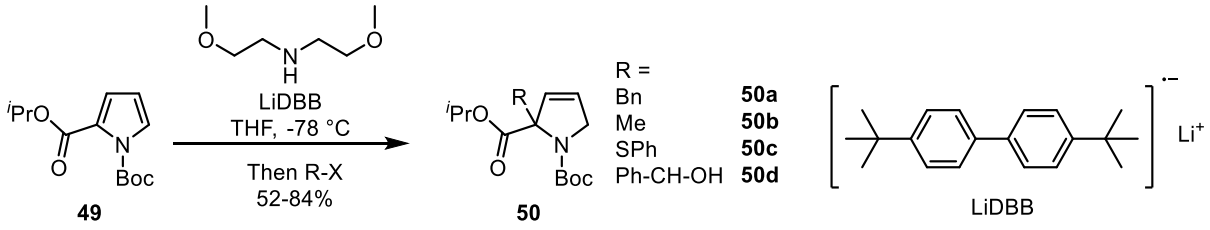

Scheme 15: Pyrrole reduction with lithium di-*tert*-butylbiphenylide (LiDBB).[59]

3.1.2. Electron-rich olefins

Electron-rich olefins such as tetrakis(dimethylamino)ethylene (**51**) (TDAE) are strong metal-free reductants under thermal conditions.[40] TDAE can perform two sequential SETs

(E_{red} ($TDAE^{\cdot+}$/TDAE) = −0.78 V vs SCE in acetonitrile, E_{red} ($TDAE^{2+}$/$TDAE^{\cdot+}$) = −0.62 V) with a reducing power similar to zinc and the driving force of oxidation is steric repulsion of the amines in planar conformation which is reduced in the oxidized form (Scheme 16A).[60] Synthetic application of TDAE includes the reduction of activated haloalkanes to radicals or anions, that can be trapped by adequate acceptors. TDAE provides a mild method for the reduction of bromodifluoromethyl heterocycles, such as **52**, to the corresponding carbanions that are subsequently trapped with aldehydes furnishing adducts like **53** (Scheme 16B).[61] A range of difluorobromo benzoxazoles have been investigated toward their debromoalkylation in the search for possible fluorinated reverse transcriptase inhibitors. Functionalization of the substrates by electrochemical reduction or activated zinc failed because of protonation after reduction. Formation of the organolithium compound resulted in decomposition. Hence the authors investigated TDAE and found efficient reduction and coupling to aldehydes by addition of the intermediate carbanion. After the reaction, $TDAEBr_2$ forms an insoluble salt that can be easily separated by filtration. The authors confirmed two sequential SETs by intercepting the radical after the first SET. Cyclic voltammetry confirmed the possibility of electron transfer from TDAE to benzoxazoles and a range of products were synthesized by using TDAE as a convenient SET reagent.[61]

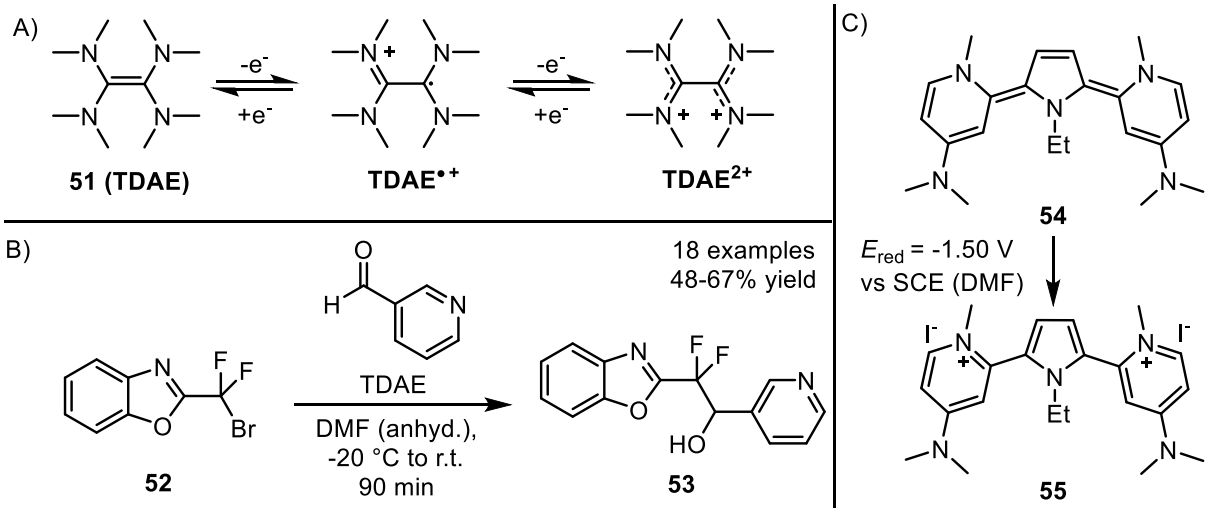

Scheme 16: A) Redox states of TDAE.[60] B) Reduction and coupling of difluorobromoalkanes by TDAE.[61] C) Strongly reducing pyrrole derivative.[60]

In comparison to thermal metal reductants, organic electron donors can be easily tuned by derivatization.[60] This offers access to a library of different reductants with redox potential significantly higher/lower than that of TDAE. Tetrathiafulvalene (TTF) is a derivative of TDAE

with significantly less reducing strength (E_{red} ($TTF^{\cdot+}$/TTF) = +0.37 V vs SCE in acetonitrile, E_{red} (TTF^{2+}/$TTF^{\cdot+}$) = +0.67 V). It has been used to reduce diarylazoniumsalts for aryl radical addition reactions to alkenes and the selective reactivity allows for the reduction of easily reducible functional groups while functional groups that would react with stronger reductants remain untouched. Likewise, TDAE derivatization can lead to stronger reductants with pyrrole derivative **54** (Scheme 16C) being among the strongest thermal organic reductants (E_{red} (**55**/**54**) = −1.50 V vs SCE in dimethylformamide).[62] The reducing power is demonstrated by several transformations including efficient reductions of Weinreb amide and tosylamides.

3.2. Photoredox Catalysis

Light-mediated catalysis benefits from reaction pathways that may be unattainable by thermal methods.[63] Photoexcited compounds can transfer the acquired energy by different mechanisms including Dexter resonance energy transfer and photoredox catalysis which involves different oxidation states of the catalyst. A characteristic property of many photoredox catalysts such as $Ir(ppy)_3$ **56** is the possibility to act as an oxidant as well as a reductant, depending on the chemical environment (Scheme 17). Absorption of the photon elevates an electron from the highest occupied molecular orbital (HOMO) to the lowest unoccupied molecular orbital (LUMO). After internal conversion to the vibrational ground state, the excited catalyst can either oxidize a donor to fill one of the single occupied molecular orbitals (SOMO) or transfer its electron to an acceptor in a process labeled photoinduced electron transfer (PET). In catalysts with efficient intersystem crossing, these processes can also occur from the triplet excited state. Another feature of most photoredox catalysts is a relatively low-wavelength absorption which prohibits unselective excitation of substrates or additives.[63]

3.2.1. Metal complexes as photoredox catalysts

Iridium polypyridyl complexes are a class of photoredox catalysts with excellent properties such as absorption in the visible region (λ_{max} = 375 nm), a long-lived excited state (τ = 1.9 µs), and a remarkable triplet energy of 56 kcal mol^{-1}.[63] Effective application in SET reactions as oxidant (E_{red} (Ir^{IV}/Ir^{*III}) = −1.73 V vs SCE) and reductant (E_{red} (Ir^{*III}/Ir^{II}) = +0.31 V vs SCE) in the excited state is possible. An example of photoredox catalysis activating substrates toward functionalization that resembles conventional methods was reported in 2010 by the group of Stephenson.[64] Tetrahydroisoquinolines, such as **57**, can be oxidized to iminium ions which

react with nitromethane to form aza-Henry products like **58** (Scheme 18A). Initially, irradiation of tetrahydroisoquinoline **57** with $Ru(bpy)_3Cl_2$ and diethyl bromomalonate as the terminal oxidant in dimethylformamide was investigated. After purification by chromatography with methanol, coupling product **59** was detected. Changing the solvent and omitting the oxidant resulted in the same product suggesting that another component can act as the oxidant. Finally, using $Ir(ppy)_2(dtbbpy)PF_6$ as a catalyst with nitromethane as the solvent, aza-Henry product **58** was isolated. Control experiments showed a very inefficient background reaction without a catalyst. A small set of tetrahydroisoquinolines and nitroalkanes were converted in excellent yields. *N*-phenyl pyrrolidine was also successfully oxidized albeit the reaction was significantly slower. As for many metal-mediated photoredox processes, the catalyst loading is very low (1%).[64]

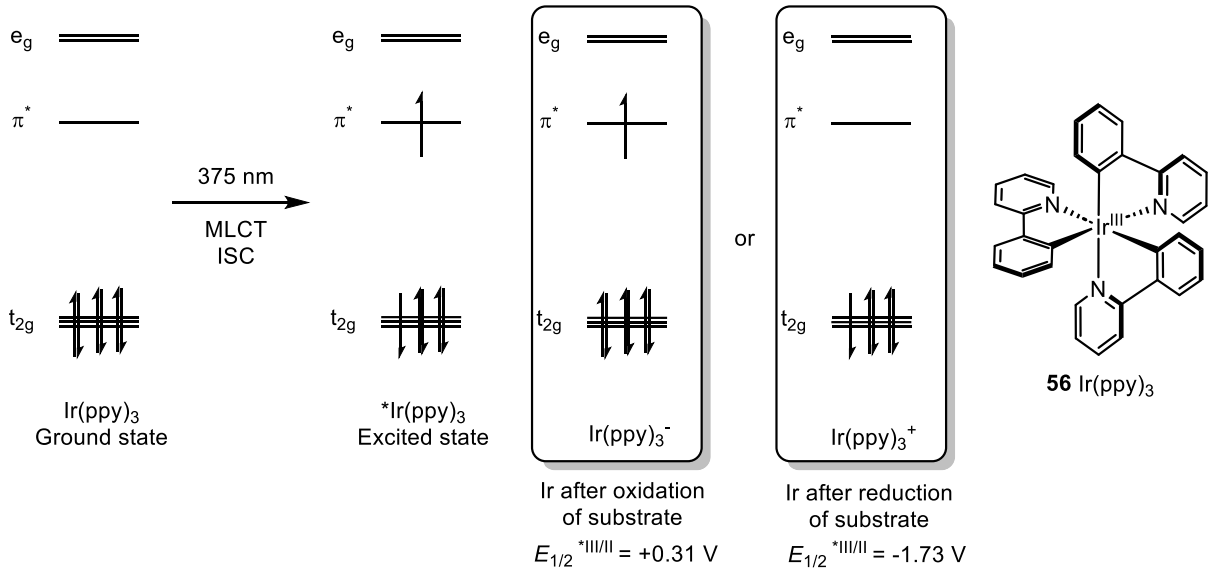

Scheme 17: Oxidative and reductive quenching after photoexcitation.[63]

The reaction commences with the absorption of a photon by Ir(III) to form photoexcited Ir(III)* (Scheme 18B).[64] Oxidation of the amine by SET occurs to form radical cation **60** and Ir(II). The latter is strongly reducing (E_{red} (Ir(III)/Ir(II)) = −1.51 V vs SCE) and converts an oxidant to the corresponding radical anion while replenishing Ir(III) for the next catalytic cycle. The oxidant is either nitromethane or oxygen, as demonstrated by lower yields under strictly degassed conditions. The radical anion can abstract a hydrogen atom from ammonium radical cation **60** to form iminium **61**. Deprotonated nitromethane adds to the sp^2 hybridized carbon to yield aza-Henry product **58**. The identity of the reduced nitromethane species is unclear and nitrosomethane could not be detected. However, performing the reaction in

dimethylformamide and a slight excess of phenyl nitromethane afforded the aza-Henry product under degassed conditions, suggesting that nitromethane is involved in catalyst regeneration. While singlet oxygen is known to oxidize amines to imines,[65] rate comparison with a reaction with a singlet oxygen sensitizer suggests inefficient singlet oxygen formation, and thus Ir(III)* mediated SET is believed to be the prime activating mechanism in this reaction.[64] Fluorescence quenching of the Ir(III)* excited state by tetrahydroisoquinolines was detected. Numerous nucleophiles were found to be adequate coupling partners in this transformation in different reports.[63]

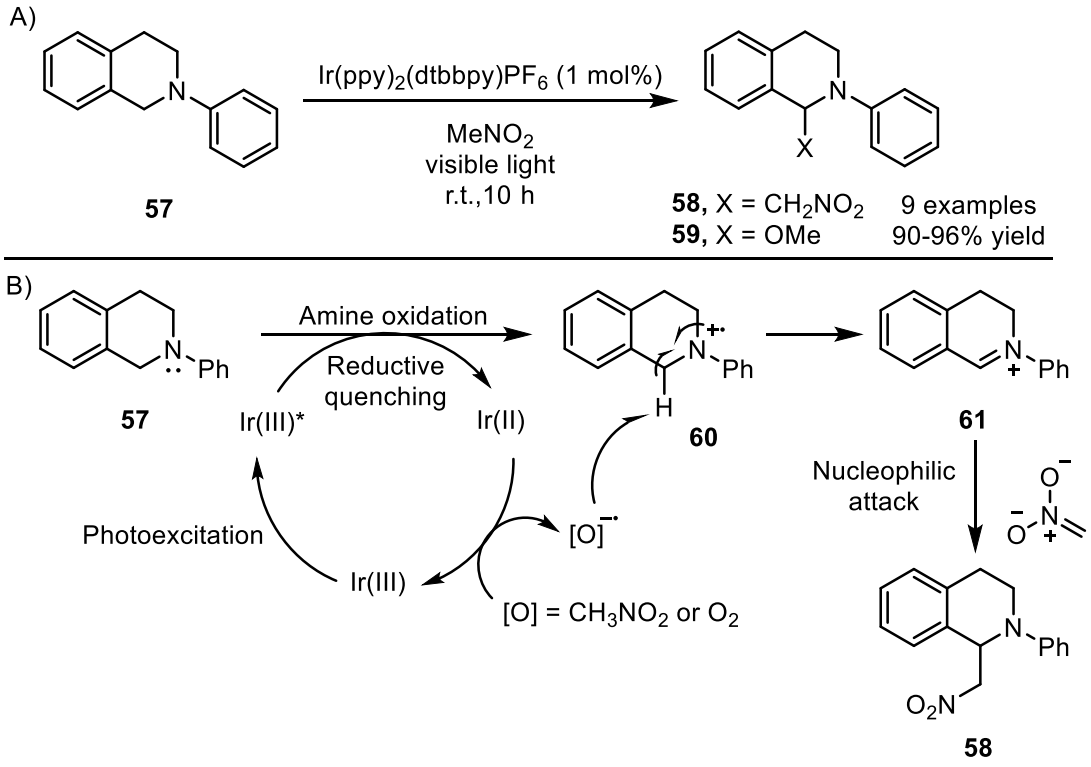

Scheme 18: A) Oxidative *α*-amino functionalization by iridium photoredox catalysis.[64] B) Suggested mechanism.

Coupling of electron-deficient cyanoarenes **62** with *N*-arylamines **63** to α-functionalized amines **64** in a net redox-neutral process by $Ir(ppy)_3$ photoredox catalysis has been reported by the MacMillan group (Scheme 19).[66] This reaction has been discovered as a result of a concept labeled "accelerated serendipity" consisting of high-throughput screening with random combinations of possibly interesting coupling partners from a substrate pool and a catalyst system in 96-well plates. The reaction outcome was assessed by gas

chromatography/mass spectrometry and one potential hit was further developed into the aforementioned coupling. The reaction tolerates cyclic amines of various ring sizes as well as a linear amine. While electron deficiency was a key requirement of the coupling partners, a range of cyanoarenes including heteroaromatics and sterically challenging substrates were successfully coupled. The photoredox catalytic cycle begins with $Ir(ppy)_3$ photoexcitation to Ir(III)* which is a strong reductant (E_{red} (Ir(IV)/Ir(III)* = −1.73 V vs SCE in acetonitrile) and reduces an electron-deficient cyanoarene **65** to its persistent radical anion **66**. Ir(IV) is a strong oxidant (E_{red} (Ir(IV)/Ir(III) = +0.77 V vs SCE in acetonitrile) and oxidizes an amine **67** to its transient radical cation **68**, thereby closing the photoredox catalytic cycle without external reductants or oxidants. The acidity of radical cation **68** is significantly increased and deprotonation by sodium acetate results in neutral radical **69**. Afterward, radical combination leads to the C-C coupling intermediate anion **70**. Cyanide is eliminated to liberate the coupled product **71**. The emission of the catalyst was quenched only by cyanoarenes and not by the amines, which excludes initial amine oxidation as a possible mechanism.[66]

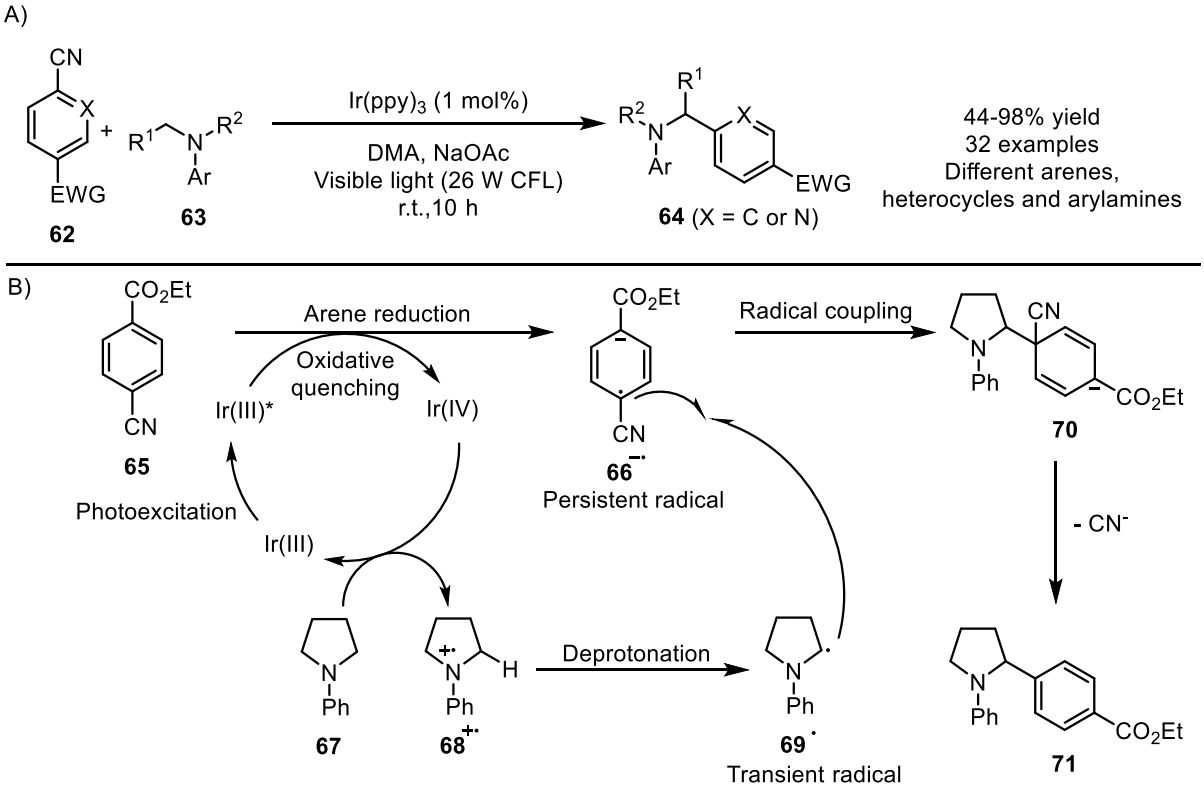

Scheme 19: A) Redox-neutral coupling of electron-deficient cyanoarenes with *N*-arylamines by photoredox catalysis.[66] B) Suggested photoredox mechanism.

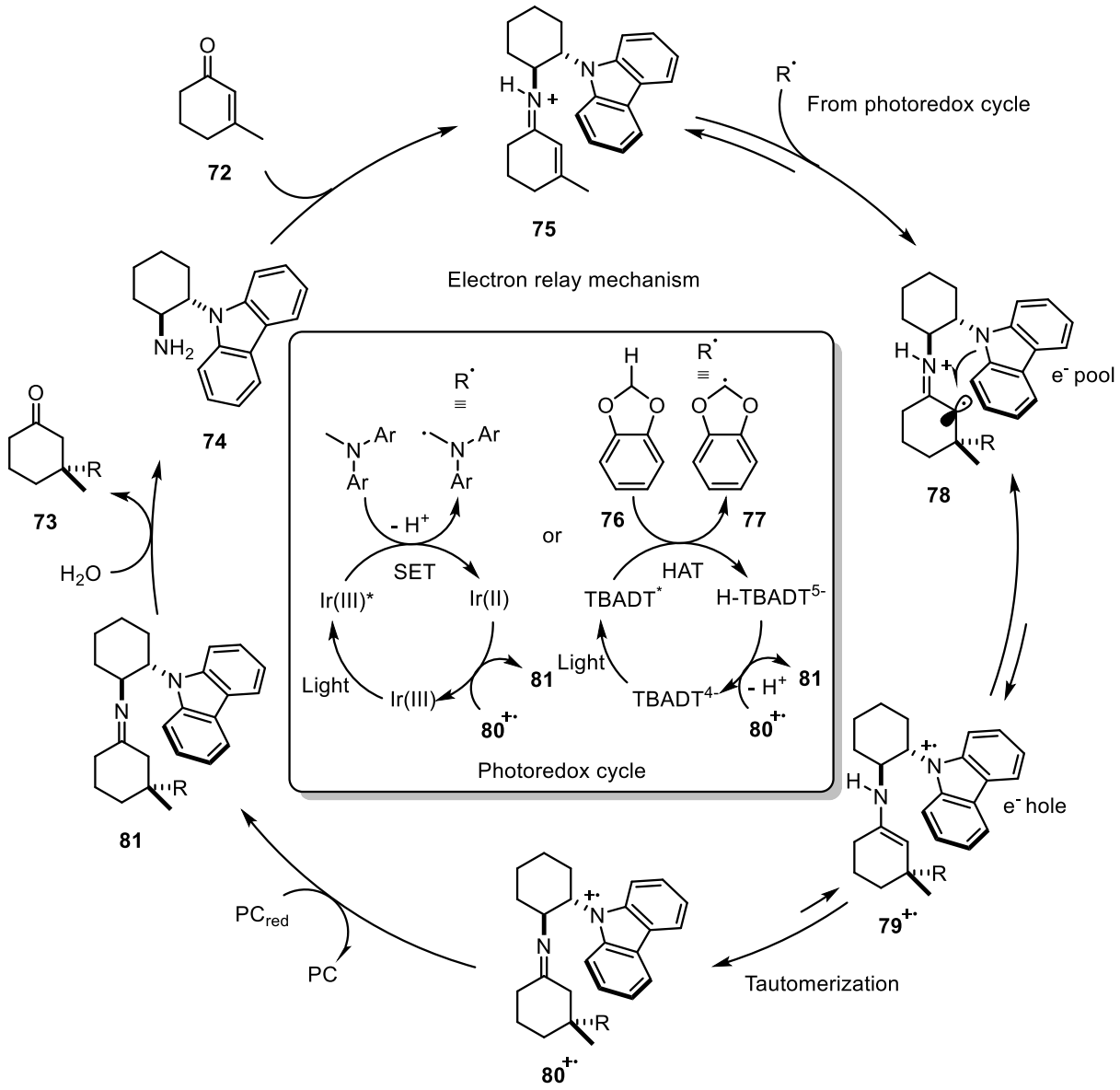

Scheme 20: Dual catalysis for asymmetric functionalization of Michael acceptors.[67]

As demonstrated, photoredox catalysis enables the activation of substrates to highly reactive intermediates that are otherwise challenging to generate. The combination of a photoredox catalyst with a chiral organic catalyst can result in an asymmetric process as demonstrated by the group of Melchiorre.[67] Substituted α,β-unsaturated cyclohexenones, such as **72**, were converted to formal Michael addition products **73** under dual catalysis by tetrabutylammonium decatungstate (TBADT) and an iminium ion precursor (Scheme 20). The formed quaternary carbon is usually accessible by the addition of organometallic reagents which require cryogenic conditions and a pre-formation of the respective organometallic reagent. The authors envisioned the formation of a chiral acceptor by iminium ion catalysis that would accept a radical with the preference of one site. However, the formed radical

cation is presumed to undergo quick β-scission, thus reversing the reaction and rendering radical addition unproductive.[67]

The development of an electron-relay catalyst **74** derived from carbazole proved successful in the desired transformation.[67] The first step of the mechanism is the acid-mediated formation of iminium **75**. TBADT is a potent HAT reagent and transforms benzodioxole **76** into a neutral carbon-centered radical **77**. This radical adds to the iminium ion in β-position **75** to form a radical in α-position in the process. This is the stereodetermining step and site selection occurs by the carbazole moiety blocking the *Si* face from addition as confirmed by crystallization and NMR studies. The electron-rich carbazole quickly performs a SET to reduce the proximate α-iminyl radical **78**. The resulting enamine **79** quickly tautomerizes to imine **80**, hence suppressing back electron transfer. The deprotonated photocatalyst $TBADT^{4-}$ now reduces the carbazole, thereby closing the photoredox cycle, and after amine dissociation of intermediate **81**, enantioenriched product **73** is formed. The decisive step of fast intramolecular reduction of the α-iminyl radical was further investigated by analyzing the reaction of a substrate that bears a homoallyl substituent in β-position. Hypothetic 5-*exo*-trig cyclization was not detected, confirming very fast SET from the carbazole moiety. To expand the scope of the reaction, tertiary amines have been converted to α-amino radicals by SET using an iridium catalyst. The radicals were successfully employed in the catalytic protocol.[67]

3.2.2. Organic photoredox catalysts

Metal complex photoredox catalysis suffers from the use of precious materials and numerous metal-free alternatives have been developed.[68] However, degradation occurs significantly faster and hence catalyst loadings with organic photoredox catalysts are higher. Their structural diversity enables fine-tuning to achieve novel reactivity and some compounds such as enzyme cofactors can be easily accessed from biogenic sources, thereby providing an interesting alternative regarding the scalability of photoredox processes.[68]

Acridinium salts are mostly applied as photooxidants, but by appropriate substitution can act as potent reductants under photoirradiation as demonstrated by the group of Nicewicz.[37] With an excited state redox potential of E_{red} ($Acr^{\cdot+}$/Acr*) = −3.36 V vs SCE, the novel acridinium photoreductant **82** is similar to elemental lithium in reducing power. During their studies of mesityl acridinium tetrafluoroborate which is a potent photooxidant, the authors discovered

the generation of an indefinitely stable mesityl acridine radical **83** (Mes-Acr·) upon one-electron reduction of the cationic chromophore (Scheme 21).[37]

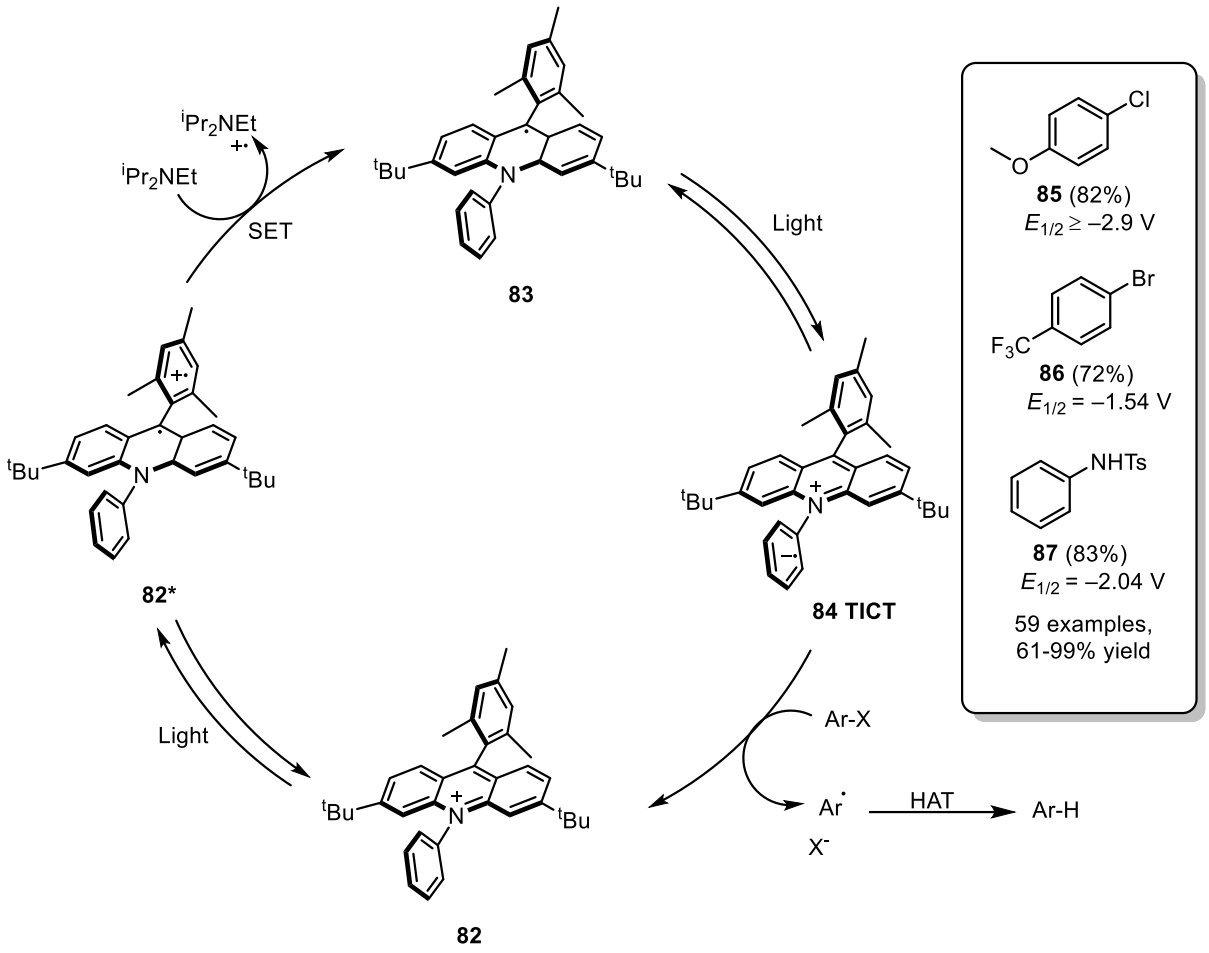

Scheme 21: Mechanism of mesityl acridine (Mes-Acr·) mediated photoreduction for challenging defunctionalization of electron-rich substrates.[37] Redox potentials vs SCE.

Two main excited states of this radical have been identified: a lower-energy doublet state D_1 and a higher-energy twisted intramolecular charge-transfer state **84** (TICT) with the latter causing the estimated redox potential of −3.36 V.[37] The energies have been determined by averaging one of the two emission maxima with the respective absorption signal identified from excitation spectra. Quantum mechanical calculations suggest a SOMO localized on the acridine core and a LUMO+1 localized on the *N*-phenyl ring of Mes-Acr· with a small spatial overlap suggesting a possible intramolecular charge-transfer state. Transient absorption spectra of the acridine radical **84** show bleaching of the ground state absorption (λ_{max} = 520 nm) after early pump-probe delays with concomitant broad increase of absorption features centered at 550 nm and 650 nm. The features suggest the presence of an aromatic

radical anion (broad absorption from 600 – 800 nm), an excited acridine radical (550 nm), and a cationic acridinium core. Further computational experiments support the calculated excited state energies and proposed molecular structures. The lower energy D_1 state matches an untwisted acridine radical excitonic structure and significant twisting (36 °) of the *N*-phenyl ring in the higher energy twisted state is observed. A mechanistic experiment with brominated *N*-phenyl acridine radical further supports the hypothesis of radical anion formation due to efficient fragmentation to an aryl radical and a bromide anion.[37]

To demonstrate the redox potential of the acridine radical **84**, a range of aryl bromides and aryl chlorides were subjected to the reaction with diisopropylethylamine as the terminal reductant in acetonitrile under irradiation at 390 nm (Scheme 21).[37] Dehalohydrogenation was successful even with challenging substrates such as *p*-chloroanisole **85** (E_{red} (**85**$^{\bullet+}$/**85**) ≥ −2.9 V vs SCE). Electron-deficient substituents sometimes negatively affected yields, possibly due to decomposition and trifluoromethyl substituted substrates, such as **86**, showed partial defluorohydrogenation. Appended aliphatic ketones and carboxylic acids, however, were well tolerated. Birch-type over-reduction was not observed, and no aliphatic substrates were tested. Reductive detosylation of amines that is typically performed with strong metal reductants was also successfully achieved with the described protocol as demonstrated in the detosylation of compound **87**. Interestingly, halogenated compounds were tolerated without dehalohydrogenation in good yields. The authors ascribe this to the lower concentration of the performed detosylation reactions. Notably, selective deprotection of tosyl amines over mesyl-protected amines can be achieved and the reaction can be conducted on a gram-scale with medicinally relevant heterocycles. The reaction mechanism proceeds by excitation of the cationic acridinium **82** which is reduced by diisopropylethylamine to the acridine radical **83**. Another photon is absorbed to furnish the twisted intramolecular charge-transfer state **84** which performs SET to furnish acridinium **82** and a substrate radical which is saturated by HAT.[37]

3.2.3. Flavins in photoredox catalysis

Owing to its function as a cofactor in flavoenzymes, riboflavin is readily available and can be used outside of the enzymatic environment as a photocatalyst in various oxidations such as the oxidation of carboxylic acids.[69] Traditional preparation of aliphatic nitriles relies on nucleophilic substitution of primary halides or treatment of carboxylic acids with strong bases

and subsequent decarboxylation to generate carbanions. Irradiation with riboflavin tetraacetate provides an alternative method without bases or metals from readily available carboxylic acids, such as **88**, and tosyl cyanide (Scheme 22A).[69]

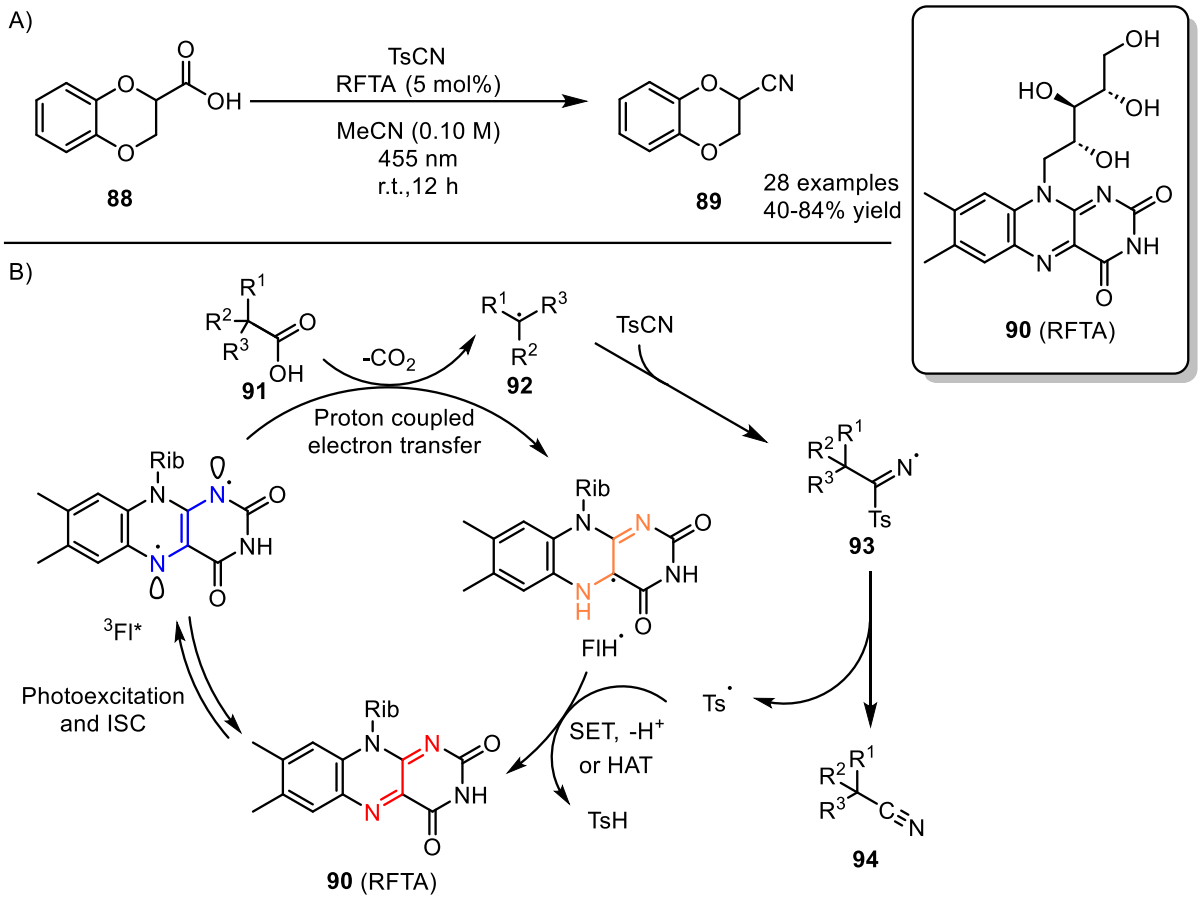

Scheme 22: A) Flavin catalyzed cyanation by oxidation of carboxylic acids.[69] B) Mechanistic proposal.

A range of primary, secondary, and tertiary carboxylic acids were successfully decarboxylated and functionalized to nitriles, such as **89**.[69] While better yields were achieved with α-heteroatom substituted derivatives due to better radical stabilization, some less stabilized examples also reacted to the corresponding nitriles. The mechanism commences with excitation of flavin **90** that quickly undergoes intersystem crossing to its excited triplet state $^3Fl^*$ which is highly oxidizing (Scheme 22B). Proton-coupled electron transfer to carboxylic acid **91** furnishes semiquinoid flavin $FlH^\cdot$ and a carbon-centered radical **92** which could be intercepted by persistent radicals in mechanistical investigations. Addition to tosyl cyanide and subsequent radical cleavage of intermediate **93** liberates nitrile **94** and a tosyl radical $Ts^\cdot$. Reaction of $Ts^\cdot$ with semiquinoid flavin by either SET and consecutive proton transfer or HAT

closes the catalytic cycle. Owing to the high molar absorption coefficient of oxidized flavins, 90 % of the light is absorbed within 0.2 mm of the solution of this particular setup. To increase the scalability of the reaction, the authors successfully demonstrated the application of their method in a flow reactor by preparation of a pharmacological precursor on a 2 mmol scale.[69]

Photoredox catalysis is not limited to chemical systems and can also be performed with enzymatic catalysts as demonstrated by the group of Hyster.[70] Flavin-dependent 'ene' reductases do not require light for their physiological function, but several examples have been shown to be competent in the enantioselective reduction of α,β-unsaturated amides.[70]

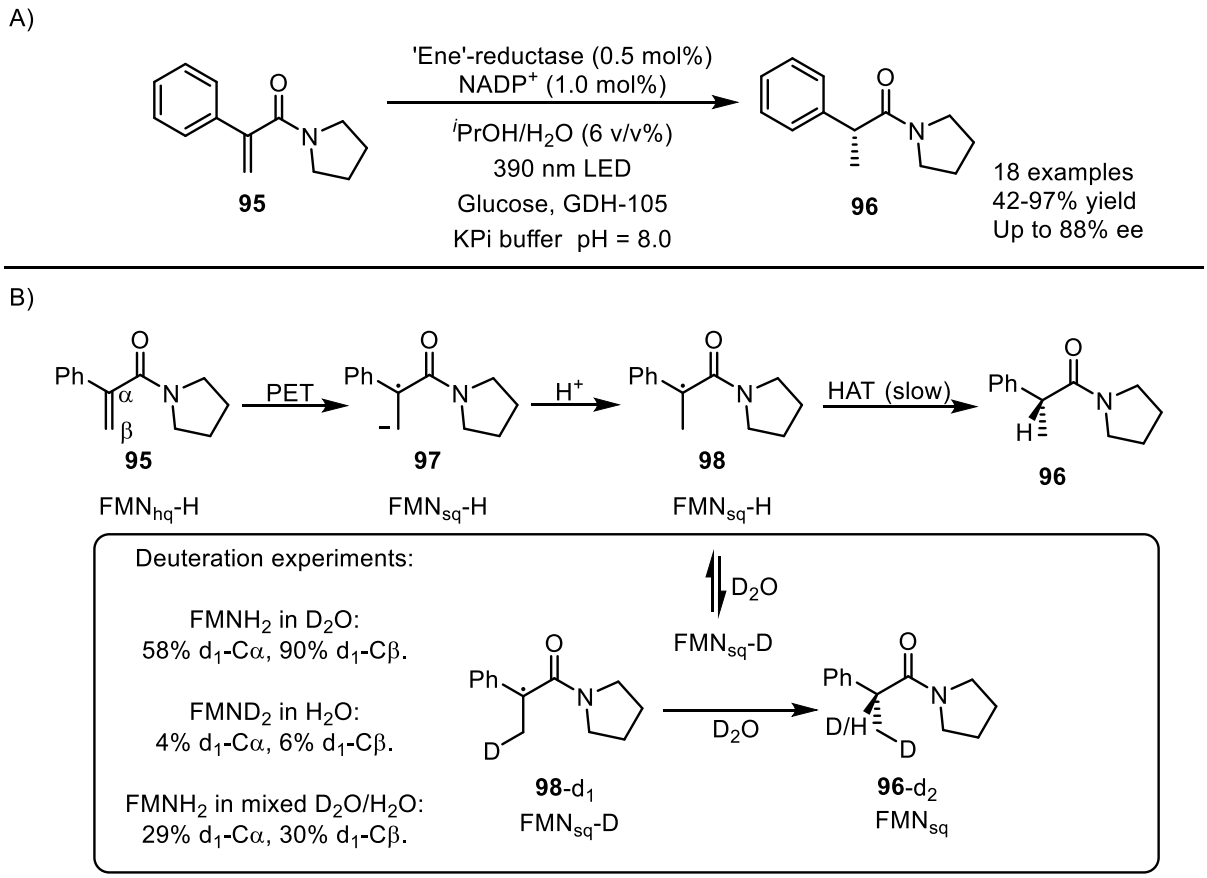

Scheme 23: A) Reduced flavin as photocatalytic SET reagent in “ene”-reductases.[70] B) Mechanistic proposal and deuteration experiments.

The reaction system typically includes a photocatalytic enzyme in a basic aqueous buffer with catalytic $NADP^+$ as a cofactor.[70] Glucose dehydrogenase ensures terminal oxidation of glucose by reducing $NADP^+$ which in turn transfers electrons to the flavin cofactor. After initial screening of different reductases, OYE1 has been identified as the most promising and selective mutation revealed an enzyme with a phenylalanine changed to a glycine (OYE1-F269G) optimized for the transformation. A range of moderately electrophilic amides, such as

95, were reduced to α-methyl amides, such as **96**, in excellent yields and enantiomeric excesses (Scheme 23A). It is also demonstrated that defluorohydrogenation and radical interception by intramolecular 5-*exo*-trig cyclization can be carried out in an enantioselective fashion (albeit with lower selectivity).[70]

After ruling out the possibility of a charge-transfer complex between enzyme-bound flavin and the substrate, transient absorption spectroscopy was performed to elucidate the reaction mechanism with the result that hydroquinoid flavin is capable of a SET to the substrate , such as **95** after excitation.[70] Concomitant with hydroquinoid flavin decay, a spectrum corresponding to semiquinoid flavin $FlH^{\cdot}$ appears. Further decay to a combination of neutral and anionic semiquinoid flavin takes place. This combination is relatively long-lived ($\tau > 80$ ns). The formed radical anion **97** is quickly protonated to a prochiral neutral radical **98** (Scheme 23B). Radical termination occurs by stereodetermining HAT from semiquinoid flavin. Deuterium experiments suggest that this step is slow. In a D_2O buffer with $FMNH_2$, full deuterium incorporation at the β-position occurs while the α-position showed only partial deuterium incorporation. With $FMND_2$ in H_2O, almost no deuterium was incorporated in the α-position and in a mixed H_2O/D_2O buffer partial incorporation at both positions was observed. These results indicate slow HAT, presumably from long-lived semiquinoid flavin N^5-position with slow exchange of the isotopic label.[70]

4. Aim and Motivation

The DNA photolyase was presented as a unique example of the usage of a reduced flavin as a photoexcitable SET reagent in the splitting of thymine dimers. The photochemistry of this reaction and overall reaction conditions in the enzymatic scaffold were described to identify a possible strategy to utilize reduced flavins in a synthetic environment. The application of reductants in several reactions has been outlined to point out interesting transformations that could be targeted with reduced flavins. The use of molecular flavins in photocatalysis is known for oxidative transformations and the strong reductive potential observed in the DNA photolyase enables a range of possible reductions that could be carried out with flavins. The objective of this work is to establish a catalytic system that enables the use of molecular flavins as reductants under photoirradiative conditions. This includes rational catalyst design to circumvent the problems associated with reduced flavins. The catalytic system is aimed to be able to reduce challenging substrates in transformations that would otherwise require a strong rare earth metal reductant. After establishing such a catalytic system, differences in reactivity should be identified to expand the scope of the novel reduced flavin method over the conventional method.

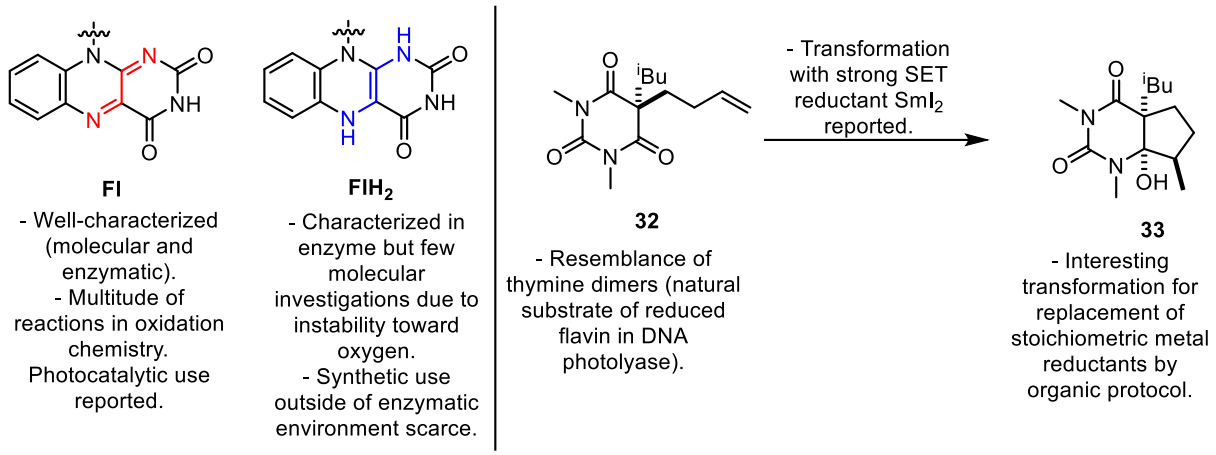

Scheme 24: Motivation and target for molecular reduced flavin photoredox catalysis.

Prior to this report, exploitation of reduced molecular flavins in synthetic transformations of organic substrates was scarce. This is surprising because the DNA photolyase poses an example of reduced flavin being utilized as an SET reagent and synthetic use in 'ene' reductases has been reported. The probable reason for the lack of research regarding molecular reduced flavins in synthesis is their instability toward molecular oxygen which impedes reliable application and thus the development of a catalytic protocol.

5. Information on Original Publications

5.1. Reduced Molecular Flavins as Single-Electron Reductants after Photoexcitation

Bibliographic information:

Foja, R.; Walter, A.; Jandl, C.; Thyrhaug, E.; Hauer, J.; Storch, G., *J. Am. Chem. Soc.* **2022**, *144*, 11, 4721 – 4726. Published on 08.03.2022 (see on page 37).[71]

Summary:

A novel air-stable reduced flavin is synthesized by a steric bias approach and was characterized by UV/Vis and fluorescence spectroscopy. Crystallization and characterization by XRD was also realized. This air-stable reduced flavin and other oxidized flavins are employed as SET catalysts under irradiation with γ-terpinene as the sacrificial reductant. Barbituric acid derivatives are reduced and the formed ketyl radical can undergo subsequent cyclization reaction to form 5-membered bicyclic compounds in good to excellent yields and excellent diastereoselectivities. Substituted alkenes, an allene, an alkyne and a precursor to a 6-membered bicyclic compound are tolerated. Haloalkanes and α,β-unsaturated amides are also successfully reduced. Measurement of the excited state lifetimes and the reaction quantum yield were performed to rationalize the relatively long irradiation times (20 h).

Author contributions:

All synthetic and catalytic experiments were planned and analyzed by R. Foja. Catalyst design was provided by R. Foja and G. Storch. The catalytic experiments were planned, performed and analyzed by R. Foja. A. Walter performed and analyzed the cyclic voltammetry measurements. Crystallographic data were gathered and analyzed by C. Jandl. Spectroscopic measurements were performed and analyzed by E. Thyrhaug, J. Hauer and R. Foja. R. Foja wrote the supplementary information file which contains all experimental data. The manuscript was written by R. Foja, A. Walter and G. Storch.

5.2. Chemoselective Reduction of Barbiturates by Photochemically Excited Flavin Catalysts

Bibliographic information:

Foja, R.; Walter, A.; Storch, G., *Synlett* **2023**, *35*, 09, 952 – 956. Published on 08.12.2023 (see on page 43).[72]

Summary:

Barbituric acid derivatives with ketones in the side-chains were investigated regarding their chemoselectivity upon reduction with either reduced flavins or samarium (II) iodide. A competition between pinacol formation and alicycle formation was chosen as method of determining the initial site of reduction. It was found, that flavin selectively forms the alicycle, while SmI_2 always forms the pinacol. By variation of the side-chain length, it was determined that the appended ketone is reduced rather than the barbituric acid carbonyl, which rationalizes the pinacol formation. Reduced flavins selectively reduced the barbituric acid carbonyl due to the more positive redox potential of this carbonyl. *N*-methyl oxime derivatives were prepared and cyclized with reduced flavin, which could not be realized with SmI_2.

Author contributions:

All synthetic and catalytic experiments were planned and analyzed by R. Foja. Catalyst design was provided by R. Foja and G. Storch. The catalytic experiments were planned, performed and analyzed by R. Foja. A. Walter performed and analyzed the cyclic voltammetry measurements. R. Foja wrote the supplementary information file which contains all experimental data. The manuscript was written by R. Foja, A. Walter and G. Storch.

JACS
JOURNAL OF THE AMERICAN CHEMICAL SOCIETY
pubs.acs.org/JACS
Communication

Reduced Molecular Flavins as Single-Electron Reductants after Photoexcitation

Richard Foja, Alexandra Walter, Christian Jandl, Erling Thyrhaug, Jürgen Hauer, and Golo Storch*

Cite This: J. Am. Chem. Soc. 2022, 144, 4721−4726
Read Online
ACCESS | Metrics & More | Article Recommendations | Supporting Information

ABSTRACT: Flavoenzymes mediate a multitude of chemical reactions and are catalytically active both in different oxidation states and in covalent adducts with reagents. The transfer of such reactivity to the organic laboratory using simplified molecular flavins is highly desirable, and such applications in (photo)oxidation reactions are already established. However, molecular flavins have not been used for the reduction of organic substrates yet, although this activity is known and well-studied for DNA photolyase enzymes. We report a catalytic method using reduced molecular flavins as photoreductants and γ-terpinene as a sacrificial reductant. Additionally, we present our design for air-stable, reduced flavin catalysts, which is based on a conformational bias strategy and circumvents the otherwise rapid reduction of O_2 from air. Using our catalytic strategy, we were able to replace superstoichiometric amounts of the rare-earth reductant SmI_2 in a 5-*exo*-trig cyclization of substituted barbituric acid derivatives. Such flavin-catalyzed reductions are anticipated to be beneficial for other transformations as well and their straightforward synthesis indicates future use in stereo- as well as site-selective transformations.

Flavins are versatile cofactors in enzymes and are involved in a variety of chemical transformations either as flavin adenine dinucleotide (FAD) or flavin mononucleotide (FMN).[1] This diversity stems from the occurrence of different catalytically active cofactor states and depends on oxidation or reduction (FAD vs $FADH_2$) as well as photochemical excitation. Among the known reactions of flavoenzymes, the cleavage of thymine dimers **1** by DNA photolyase is a particularly interesting and relevant reaction, which is mediated by excited hydroquinoid $FADH^{-}$* (**2**$^{-}$*). Thymine dimers (T⟨⟩T) **1** are the result of a UV-light-mediated [2 + 2]-cycloaddition reaction between adjacent thymines in DNA, and their formation hampers correct transcription or replication. The enzymatic strategy to revert such DNA damage relies on the excitation of reduced cofactor **2**$^{-}$ and subsequent one-electron reduction of (T⟨⟩T) **1** (Figure 1).[2] Ketyl radical intermediate **1**$^{\bullet-}$ undergoes rapid cyclobutane ring-opening and back electron transfer to semiquinone **2**$^{\bullet}$, which leads to the release of both thymines and closes the catalytic cycle. The very negative redox potential $E(\mathbf{1}/\mathbf{1}^{\bullet-})$ = −2.2 V vs SCE (in CH_3CN) of thymine dimer **1** highlights the strong reducing capacity of excited cofactor **2**$^{-}$*.[3] Despite the great potential for synthetic transformations, such one-electron reductions have not yet been applied using molecular flavin catalysts in the organic laboratory, although the photosensitized[4] and oxidative[5] cleavage of thymine dimers with molecular flavins has been studied. The general usefulness of reduced flavin catalysts is highlighted by recent reductive catalytic reactions with flavoenzymes[6] and a deazaflavin.[7] We found it remarkable that in organic synthesis molecular flavins are extensively applied for oxidations,[8] for example, using commercially available (−)-riboflavin,[9] but they are not applied for reductions. Therefore, we aimed for finding a strategy to use molecular flavins in the reductive 5-*exo*-trig cyclization of barbituric acid derivatives, which had previously only been reported with superstoichiometric metal reductants (Figure 1B).[10,11]

We hypothesized that the instability of reduced flavins such as **2** toward oxygen from air is one reason for the above-described discrepancy since it renders studies of the reduced cofactor very impractical. The instability itself is the result of a rapid reduction of O_2 to $O_2^{\bullet-}$ and subsequent formation of covalently bound flavin hydroperoxides.[12] The initial reduction of molecular oxygen [$E(O_2/O_2^{\bullet-})$ = −0.55 V vs SCE] by a reduced *N*5-ethyl-flavin [$E(Fl^{\bullet+}/Fl_{red})$ = −0.05 V vs SCE] (both values in aqueous buffer at pH 4.6) is disfavored, but the net reaction becomes exergonic upon formation of the thermodynamically favored oxidized flavin and hydrogen peroxide.[13] We decided to base our strategy for air-stable, reduced flavin catalysts on a conformational bias for the reduced form,[14] which is typically bent along the N5−N10 axis with a ring puckering angle of 27.3°.[15] Both the oxidized as well as the semiquinone states are (almost) planar.[16] The conformational bias was achieved by double substitution of the N5- and C6-positions via reductive alkylation of flavin **3** and reduced catalyst **4** was obtained as an air-stable solid (Figure 2A). However, unsubstituted analog **5** did not yield the reduced flavin and was instead oxidized by air. Both oxidized flavins have similar redox properties: $E_{1/2}$ = −0.78 V vs SCE (**3**) and $E_{1/2}$ = −0.85 V vs SCE (**5**). The bent structure

Received: December 17, 2021
Published: March 8, 2022

https://doi.org/10.1021/jacs.1c13285
J. Am. Chem. Soc. 2022, 144, 4721−4726

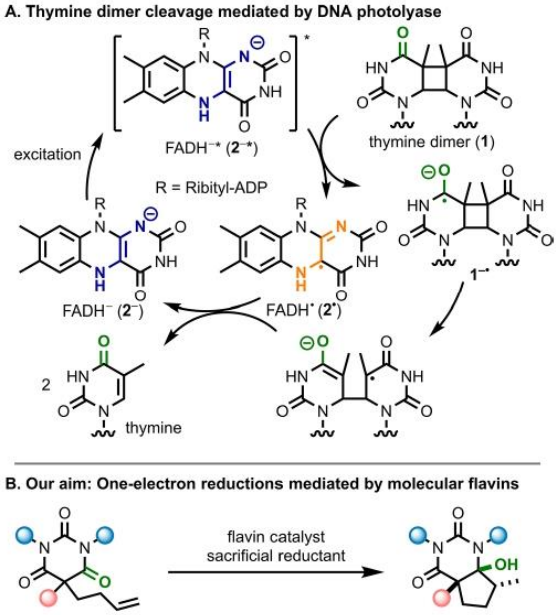

Figure 1. Mechanism of enzymatic thymine dimer **1** cleavage mediated by DNA photolyase (A). In the key step, an electron is transferred from excited cofactor $\mathbf{2}^{-*}$ to dimerized thymine **1**. Our envisioned transformation using molecular, reduced flavin catalysts relies on similar one-electron transfer (B). Carbonyl groups involved in reduction are highlighted in green.

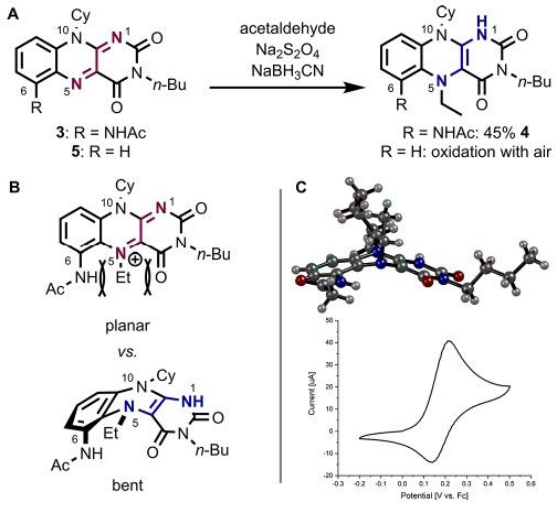

Figure 2. Synthesis and characterization of an air-stable reduced flavin. Conformational bias is realized by reductive alkylation (A), which results in steric destabilization of the planar states (B). The bent structure of flavin **4** is visible in the X-ray structure (C), and cyclic voltammetry in CH_3CN shows partially reversible electron transfer.

of flavin **4** (Figure 2B) was further characterized by single-crystal X-ray diffraction, and a ring puckering angle of 32.1° was found along the N5–N10 axis (Figure 2C). Cyclic voltammetry confirmed that oxidation [$E_{1/2}$ = +0.46 V vs SCE ($\mathbf{4}$) in CH_3CN] of reduced flavin **4** is at least partially reversible (Figure 2C). When the measurement was continued to more positive potentials, irreversible processes were detected, an observation which is in line with our strategy of destabilizing the planar oxidized states.

We then turned our attention to the photophysical properties of air-stable flavin **4** and its oxidized counterpart **3** (Figure 3). The first major difference is the blueshift of the

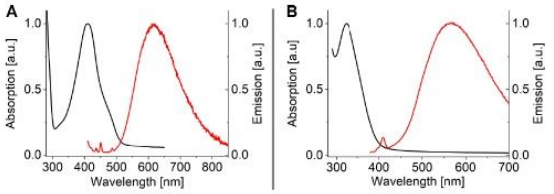

Figure 3. Normalized absorption (in black) and emission (in red) spectra of flavin **3** (A) and reduced flavin **4** (B) in CH_3CN solution. Quinoid flavin **3**: $\lambda_{A,max}$ = 411 nm; $\lambda_{E,max}$ = 620 nm. Hydroquinoid flavin **4**: $\lambda_{A,max}$ = 324 nm; $\lambda_{E,max}$ = 567 nm.

absorption maximum, which is at $\lambda_{A,max}$ = 324 nm for the reduced catalyst. The same trend is observed for the emission with fluorescence occurring at $\lambda_{E,max}$ = 567 nm. In analogy to the natural cofactor ($FADH_2$ vs $FADH^-$), the emission of **4** is shifted to $\lambda_{E,max}$ = 533 nm upon addition of triethylamine base.[2c] We observed two long lifetime components of flavin **4** in the excited state (see the Supporting Information): τ = 1.1 ns (78%) and τ = 11.7 ns (22%).

With this information in hand, we started our catalysis studies and chose barbituric acid derivative **6** as a promising substrate for one-electron reduction due to its structural and electronic similarity to thymine dimer **1**. The 5-*exo*-trig cyclization of substrate **6** had previously been reported using 6 equiv of rare-earth reductant SmI_2,[10] thus making this reaction an ideal target for a mild catalytic protocol. Optimization of the catalytic conditions (see the Supporting Information for details) quickly revealed that **4** is indeed a suitable electron donor in the excited state. Several sacrificial reductants turned out to be applicable, but we decided to move forward with γ-terpinene, which is an inexpensive and commercially available essential oil.[17] With a catalytic amount of triethylamine and a catalytic amount of cysteine as a hydrogen atom donor,[18] we obtained bicycle **7** in 90% yield (Table 1, entry 1).

Leaving out the amine base resulted in no conversion. This is in analogy to the enzymatic process, which relies on the deprotonated cofactor $FADH^-$ (entry 2).[2f] The γ-terpinene is required as a sacrificial reductant, and only a trace amount of product is formed in its absence due to irreversible catalyst oxidation (entry 3). Cysteine improves the yield significantly but is not essential for catalysis (entry 4). We also verified that catalyst and irradiation are necessary (entries 5 and 6). Increasing amounts of triethylamine led to quantitative conversion (entry 7), and other bases such as quinuclidine are also suitable (see the Supporting Information). Cystine and cysteine perform equally well, which implies that the former is efficiently reduced under the reaction conditions as well (entry 8). Under our optimized conditions, *in situ* reduced quinoid flavin **3** and even (−)-riboflavin tetraacetate **8** also led to product formation (entries 9 and 10), which highlights the applicability of our method. Consistent with the short excited-

https://doi.org/10.1021/jacs.1c13285
J. Am. Chem. Soc. 2022, 144, 4721−4726

Table 1. Flavin-Catalyzed Net-Reductive Cyclization of Substituted Barbituric Acid Derivative 6

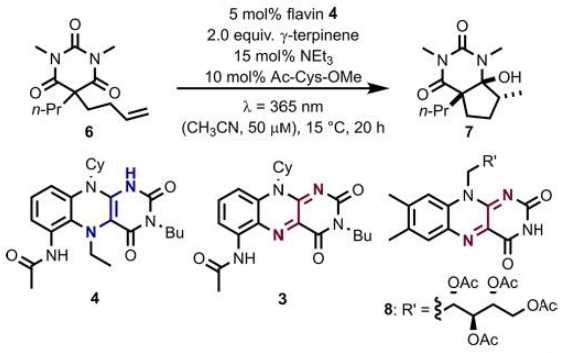

entry	deviation from standard conditions	yield[a]
1	none	90%
2	no NEt_3	nd
3	no γ-terpinene	<5%
4	no Ac-Cys-OMe	39%
5	no flavin catalyst	nd
6	no irradiation	nd
7	with 4.0 equiv of NEt_3	quant.[b]
8[c]	10 mol % $(Ac\text{-}Cys\text{-}OMe)_2$	quant.
9[c]	5 mol % flavin catalyst **3**	46
10[c]	5 mol % flavin catalyst **8**	88

[a]Measured by NMR spectroscopy with internal standard. nd: Not detected. [b]Isolated yield on 0.1 mmol substrate scale. [c]With 4.0 equiv of NEt_3.

state lifetime outside an enzyme environment,[2c,19] increasing the substrate concentration to 0.4 M led to accelerated product formation (see Table SI-1, entry 7).

According to our mechanistic proposal, the catalytic reaction is initiated by a one-electron reduction of barbiturate **6**, very similar to the first step in DNA photolyase (Figure 4). Our flavin catalysis proceeds relatively slowly with a quantum yield of $\Phi = 1.8 \times 10^{-3}$ (see the Supporting Information), and in line with this observation, no significant fluorescence quenching of $\mathbf{4}^{-}$* occurs upon addition of substrate **6** presumably due to inefficient electron transfer. Additionally, the low quantum yield points against a radical chain process. The intermediate ketyl radical next undergoes rapid 5-*exo*-trig cyclization to anion $\mathbf{7}^{\bullet-}$ which is further reduced and protonated to yield bicyclic product **7**. Hydrogen atom transfer from γ-terpinene (BDE of 1,4-cyclohexadiene is 77 kcal mol^{-1})[20] resulting in *para*-cymene (observed by NMR) via **9** seems plausible for reduction of both intermediate $\mathbf{7}^{\bullet-}$ and semiquinone $\mathbf{4}^{\bullet}$. The latter species is also a strong photoreductant and can be excited by visible light (neutral semiquinones: $\lambda_{max} \approx 330$, 490, and 600 nm; anionic semiquinones: $\lambda_{max} \approx 370$ and 490 nm).[7,21] This opens up the possibility for two catalytic cycles (A and B) in which either the hydroquinoid or the semiquinoid catalyst acts as the substrate reductant. Interestingly, the catalytic reaction also proceeds at irradiation with $\lambda = 451$ nm when using RFTA (**8**), while no conversion was observed under these conditions with flavin **4** (see the Supporting Information). When conducting the reaction with flavin **4** in an NMR tube under inert conditions, measurements after several time intervals only show the hydroquinoid catalyst and no quinoid species (see

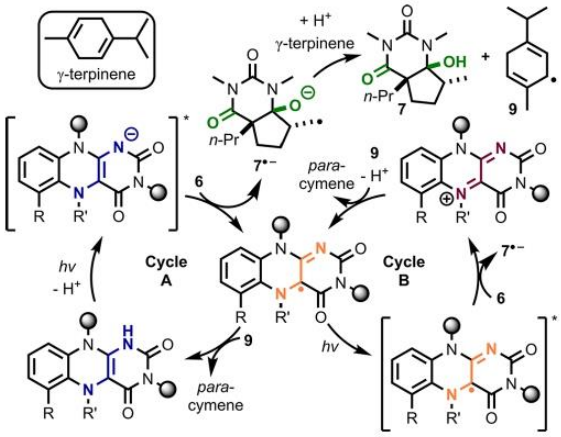

Figure 4. Simplified mechanistic proposal for the flavin-catalyzed reduction of barbituric acid derivative **6**. The carbonyl groups, one of which is initially reduced, are highlighted in green. For flavin **4**: R = NHAc and R′ = Et. For RFTA (methyl groups in the C7 and C8 positions not shown): R, R′ = H. Reduction of substrate **6** in cycle B with RFTA is also possible via a HAT from the semiquinone or electron transfer from the deprotonated form of the latter species (resulting in the neutral quinoid flavin with a lone pair instead of R′ = H).

the Supporting Information). We conclude that both cycles A and B are plausible with RFTA, while a substituent in the catalyst's N5-position seems to hamper cycle B. The cysteine cocatalyst was not included in this mechanistic discussion since it is not necessary for product formation but its function as a hydrogen atom donor leads to increased yields.

Gratifyingly, flavin catalysis also allows efficient reductive conversion of a series of barbituric acid derivatives (Figure 5).

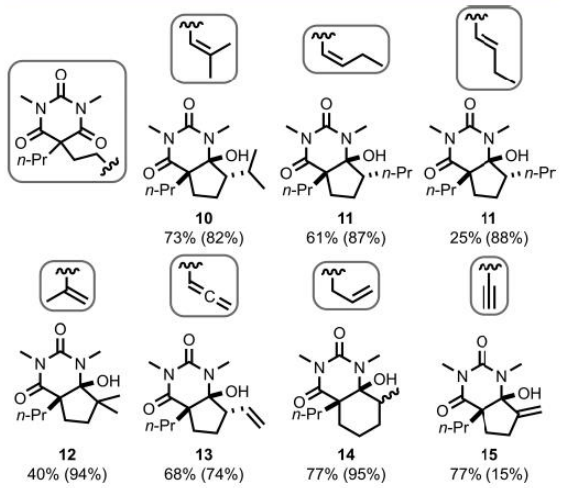

Figure 5. Application of the flavin catalysis to a variety of barbituric acid derivatives. Reaction conditions: 5 mol % **4** (10 mol % for product **11**), 2.0 equiv of γ-terpinene, 1.0 equiv of NEt_3, $\lambda = 365$ nm, (CH_3CN), 15 h. Results for the catalytic reactions with RFTA (**8**) are given in parentheses. Yields were determined by NMR spectroscopy with internal standard. Compound **14** was obtained as a mixture of diastereomers with d.r. ≈ 2:1.

https://doi.org/10.1021/jacs.1c13285
J. Am. Chem. Soc. 2022, 144, 4721−4726

The 5-*exo*-trig cyclization is initiated with different substituted alkene side chains (**10**-**12**) and di- as well as trisubstitution is tolerated. With allene substrates, terminal alkene product **13** is formed. An analogous cyclization forming six-membered rings is also possible, but bicycle **14** was obtained as a mixture of diastereomers. With terminal alkynes, 5-*exo*-dig cyclization results in exocyclic alkene **15**.

We next probed for potential differences between flavin-mediated reductions and conventional reactions using SmI_2. In this context, barbituric acid derivative **16** was chosen, which was reported to result in pinacol coupling product **17** upon reduction with SmI_2 (Figure 6).[22] Here, three carbonyl sites

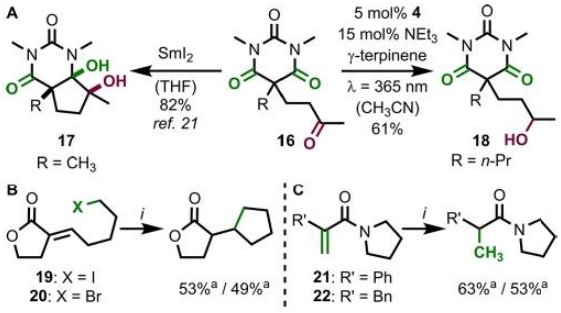

Figure 6. Application of flavin catalysis to other substrates. Reduction of ketone **16** shows distinct differences between SmI_2-mediated and flavin-catalyzed reactions (A). Flavin catalysis also mediates the reductive cyclization of alkyl halides (B) and the reduction of unsaturated amides (C). Reaction conditions (i): 10 mol % **4**, 2.0 equiv of γ-terpinene, 4.0 equiv of NEt_3, λ = 365 nm (CH_3CN), 20 h. [a]Measured by NMR spectroscopy with an internal standard.

compete for the one-electron reduction, and the formation of the pinacol product was rationalized based on a favored (E = −2.2 V vs SCE) initial reduction of a barbituric acid carbonyl group compared to the ketone (E < −2.5 V vs SCE).[22] In contrast, when applying flavin catalyst **4**, no pinacol product was obtained, and secondary alcohol **18** was formed instead. This reactivity difference could be explained by substrate chelation when using SmI_2, which allows flavin **4** to leave the carbonyl groups in the heterocycle fully intact. Additionally, we probed for flavin-catalyzed reductions of entirely different substrate classes, which were previously described using flavoenzymes.[6a,c] Fortunately, we observed product formation in a reductive cyclization reaction of alkyl iodide **19**, even when using alkyl bromide analog **20** (Figure 6B). Reduced flavin **4** was also competent in the reduction of unsaturated amides **21** and **22** (Figure 6C), where it complements flavoenzyme activity.

In summary, we report reduced molecular flavins as catalysts in organic transformations. While so far such reduced flavins have been exclusively used as O_2-reductants, our combination of the essential oil reductant γ-terpinene, photochemical excitation, and mild basic conditions allow the conversion of other, useful organic substrates. Inspired by DNA photolyase, we focused on barbituric acid derivatives in this study but envision broad applicability to other substrate classes based on the strong reducing power of excited flavins. Additionally, we observed differences between traditional metal reductants and flavin catalysts, which stimulate our continuing search for other challenging transformations as well as chiral catalyst versions for stereoselective reductions.

■ ASSOCIATED CONTENT

Supporting Information

The Supporting Information is available free of charge at https://pubs.acs.org/doi/10.1021/jacs.1c13285.

Experimental procedures and analytical data for all new compounds and additional experiments (PDF)
NMR data (ZIP)

Accession Codes

CCDC 2126062 contains the supplementary crystallographic data for this paper. These data can be obtained free of charge via www.ccdc.cam.ac.uk/data_request/cif, or by emailing data_request@ccdc.cam.ac.uk, or by contacting The Cambridge Crystallographic Data Centre, 12 Union Road, Cambridge CB2 1EZ, UK; fax: +44 1223 336033.

■ AUTHOR INFORMATION

Corresponding Author

Golo Storch − *Department of Chemistry, Technical University of Munich, 85747 Garching, Germany;* orcid.org/0000-0002-6747-3035; Email: golo.storch@tum.de

Authors

Richard Foja − *Department of Chemistry, Technical University of Munich, 85747 Garching, Germany*
Alexandra Walter − *Department of Chemistry, Technical University of Munich, 85747 Garching, Germany*
Christian Jandl − *Department of Chemistry, Technical University of Munich, 85747 Garching, Germany*
Erling Thyrhaug − *Department of Chemistry, Technical University of Munich, 85747 Garching, Germany*
Jürgen Hauer − *Department of Chemistry, Technical University of Munich, 85747 Garching, Germany;* orcid.org/0000-0002-6874-6138

Complete contact information is available at: https://pubs.acs.org/10.1021/jacs.1c13285

Notes

The authors declare no competing financial interest.

■ ACKNOWLEDGMENTS

The Fonds der Chemischen Industrie (FCI, Ph.D. Fellowship to A.W. and Liebig Fellowship to G.S.) is gratefully acknowledged. R.F. thanks the Studienstiftung des Deutschen Volkes for a Ph.D. fellowship. The project was funded by the Deutsche Forschungsgemeinschaft (DFG, German Research Foundation, TRR 325−444632635). We thank K. Rickmeyer and L. Niederegger (research group of Prof. C. Hess) for their assistance with cyclic voltammetry, D. P. Schwinger and J. Großkopf for spectroscopic measurements, and O. Ackermann for HPLC analyses. G.S. is supported by the Emmy Noether Programme (DFG, STO 1175/3-1) and the Technical University of Munich (Junior Fellow Programme). He is very grateful to Prof. T. Bach for his continuous support.

■ REFERENCES

(1) (a) Mansoorabadi, S. O.; Thibodeaux, C. J.; Liu, H.-w. The Diverse Roles of Flavin Coenzymes − Nature's Most Versatile Thespians. *J. Org. Chem.* **2007**, *72*, 6329−6342. (b) Joosten, V.; van Berkel, W. J. H. Flavoenzymes. *Curr. Opin. Chem. Biol.* **2007**, *11*,

195−202. (c) Walsh, C. T.; Wencewicz, T. A. Flavoenzymes: Versatile catalysts in biosynthetic pathways. *Nat. Prod. Rep.* **2013**, *30*, 175−200.
(2) (a) Sancar, A. Structure and function of DNA photolyase. *Biochemistry* **1994**, *33*, 2−9. (b) Kao, Y.-T.; Saxena, C.; Wang, L.; Sancar, A.; Zhong, D. Direct observation of thymine dimer repair in DNA by photolyase. *Proc. Natl. Acad. Sci. U.S.A.* **2005**, *102*, 16128−16132. (c) Kao, Y.-T.; Saxena, C.; He, T.-F.; Guo, L.; Wang, L.; Sancar, A.; Zhong, D. Ultrafast Dynamics of Flavins in Five Redox States. *J. Am. Chem. Soc.* **2008**, *130*, 13132−13139. (d) Harbach, P. H. P.; Schneider, M.; Faraji, S.; Dreuw, A. Intermolecular Coulombic Decay in Biology: The Initial Electron Detachment from $FADH^-$ in DNA Photolyases. *J. Phys. Chem. Lett.* **2013**, *4*, 943−949. (e) Tan, C.; Liu, Z.; Li, J.; Guo, X.; Wang, L.; Sancar, A.; Zhong, D. The molecular origin of high DNA-repair efficiency by photolyase. *Nat. Commun.* **2015**, *6*, 7302. (f) Zhong, D. Electron Transfer Mechanisms of DNA Repair by Photolyase. *Annu. Rev. Phys. Chem.* **2015**, *66*, 691−715. (g) Sancar, A. Mechanisms of DNA Repair by Photolyase and Excision Nuclease (Nobel Lecture). *Angew. Chem., Int. Ed.* **2016**, *55*, 8502−8527. (h) Zhang, M.; Wang, L.; Shu, S.; Sancar, A.; Zhong, D. Bifurcating electron-transfer pathways in DNA photolyases determine the repair quantum yield. *Science* **2016**, *354*, 209−213.
(3) Scannell, M. P.; Fenick, D. J.; Yeh, S.-R.; Falvey, D. E. Model Studies of DNA Photorepair: Reduction Potentials of Thymine and Cytosine Cyclobutane Dimers Measured by Fluorescence Quenching. *J. Am. Chem. Soc.* **1997**, *119*, 1971−1977.
(4) (a) Rokita, S. E.; Walsh, C. T. Flavin and 5-deazaflavin photosensitized cleavage of thymine dimer: a model of in vivo light-requiring DNA repair. *J. Am. Chem. Soc.* **1984**, *106*, 4589−4595. (b) Pac, C.; Miyake, K.; Masaki, Y.; Yanagida, S.; Ohno, T.; Yoshimura, A. Flavin-photosensitized monomerization of dimethylthymine cyclobutane dimer: remarkable effects of perchloric acid and participation of excited-singlet, triplet, and chain-reaction pathways. *J. Am. Chem. Soc.* **1992**, *114*, 10756−10762. (c) Yasuda, M.; Nishinaka, Y.; Nakazono, T.; Hamasaki, T.; Nakamura, N.; Shiragami, T.; Pac, C.; Shima, K. Photochemistry of Flavins in Micelles: Specific Effects of Anionic Surfactants on the Monomerization of Thymine Cyclobutane Dimers Photosensitized by Tetra-*O*-acyl Riboflavins. *Photochem. Photobiol.* **1998**, *67*, 192−197.
(5) Hartman, T.; Cibulka, R. Photocatalytic Systems with Flavinium Salts: From Photolyase Models to Synthetic Tool for Cyclobutane Ring Opening. *Org. Lett.* **2016**, *18*, 3710−3713.
(6) (a) Clayman, P. D.; Hyster, T. K. Photoenzymatic Generation of Unstabilized Alkyl Radicals: An Asymmetric Reductive Cyclization. *J. Am. Chem. Soc.* **2020**, *142*, 15673−15677. (b) Huang, X.; Wang, B.; Wang, Y.; Jiang, G.; Feng, J.; Zhao, H. Photoenzymatic enantioselective intermolecular radical hydroalkylation. *Nature* **2020**, *584*, 69−74. (c) Sandoval, B. A.; Clayman, P. D.; Oblinsky, D. G.; Oh, S.; Nakano, Y.; Bird, M.; Scholes, G. D.; Hyster, T. K. Photoenzymatic Reductions Enabled by Direct Excitation of Flavin-Dependent "Ene"-Reductases. *J. Am. Chem. Soc.* **2021**, *143*, 1735−1739. (d) Gao, X.; Turek-Herman, J. R.; Choi, Y. J.; Cohen, R. D.; Hyster, T. K. Photoenzymatic Synthesis of α-Tertiary Amines by Engineered Flavin-Dependent "Ene"-Reductases. *J. Am. Chem. Soc.* **2021**, *143*, 19643−19647.
(7) Graml, A.; Neveselý, T.; Jan Kutta, R.; Cibulka, R.; König, B. Deazaflavin reductive photocatalysis involves excited semiquinone radicals. *Nat. Commun.* **2020**, *11*, 3174.
(8) For reviews, see (a) Imada, Y.; Naota, T. Flavins as organocatalysts for environmentally benign molecular transformations. *Chem. Rec.* **2007**, *7*, 354−361. (b) Cibulka, R. Artificial Flavin Systems for Chemoselective and Stereoselective Oxidations. *Eur. J. Org. Chem.* **2015**, *2015*, 915−932. Examples for recent reports on photo-oxidation with flavins: (c) Bloom, S.; Liu, C.; Kölmel, D. K.; Qiao, J. X.; Zhang, Y.; Poss, M. A.; Ewing, W. R.; MacMillan, D. W. C. Decarboxylative alkylation for site-selective bioconjugation of native proteins via oxidation potentials. *Nat. Chem.* **2018**, *10*, 205−210. (d) Tagami, T.; Arakawa, Y.; Minagawa, K.; Imada, Y. Efficient Use of Photons in Photoredox/Enamine Dual Catalysis with a Peptide-Bridged Flavin−Amine Hybrid. *Org. Lett.* **2019**, *21*, 6978−6982. (e) Chilamari, M.; Immel, J. R.; Bloom, S. General Access to C-Centered Radicals: Combining a Bioinspired Photocatalyst with Boronic Acids in Aqueous Media. *ACS Catal.* **2020**, *10*, 12727−12737.
(9) For general reviews on the use of molecular flavins in catalysis, see (a) de Gonzalo, G.; Fraaije, M. W. Recent Developments in Flavin-based Catalysis. *ChemCatChem.* **2013**, *5*, 403−415. (b) Rehpenn, A.; Walter, A.; Storch, G. Molecular Editing of Flavins for Catalysis. *Synthesis* **2021**, *53*, 2583−2593.
(10) Szostak, M.; Sautier, B.; Spain, M.; Behlendorf, M.; Procter, D. J. Selective Reduction of Barbituric Acids Using SmI_2/H_2O: Synthesis, Reactivity, and Structural Analysis of Tetrahedral Adducts. *Angew. Chem., Int. Ed.* **2013**, *52*, 12559−12563.
(11) For related, reductive cyclization reactions of barbituric acid derivatives with SmI_2, see (a) Huang, H.-M.; Procter, D. J. Radical−Radical Cyclization Cascades of Barbiturates Triggered by Electron-Transfer Reduction of Amide-Type Carbonyls. *J. Am. Chem. Soc.* **2016**, *138*, 7770−7775. (b) Huang, H.-M.; Procter, D. J. Dearomatizing Radical Cyclizations and Cyclization Cascades Triggered by Electron-Transfer Reduction of Amide-Type Carbonyls. *J. Am. Chem. Soc.* **2017**, *139*, 1661−1667.
(12) Kemal, C.; Chan, T. W.; Bruice, T. C. Reaction of $^3O_2$ with dihydroflavins. 1. *N*3,5-Dimethyl-1,5-dihydrolumiflavin and 1,5-dihydroisoalloxazines. *J. Am. Chem. Soc.* **1977**, *99*, 7272−7286.
(13) Eberlein, G.; Bruice, T. C. The chemistry of a 1,5-diblocked flavin. 2. Proton and electron transfer steps in the reaction of dihydroflavins with oxygen. *J. Am. Chem. Soc.* **1983**, *105*, 6685−6697.
(14) (a) Hasford, J. J.; Kemnitzer, W.; Rizzo, C. J. Conformational Effects on Flavin Redox Chemistry. *J. Org. Chem.* **1997**, *62*, 5244−5245. (b) Reibenspies, J. H.; Guo, F.; Rizzo, C. J. X-ray Crystal Structures of Conformationally Biased Flavin Models. *Org. Lett.* **2000**, *2*, 903−906.
(15) (a) Tauscher, L.; Ghisla, S.; Hemmerich, P. NMR.-Study of Nitrogen Inversion and Conformation of 1,5-Dihydro-isoalloxazines ('Reduced Flavin'). Studies in the flavin series, XIX. Communication. *Helv. Chim. Acta* **1973**, *56*, 630−644. (b) Zheng, Y.-J.; Ornstein, R. L. A Theoretical Study of the Structures of Flavin in Different Oxidation and Protonation States. *J. Am. Chem. Soc.* **1996**, *118*, 9402−9408. (c) Rodríguez-Otero, J.; Martínez-Núñez, E.; Peña-Gallego, A.; Vázquez, S. A. The Role of Aromaticity in the Planarity of Lumiflavin. *J. Org. Chem.* **2002**, *67*, 6347−6352.
(16) Walsh, J. D.; Miller, A.-F. Flavin reduction potential tuning by substitution and bending. *J. Mol. Struct. Theochem* **2003**, *623*, 185−195.
(17) Selected examples for using γ-terpinene as a sacrificial reductant in photochemical transformations: (a) Schweitzer-Chaput, B.; Horwitz, M. A.; de Pedro Beato, E.; Melchiorre, P. Photochemical generation of radicals from alkyl electrophiles using a nucleophilic organic catalyst. *Nat. Chem.* **2019**, *11*, 129−135. (b) de Pedro Beato, E.; Mazzarella, D.; Balletti, M.; Melchiorre, P. Photochemical generation of acyl and carbamoyl radicals using a nucleophilic organic catalyst: applications and mechanism thereof. *Chem. Sci.* **2020**, *11*, 6312−6324.
(18) For the BDE of cysteine, see Roux, M. V.; Foces-Foces, C.; Notario, R.; Ribeiro da Silva, M. A. V.; Ribeiro da Silva, M. d. D. M. C.; Santos, A. F. L. O. M.; Juaristi, E. Experimental and Computational Thermochemical Study of Sulfur-Containing Amino Acids: l-Cysteine, l-Cystine, and l-Cysteine-Derived Radicals. S−S, S−H, and C−S Bond Dissociation Enthalpies. *J. Phys. Chem. B* **2010**, *114*, 10530−10540.
(19) Li, G.; Glusac, K. D. The Role of Adenine in Fast Excited-State Deactivation of FAD: a Femtosecond Mid-IR Transient Absorption Study. *J. Phys. Chem. B* **2009**, *113*, 9059−9061.
(20) Gao, Y.; DeYonker, N. J.; Garrett, E. C.; Wilson, A. K.; Cundari, T. R.; Marshall, P. Enthalpy of Formation of the Cyclohexadienyl Radical and the C−H Bond Enthalpy of 1,4-Cyclohexadiene: An Experimental and Computational Re-Evaluation. *J. Phys. Chem. A* **2009**, *113*, 6955−6963.

https://doi.org/10.1021/jacs.1c13285
J. Am. Chem. Soc. 2022, 144, 4721−4726

(21) (a) Kabir, M. P.; Orozco-Gonzalez, Y.; Gozem, S. Electronic spectra of flavin in different redox and protonation states: a computational perspective on the effect of the electrostatic environment. *Phys. Chem. Chem. Phys.* **2019**, *21*, 16526−16537. (b) Su, D.; Kabir, M. P.; Orozco-Gonzalez, Y.; Gozem, S.; Gadda, G. Fluorescence Properties of Flavin Semiquinone Radicals in Nitronate Monooxygenase. *ChemBioChem.* **2019**, *20*, 1646−1652.

(22) Kise, N.; Tuji, T.; Sakurai, T. Stereoselective intramolecular coupling of barbituric acids with aliphatic ketones and *O*-methyl oximes by electroreduction: radical cyclization mechanism supported by DFT study. *Tetrahedron Lett.* **2016**, *57*, 1790−1793.

https://doi.org/10.1021/jacs.1c13285
J. Am. Chem. Soc. 2022, 144, 4721−4726

Synlett R. Foja et al. Cluster

Chemoselective Reduction of Barbiturates by Photochemically Excited Flavin Catalysts

Richard Foja
Alexandra Walter
Golo Storch*

School of Natural Sciences and Catalysis Research Center (CRC), Technical University of Munich (TUM), Lichtenbergstr. 4, 85747 Garching, Germany
golo.storch@tum.de

Published as part of the Cluster
Chemical Synthesis and Catalysis in Germany

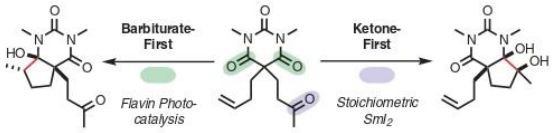

Received: 19.09.2023
Accepted after revision: 30.10.2023
Published online: 30.10.2023 (Accepted Manuscript), 08.12.2023 (Version of Record)
DOI: 10.1055/a-2201-7141; Art ID: ST-2023-09-0412-L

Crowd-Reviewed

Abstract Photocatalytic reductive cyclizations are powerful methods for obtaining structurally complex molecules. Achieving noninherent reactivity in substrates with more than one potential site of reduction is a difficult challenge. We disclose the use of flavin catalysis for the chemoselective reductive cyclization of barbiturates with additional reactive functional groups. Our method provides orthogonal selectivity in comparison to the well-established reductant samarium(II) iodide, which preferentially reduces substrate ketone groups. Flavin catalysis first leads to barbiturate reduction and allows a complete change of chemoselectivity in barbiturates with appended ketones. Additionally, flavin photocatalysis enables the reductive cyclization of substrates with appended oxime ethers in >99% yield, which is not possible with SmI_2.

Key words flavin catalysis, photochemistry, chemoselectivity, reductive catalysis, barbiturates

The single-electron reduction of carbonyls to ketyl radicals is a valuable strategy that has emerged as a powerful tool in chemical synthesis.[1] A large part of the synthetic utility stems from subsequent intra- or intermolecular reactivity of the initially generated ketyl radicals, which facilitate a broad range of C–C bond formation reactions.[2] However, achieving desired reactivity becomes challenging for substrates with multiple carbonyl groups, where chemoselective reduction is required. With samarium(II) iodide as a versatile single-electron donor,[3] orthogonal selectivity[4] has been, for example, reported as a function of an added proton source in the reduction of unsaturated lactone **1** (Scheme 1A).[5] The reactivity difference results from the formation of either the anionic ketyl radical or its neutral form after protonation,[6] which leads to spirocyclic lactone **2** or cyclobutane **3**. However, these reactions still build upon the same lactone position of initial reduction (green color).

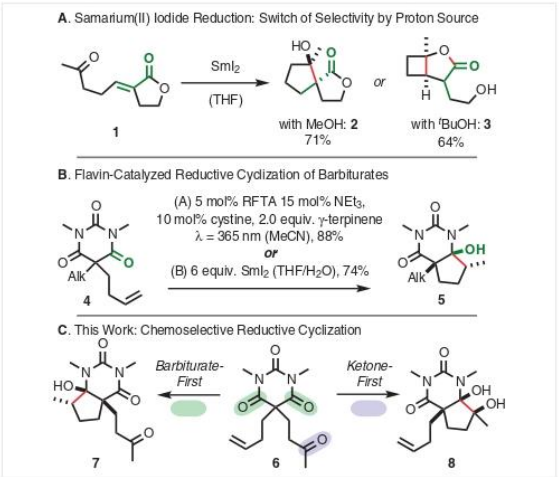

Scheme 1 (A) Reductive cyclization reactions with SmI_2 and (B) reductive flavin photocatalysis as an alternative method. (C) Chemoselective reductions of hybrid substrates such as barbiturate **6** are the aim of this study.

Chemoselective reductions of substrates containing several different functional groups are, therefore, typically determined by the relative inherent reactivity with the reductant. Reductions with noninherent selectivity require a switch in the reduction mechanism or an alternate pathway of substrate activation.[7] The SmI_2 reagent is active in the reduction of a wide variety of functional groups, including barbiturates[8] such as alkyl-substituted derivative **4**.[9] Besides metal reductants, photoredox catalysis[10] has emerged as another powerful strategy for reductive C–C bond formation with ketone-containing substrates.[11] In search for such an orthogonal reduction reaction, we recently disclosed

that photochemically excited reduced flavins[12,13] also serve as reductants for barbiturates and yield the bicyclic hemiaminal **5** (Scheme 1B).[14] Similar reactivity is also found in DNA photolyase enzymes, where excited hydroquinoid flavins reduce thymine dimers and trigger DNA repair.[15]

Reductive flavoenzyme chemistry offers diverging pathways such as direct excitation of the hydroquinoid flavin,[16] excitation of a charge-transfer complex between the reduced cofactor and a substrate,[17] or the activity of the radical semiquinoid flavin.[18] In contrast to reductions with SmI_2, aliphatic ketone functional groups tend to remain unconverted by reductive flavin-dependent 'ene' reductases.[19] This study aimed to achieve flavin-catalyzed[20] chemoselective reductive cyclizations. Substrates such as barbiturate **6** contain two different sites of potential initial reduction, which ultimately leads to divergent reaction products (Scheme 1C).

We initially probed the intrinsic reactivity of hybrid barbiturate **6** towards SmI_2 (Scheme 2).[21] This reaction proceeded with exquisite selectivity and provided the pinacol-type product **8** exclusively.[22] Both hydroxy groups are in a *cis* arrangement, presumably as a result of chelation with the samarium reductant.

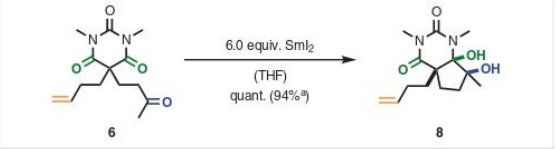

Scheme 2 Samarium(II)-mediated reduction of hybrid barbiturate **6**. The yield was determined by NMR spectroscopy *versus* internal standard. [a] Yield of isolated material.

We then probed whether hydroquinoid flavins reduce hybrid substrate **6** analogously under photochemical excitation. Such a direct comparison experiment requires the flavin reductant in stoichiometric quantities and we explored two strategies for achieving quantitative flavin reduction (Scheme 3A). The first approach (method A) builds upon the photochemical reduction of the *N*-methyl (–)-riboflavin tetraacetate **9** using γ-terpinene as the reductant.[23] The desired hydroquinone **10** was isolated in 71% yield and was found to be stable towards air for several hours in the solid state (see the Supporting Information for details). As an alternative (method B), we reduced the quinoid flavin **9** with Pd/Al_2O_3 under an atmosphere of dihydrogen and filtered the solution under rigorously inert conditions. Hydroquinoid flavins obtained by both methods were then applied in the reduction of hybrid barbiturate **6** under irradiation (Scheme 3B). These reductions typically benefit from a base in analogy to the natural photolyase system, in which $FADH^{-*}$ is the active single-electron donor.[24] We studied triethylamine (NEt_3), quinuclidine (Quin), and imidazole (Im). The latter was added since it is just basic enough (pK_a = ca. 7 for the conjugated acid) to deprotonate the reduced flavin at the N1 position (pK_a = ca. 6).[25] Imidazole was also chosen based on the importance of histidine as a proton shuttle in (6-4)-DNA photolyase.[26] We observed productive conversion of substrate **6** in all cases, albeit in varying quantities ranging from 4% to 44%. Incomplete conversions were to be expected since the concomitantly formed quinoid flavin **9** is very colorful and intense darkening of the solution prohibits efficient excitation of the remaining hydroquinone **10**. Interestingly, the flavin-mediated reduction did not lead to pinacol **8**, but exclusively resulted in the formation of alicyclic hemiaminal $\mathbf{7}_{ketone}$, which shows partial intramolecular ring closure to $\mathbf{7}_{lactol}$. Deliberate reduction of the aliphatic ketone with $NaBH_4$ converted the equilibrating mixture into the secondary alcohol product **11**.

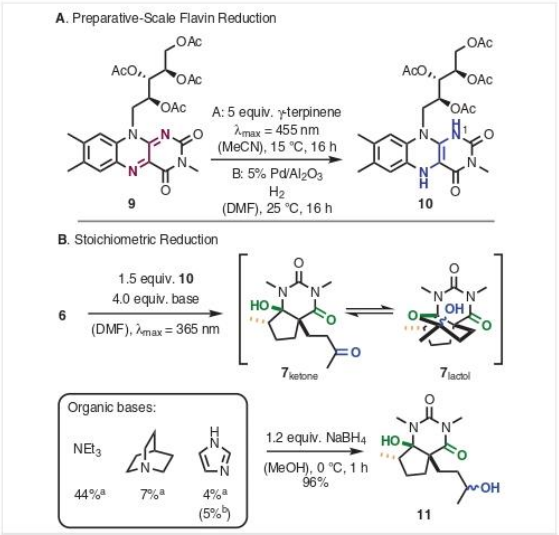

Scheme 3 (A) Stoichiometric reduction of (–)-riboflavin tetraacetate (B) and its application as a reductant for barbiturate **6**. [a] With hydroquinoid flavin **10** obtained by method B (Pd/Al_2O_3 and H_2) and determined by NMR spectroscopy with an internal standard. [b] With hydroquinoid flavin **10** obtained by method A (photochemical reduction) and 8 equiv. of 1*H*-imidazole.

With the stoichiometric reactivity of reduced flavins determined, we turned our attention to finding a catalytic method for the conversion of barbiturate **6** with the aim to maintain the orthogonal reactivity compared to SmI_2. We chose the essential oil γ-terpinene as a sacrificial reductant and focused on using quinoid flavin **9** as a precatalyst, which is reduced in situ (Table 1). Suitable conditions were identified when using dimethylformamide as the solvent and a catalyst loading of 20 mol% (entry 1).[27,28] Omitting the stoichiometric reductant γ-terpinene (entries 2–4) resulted in no conversion with imidazole and quinuclidine. Minor quantities (33%) of product **7** were observed with the triethylamine base, which indicates that it also serves as a re-

ductant for excited quinoid flavins. The flavin catalyst loading could be lowered to 5 mol% with an unaltered high product yield of 96% (entry 5). Switching the solvent to acetonitrile was less favorable and also resulted in minor quantities of the over-reduction product **11** (entry 6). At 5 mol% of flavin catalyst, the three bases could also be used in catalytic quantities (entries 7–9). No product formation was detected in the absence of a flavin catalyst or without irradiation (entries 10 and 11). The addition of $Sm(OTf)_3$ as a Lewis acid did not alter the chemoselectivity of the flavin-catalyzed reaction.

Table 1 Catalytic Flavin-Mediated Reduction: Barbiturate-First Mechanism[a]

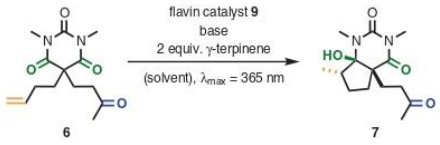

Entry	Flavin (mol%)	Base	Solvent[b]	Yield (%)[c]
1	20	8 equiv. Im	DMF	95
2[d]	20	4 equiv. Im	DMF	n.d.
3[d]	20	4 equiv. Quin	DMF	n.d.
4[d]	20	4 equiv. NEt_3	DMF	33
5	5	8 equiv. Im	DMF	96
6	5	8 equiv. Im	MeCN	25[e]
7	5	40 mol% Im	DMF	61
8	5	40 mol% NEt_3	DMF	83
9	5	40 mol% Quin	DMF	35
10	none	8 equiv. Im	DMF	n.d.
11[f]	20	8 equiv. Im	DMF	n.d.

[a] Compound **7** was obtained as an equilibrium between ketone $\mathbf{7}_{ketone}$ and lactol $\mathbf{7}_{lactol}$ form.
[b] All reactions were performed at 15 °C with a substrate concentration of 0.2 M.
[c] Determined by NMR spectroscopy vs internal standard.
[d] No γ-terpinene was used.
[e] Additional over-reduction to secondary alcohol **11** was observed in 16% yield.
[f] No irradiation. n.d.: No product formation was determined.

The flavin-mediated formation of alicyclic hemiaminal **7** requires the initial reduction of one of the two barbituric acid carbonyl groups highlighted in green (barbiturate-first mechanism). On the other hand, the order of events is less clear in the SmI_2-mediated reduction to pinacol **8**, which can either be formed upon the initial reduction of the barbiturate or the aliphatic ketone.

We concluded that a telling mechanistic experiment would be to separate the two reactive functional groups by an aliphatic spacer of increasing length (Table 2). Ketone **12** resembles the hybrid barbiturate **6** but lacks the terminal alkene group. We observed the selective formation of pinacol-type product **13** (entries 1 and 2) even in the presence of 20% (v/v) water, which is typically added to SmI_2-mediated ketone reductions in order to favor the formation of secondary alcohols.[29] While the elongated ketone **14** still exclusively yielded pinacol **15** in pure tetrahydrofuran, this selectivity was completely reversed with the addition of water, and secondary alcohol **16** was obtained as the sole product under these conditions. Ketone substrate **17** contains an additional methylene unit and secondary alcohol formation (**18**) was observed independent of the reaction conditions. These experiments clearly show that SmI_2 leads to the initial reduction of the aliphatic ketone (ketone-first mechanism) and cyclization with the barbiturate depends on the spatial distance and the addition of water. Cyclic voltammetry measurements (see the Supporting Information) revealed that the initial site of reduction should indeed be the barbiturate heterocycle (E = ca. –1.8 V vs SCE). However, SmI_2 favored the reduction of the side-chain ketone.[30,31] This change of reactivity likely originates from the favored formation of the ketone-derived ketyl radical samarium(III) complex.[32]

Table 2 Variation of the Spacer Length in SmI_2 Reduction of Barbiturates: Ketone-First Mechanism[a]

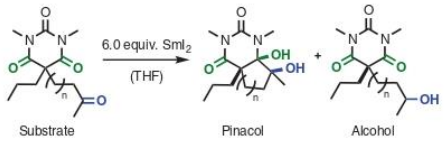

Entry	Substrate	Additive	Pinacol (%)	Alcohol (%)
1	n = 1 **12**	none	>99 **13**	0
2	n = 1 **12**	20% H_2O (v/v)	>99 **13**	0
3	n = 2 **14**	none	75 **15**	0
4	n = 2 **14**	20% H_2O (v/v)	0	46 **16**
5	n = 3 **17**	none	0	59 **18**

[a] All reactions were performed at 25 °C and required 30 min up to 24 h until completion. See the Supporting Information for details.

We next aimed for flavin-mediated reductions that are otherwise not possible with SmI_2 (Scheme 4) and moved to aliphatic oxime ethers, which are suitable radical addition partners.[33] Indeed, no conversion of barbiturate **19** was observed using SmI_2.[34] Here, productive reductive cyclization seems to require efficient barbiturate reduction and subsequent C–C bond formation by radical addition to the oxime ether. Flavin catalysis led to efficient reductive cyclization and formation of the corresponding β-amino alcohol **20**. Interestingly, this chemoselective barbiturate-first reduction occurs with high diastereoselectivity of 92:8. We assigned the major diastereomer as *trans*-configured based on NOE contacts (see the Supporting Information). The related hy-

brid substrate **21** again only leads to product formation if the barbiturate is reduced first, and no conversion is observed with SmI_2. In contrast, flavin catalysis led to exclusive cyclization with the more accessible terminal alkene to form alicyclic hemiaminal **22** in >99% yield.

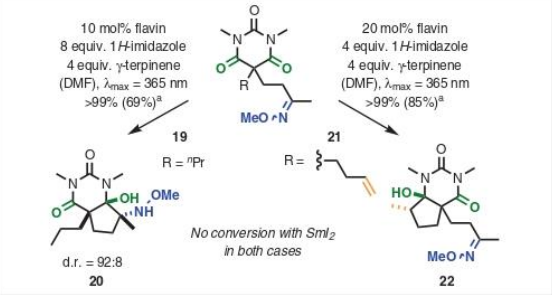

Scheme 4 Chemoselective barbiturate-first reduction of oxime ethers by flavin catalysis. Reductions with SmI_2 were attempted with 6 equiv. of the reagent. No conversion was observed in THF solution, while unselective decomposition occurred in THF/H_2O. [a] Yield of isolated material.

In summary, we disclose a series of chemoselective reductive cyclizations mediated by flavin photocatalysis and describe orthogonal selectivity when compared to the well-established SmI_2 reductant. Systematic investigation of barbiturate substrates with appended ketones separated by a varying number of methylene groups led to the conclusion that flavin catalysis proceeds via the initial reduction of the barbiturate core, while SmI_2 favors a first reduction of the ketone. Building upon this orthogonal activity, barbiturate substrates with appended oximes led to β-amino alcohol products with flavin photocatalysis, while SmI_2 does not serve as a competent reductant in these cases. We anticipate the flavin-catalyzed reductive cyclization method to be beneficial for a variety of transformations that require reductive activation of carbonyl functional groups.

Conflict of Interest

The authors declare no conflict of interest.

Funding Information

The Fonds der Chemischen Industrie (FCI, PhD Fellowship to A.W. and Liebig Fellowship to G.S.) is gratefully acknowledged. R.F. thanks the Studienstiftung des Deutschen Volkes for a PhD fellowship. G.S. thanks the Deutsche Forschungsgemeinschaft (DFG) for support through the Emmy Noether Programme (STO 1175/3-1) and the TRR 325 (444632635, Project B7).

Acknowledgment

G.S. is very grateful to Prof. T. Bach for his continuous support.

Supporting Information

Supporting information for this article is available online at https://doi.org/10.1055/a-2201-7141.

Primary Data

Original NMR datasets (FIDs) are available at Open Science-Framework at https://osf.io/4f6gp/.

References and Notes

(1) Péter, Á.; Agasti, S.; Knowles, O.; Pye, E.; Procter, D. J. *Chem. Soc. Rev.* **2021**, *50*, 5349.
(2) Streuff, J. *Synthesis* **2013**, *45*, 281.
(3) (a) Nicolaou, K. C.; Ellery, S. P.; Chen, J. S. *Angew. Chem. Int. Ed.* **2009**, *48*, 7140. (b) Szostak, M.; Spain, M.; Procter, D. J. *Chem. Soc. Rev.* **2013**, *42*, 9155. (c) Szostak, M.; Fazakerley, N. J.; Parmar, D.; Procter, D. J. *Chem. Rev.* **2014**, *114*, 5959. (d) Heravi, M. M.; Nazari, A. *RSC Adv.* **2022**, *12*, 9944.
(4) Mechanistic switching was also observed when coordinating additives were used: Szostak, M.; Spain, M.; Sautier, B.; Procter, D. J. *Org. Lett.* **2014**, *16*, 5694.
(5) Hutton, T. K.; Muir, K. W.; Procter, D. J. *Org. Lett.* **2003**, *5*, 4811.
(6) (a) Amiel-Levy, M.; Hoz, S. *J. Am. Chem. Soc.* **2009**, *131*, 8280. (b) Hoz, S. *Acc. Chem. Res.* **2020**, *53*, 2680.
(7) Examples of mechanistic switches in photochemical reduction: (a) Rong, J.; Seeberger, P. H.; Gilmore, K. *Org. Lett.* **2018**, *20*, 4081. (b) Bergamaschi, E.; Lunic, D.; McLean, L. A.; Hohenadel, M.; Chen, Y.-K.; Teskey, C. J. *Angew. Chem. Int. Ed.* **2022**, *61*, e202114482. (c) Du, J.; Espelt, L. R.; Guzei, I. A.; Yoon, T. P. *Chem. Sci.* **2011**, *2*, 2115.
(8) (a) Huang, H.-M.; Procter, D. J. *J. Am. Chem. Soc.* **2016**, *138*, 7770. (b) Huang, H.-M.; Procter, D. J. *J. Am. Chem. Soc.* **2017**, *139*, 1661.
(9) Szostak, M.; Sautier, B.; Spain, M.; Behlendorf, M.; Procter, D. J. *Angew. Chem. Int. Ed.* **2013**, *52*, 12559.
(10) Reviews on photoredox catalysis: (a) Prier, C. K.; Rankic, D. A.; MacMillan, D. W. C. *Chem. Rev.* **2013**, *113*, 5322. (b) Romero, N. A.; Nicewicz, D. A. *Chem. Rev.* **2016**, *116*, 10075.
(11) Selected examples: (a) Tarantino, K. T.; Liu, P.; Knowles, R. R. *J. Am. Chem. Soc.* **2013**, *135*, 10022. (b) Fava, E.; Nakajima, M.; Nguyen, A. L. P.; Rueping, M. *J. Org. Chem.* **2016**, *81*, 6959. (c) Qi, L.; Chen, Y. *Angew. Chem. Int. Ed.* **2016**, *55*, 13312. (d) Venditto, N. J.; Liang, Y. S.; El Mokadem, R. K.; Nicewicz, D. A. *J. Am. Chem. Soc.* **2022**, *144*, 11888.
(12) For reductive photocatalysis with flavins, see: Martinez-Haya, R.; Miranda, M. A.; Marin, M. L. *Eur. J. Org. Chem.* **2017**, 2164.
(13) For reductive photocatalysis with deazaflavins, see: (a) Graml, A.; Neveselý, T.; Jan Kutta, R.; Cibulka, R.; König, B. *Nat. Commun.* **2020**, *11*, 3174. (b) Pavlovska, T.; Král Lesný, D.; Svobodová, E.; Hoskovcová, I.; Archipowa, N.; Kutta, R. J.; Cibulka, R. *Chem. Eur. J.* **2022**, *28*, e202200768.
(14) Foja, R.; Walter, A.; Jandl, C.; Thyrhaug, E.; Hauer, J.; Storch, G. *J. Am. Chem. Soc.* **2022**, *144*, 4721.
(15) (a) Sancar, A. *Biochemistry* **1994**, *33*, 2. (b) Tan, C.; Liu, Z.; Li, J.; Guo, X.; Wang, L.; Sancar, A.; Zhong, D. *Nat. Commun.* **2015**, *6*, 7302. (c) Zhong, D. *Annu. Rev. Phys. Chem.* **2015**, *66*, 691. (d) Brettel, K.; Müller, P.; Yamamoto, J. *ACS Catal.* **2022**, *12*, 3041.

(16) Sandoval, B. A.; Clayman, P. D.; Oblinsky, D. G.; Oh, S.; Nakano, Y.; Bird, M.; Scholes, G. D.; Hyster, T. K. *J. Am. Chem. Soc.* **2021**, *143*, 1735.
(17) (a) Page, C. G.; Cooper, S. J.; DeHovitz, J. S.; Oblinsky, D. G.; Biegasiewicz, K. F.; Antropow, A. H.; Armbrust, K. W.; Ellis, J. M.; Hamann, L. G.; Horn, E. J.; Oberg, K. M.; Scholes, G. D.; Hyster, T. K. *J. Am. Chem. Soc.* **2021**, *143*, 97. (b) Laguerre, N.; Riehl, P. S.; Oblinsky, D. G.; Emmanuel, M. A.; Black, M. J.; Scholes, G. D.; Hyster, T. K. *ACS Catal.* **2022**, *12*, 9801.
(18) Page, C. G.; Cao, J.; Oblinsky, D. G.; MacMillan, S. N.; Dahagam, S.; Lloyd, R. M.; Charnock, S. J.; Scholes, G. D.; Hyster, T. K. *J. Am. Chem. Soc.* **2023**, *145*, 11866.
(19) (a) Velikogne, S.; Breukelaar, W. B.; Hamm, F.; Glabonjat, R. A.; Kroutil, W. *ACS Catal.* **2020**, *10*, 13377. (b) Fu, H.; Lam, H.; Emmanuel, M. A.; Kim, J. H.; Sandoval, B. A.; Hyster, T. K. *J. Am. Chem. Soc.* **2021**, *143*, 9622. (c) Kumar Roy, T.; Sreedharan, R.; Ghosh, P.; Gandhi, T.; Maiti, D. *Chem. Eur. J.* **2022**, *28*, e202103949.
(20) Reviews on flavin catalysis in organic chemistry: (a) Sideri, I. K.; Voutyritsa, E.; Kokotos, C. G. *Org. Biomol. Chem.* **2018**, *16*, 4596. (b) Rehpenn, A.; Walter, A.; Storch, G. *Synthesis* **2021**, *53*, 2583.
(21) Kise, N.; Tuji, T.; Sakurai, T. *Tetrahedron Lett.* **2016**, *57*, 1790.
(22) **Analytical Data for Compound 8**
White solid (25.6 mg, 94 µmol, 94% (quant. NMR yield)). TLC: R_f = 0.37 (*n*-pentane/EtOAc, 50/50) [$KMnO_4$]. ^{1}H NMR (400 MHz, acetone-d_6, 298 K): δ = 5.35 (s, 1 H, O-H^3), 5.16 (s, 1 H, O-H^9), 3.08 (s, 3 H, H^5), 3.00 (s, 3 H, H^2), 2.47–2.29 (m, 1 H, H^{11a}), 1.88–1.77 (m, 1 H, H^{10a}), 1.74–1.67 (m, 2 H, H^6), 1.66–1.55 (m, 2 H, H^{10b,11b}), 1.27–1.19 (m, 1 H, H^{7a}), 1.07 (s, 4 H, H^{7b,12}), 0.82 (t, $^3J_{H-H}$ = 7.3 Hz, 3 H, H^8) ppm. ^{13}C{^{1}H} NMR (101 MHz, acetone-d_6, 298 K): δ = 173.9 (C^6), 152.7 (C^1), 91.6 (C^3), 82.7 (C^9), 55.1 (C^4), 38.4 (C^6), 37.1 (C^{10}), 30.1 (C^{11}), 28.8 (C^2), 28.1 (C^5), 24.9 (C^{12}), 18.4 (C^7), 14.7 (C^8) ppm. HRMS (ESI$^+$): *m/z* calcd for [M + H]$^+$ = [$C_{13}H_{23}N_2O_4$]$^+$: 271.1652; found: 271.1635. IR: (ATR): ν = 3400 (br OH), 2960, 2874, 2034, 1854, 1732, 1703, 1648 (C=O), 1587, 1549, 1513, 1450, 1415, 1377, 1333, 1309, 1246, 1129, 1080, 1062, 1028, 1013, 972, 942, 882, 861, 836, 795, 755, 743, 721, 698, 656 cm^{-1}.
(23) Examples of γ-terpinene as a reductant in photochemistry: (a) Schweitzer-Chaput, B.; Horwitz, M. A.; de Pedro Beato, E.; Melchiorre, P. *Nat. Chem.* **2019**, *11*, 129. (b) de Pedro Beato, E.; Mazzarella, D.; Balletti, M.; Melchiorre, P. *Chem. Sci.* **2020**, *11*, 6312.
(24) (a) Epple, R.; Carell, T. *Angew. Chem. Int. Ed.* **1998**, *37*, 938. (b) Cichon, M. K.; Arnold, S.; Carell, T. A. *Angew. Chem. Int. Ed.* **2002**, *41*, 767.
(25) (a) Ghisla, S.; Massey, V. *Eur. J. Biochem.* **1989**, *181*, 1. (b) Srivastava, V.; Singh, P. K.; Srivastava, A.; Singh, P. P. *RSC Adv.* **2021**, *11*, 14251.
(26) Hitomi, K.; Nakamura, H.; Kim, S.-T.; Mizukoshi, T.; Ishikawa, T.; Iwai, S.; Todo, T. *J. Biol. Chem.* **2001**, *276*, 10103.
(27) **Representative Procedure**
Ketone **6** (14 mg, 50 µmol, 1.00 equiv.), flavin **9** (1.4 mg, 2.5 µmol, 5 mol%), and imidazole (27 mg, 400 µmol, 8.0 equiv.) were combined in a crimp cap vial and sealed. The reaction vessel was evacuated and backfilled with argon thrice. Subsequently, *N*,*N*-dimethylformamide (anhydrous, 250 µL, 0.2 M) and γ-terpinene (16 µL, 100 µmol, 2.00 equiv.) were added, and the vial was irradiated at λ_{max} = 365 nm and a controlled reaction temperature of 15 °C for 16 h. The vial was then opened, the solution was transferred to a flask (rinsed with acetone thrice), and all volatiles were removed in vacuo. 1,3,5-Benzene tricarboxylic acid trimethyl ester (10 µmol) was added as an internal standard and the NMR spectrum was recorded. The crude compound was purified by column chromatography to afford product **7**.
(28) **Analytical Data for Compound 7**
White solid (11.1 mg, 40 µmol, 79% (96% NMR-yield)); TLC: R_f = 0.23 (*n*-pentane/EtOAc, 60/40) [$KMnO_4$]. The compound was isolated as a single diastereomer. However, compound **7** was observed to contain two isomers which are assigned to an open chain (*major*) 'H^a' and lactol (*minor*) 'H^b' form. ^{1}H NMR (400 MHz, CD_2Cl_2, 298 K): δ = 4.69 (br s, 1 H, C^3-O*H*), 3.16 (s, 3 H, H^{6a}), 3.14 (s, 3 H, H^{6b}), 2.97 (s, 3 H, H^{2b}), 2.88 (s, 3 H, H^{2a}), 2.51–2.40 (m, 3 H, H$^{8,14-1}$), 2.37–2.26 (m, 1 H, H^{11}), 2.18–2.10 (m, 1 H, H$^{7-1}$), 2.08 (s, 3 H, H^{10a}), 2.05–1.93 (m, 1 H, H$^{13-1}$), 1.83–1.75 (m, 1 H, H$^{7-2}$), 1.73–1.63 (m, 1 H, H$^{14-2}$), 1.42 (s, 3 H, H^{10b}), 1.18–1.02 (m, 1 H, H$^{13-2}$), 0.69 (d, $^3J_{H-H}$ = 7.5 Hz, 3 H, H^{12a}), 0.63 (d, $^3J_{H-H}$ = 7.5 Hz, 3 H, H^{12b}) ppm. ^{13}C{^{1}H} NMR (101 MHz, CD_2Cl_2, 298 K): δ = 210.9 (C^{9a}), 175.1 (C^{5b}), 172.9 (C^{5a}), 152.3 (C^1), 95.6 (C^{9b}), 94.2 (C^{3b}), 92.8 (C^{3a}), 55.8 (C^{4a}), 47.7 (C^{4b}), 45.4 (C^{11b}), 44.6 (C^{11a}), 38.9 (C^{8a}), 33.5 (C^{14a}), 30.5 (C^{13b}), 30.2 (C^{14b}), 30.1 (C^{2b}), 29.8 (C^{10b}), 29.7 (C^{10a}), 28.8 (C^{13a}), 28.6 (C^{2a}), 28.1 (C^{6b}), 27.8 (C^{7b}), 27.8 (C^{6a}), 27.1 (C^{8b}), 26.2 (C^{7a}), 17.2 (C^{12a}), 14.5 (C^{12b}) ppm. HRMS (ESI$^+$): *m/z* calcd for [M + H]$^+$ = [$C_{14}H_{23}N_2O_4$]$^+$: 283.1652; found: 283.1658. IR (ATR): 3346 (OH), 2960, 2877, 1733, 1684, 1649 (C=O), 1549, 1449, 1414, 1382, 1340, 1308, 1259, 1172, 1153, 1122, 1094, 1061, 1002, 961, 929, 885, 843, 755, 735, 722, 661.9 cm^{-1}.
(29) (a) Singh, A. K.; Bakshi, R. K.; Corey, E. J. *J. Am. Chem. Soc.* **1987**, *109*, 6187. (b) Hasegawa, E.; Curran, D. P. *J. Org. Chem.* **1993**, *58*, 5008.
(30) For the related SmI_2-mediated reduction of γ-indolylketones, see: Beemelmanns, C.; Nitsch, D.; Bentz, C.; Reissig, H.-U. *Chem. Eur. J.* **2019**, *25*, 8780.
(31) For the related SmI_2-mediated reduction of α,β-unsaturated esters in cyclic imide substrate side chain, see: (a) Shi, S.; Szostak, M. *Org. Lett.* **2015**, *17*, 5144. (b) Shi, S.; Lalancette, R.; Szostak, R.; Szostak, M. *Chem. Eur. J.* **2016**, *22*, 11949.
(32) Computational study of a SmI_2-mediated reduction with chelate complex intermediates: Achazi, A. J.; Andrae, D.; Reissig, H.-U.; Paulus, B. *J. Comput. Chem.* **2017**, *38*, 2693.
(33) (a) Chiara, J. L.; Marco-Contelles, J.; Khiar, N.; Gallego, P.; Destabel, C.; Bernabe, M. *J. Org. Chem.* **1995**, *60*, 6010. (b) Marco-Contelles, J.; Gallego, P.; Rodríguez-Fernández, M.; Khiar, N.; Destabel, C.; Bernabé, M.; Martínez-Grau, A.; Chiara, J. L. *J. Org. Chem.* **1997**, *62*, 7397.
(34) On the reduced reactivity of SmI_2 towards oxime ethers, see: Ning, L.; Li, H.; Lai, Z.; Szostak, M.; Chen, X.; Dong, Y.; Jin, S.; An, J. *J. Org. Chem.* **2021**, *86*, 2907.

6. Summary

Since instability toward molecular oxygen is the main deactivation pathway for reduced flavins, the molecular design and synthesis of air-stable reduced flavins were tackled first. Adaptation of a synthetic protocol (reduction of flavin **99**) developed in the group, led to the isolation of N^5 alkylated reduced flavin **100** as a white or slightly yellow solid (Scheme 25A). This compound showed remarkable stability under air, as it could be isolated by column chromatography and showed only slow decomposition in solution under aerobic conditions. Analogous reduction of flavin **101** did not result in a compound that could be isolated. Reduced flavin **100** was successfully crystallized and a single-crystal X-ray diffractogram was determined. A bent structure that has been proposed for reduced flavins[24] was confirmed and the stability toward oxygen is rationalized by the concept of confirmational bias (Scheme 25B).

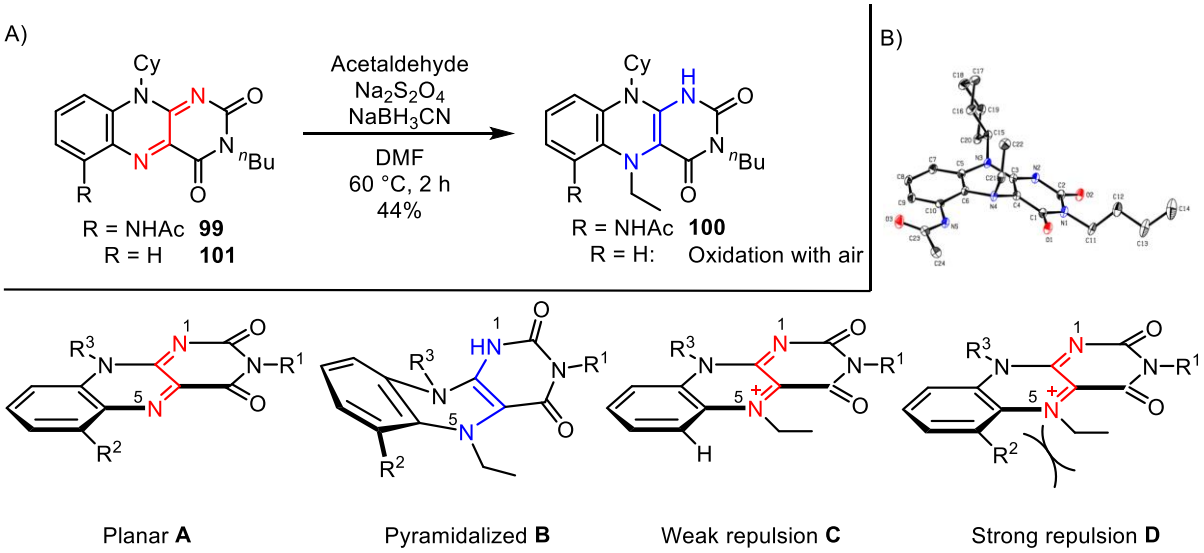

Scheme 25: A) Synthesis of air-stable reduced flavin **100**. B) X-ray diffractogram and rationalization of stability toward oxygen by conformational bias.

Upon oxidation of reduced flavin **100** a change in geometry must take place from a bent structure in the reduced state to a planar structure in the oxidized state. Steric interaction of the C^6 amide group and the N^5 ethyl group is presumed to hamper this process and thus stabilize the resulting geometry in the reduced state. Cyclic voltammetry supports this assumption as a partially reversible electron transfer at $E_{1/2}$ = +0.46 V vs SCE in acetonitrile is detected while an irreversible electron transfer is observed at more positive potentials. Next, the photophysical properties of reduced flavin **100** were determined. An absorption maximum

at $\lambda_{A,max}$ = 324 nm and an emission maximum of $\lambda_{E,max}$ = 567 nm were determined which is in line with prior reports of reduced flavin spectroscopy. A shift of the emission maximum ($\lambda_{E,max}$ = 533 nm) is observed upon the addition of triethylamine as a base. The excited state decay of the emission maximum is biexponential with τ_1 = 1.1 ns (78 % contribution) and τ_2 = 11.7 ns (22 % contribution).

After the determination of the properties of reduced flavin **100**, application in a synthetic protocol was developed. Samarium (II) iodide as a strong earth-metal reductant is able to reduce barbituric acids **102** with appended acceptors for radical addition furnishing bicyclic products **103**.[42] This transformation was selected as an appropriate target because of its resemblance to thymine dimers which are the natural substrates of the DNA photolyase. 5-*exo*-trig cyclization of barbituric acids **102** were achieved under irradiation at λ = 365 nm of reduced flavin **100** as a catalyst in acetonitrile with triethylamine as a base, *γ*-terpinene as sacrificial reductant and a cysteine derivative as an additive (Scheme 26A). Apart from cysteine, which increases the yield presumably as a HAT reagent, every component was essential, and omission would shut down the reaction. Under these conditions, oxidized precursor flavin **99** and even riboflavin tetraacetate which is derived from natural riboflavin were active in the reaction after *in situ* reduction by γ-terpinene. Changing the wavelength to 450 nm shuts down the reaction of air-stable reduced flavin **100** while riboflavin tetraacetate still showed activity. This is rationalized by the fact that reduced riboflavin is still slightly yellow. The scope of the reaction includes several barbituric acids with different alkenes as acceptors for the addition of a ketyl radical (Scheme 26B). An alkyne and an allene were employed as acceptors and a six-membered ring could be formed with appropriate chain-length of the alkenyl chain. To expand the scope of the reaction, haloalkanes **104** and α,β-unsaturated amides **105** that were demonstrated as suitable substrates for flavoenzyme mediated reduction[70] were synthesized and successfully employed in the catalytic protocol yielding cyclized products **106** and saturated amides **107** respectively (Scheme 26C). Notably, two substrates that were not reduced under flavoenzyme conditions could be reduced with molecular reduced flavin. Barbituric acids with an appended ketone instead of an alkene were reduced to the corresponding secondary alcohols while reduction with SmI_2 led to the formation of the pinacols.

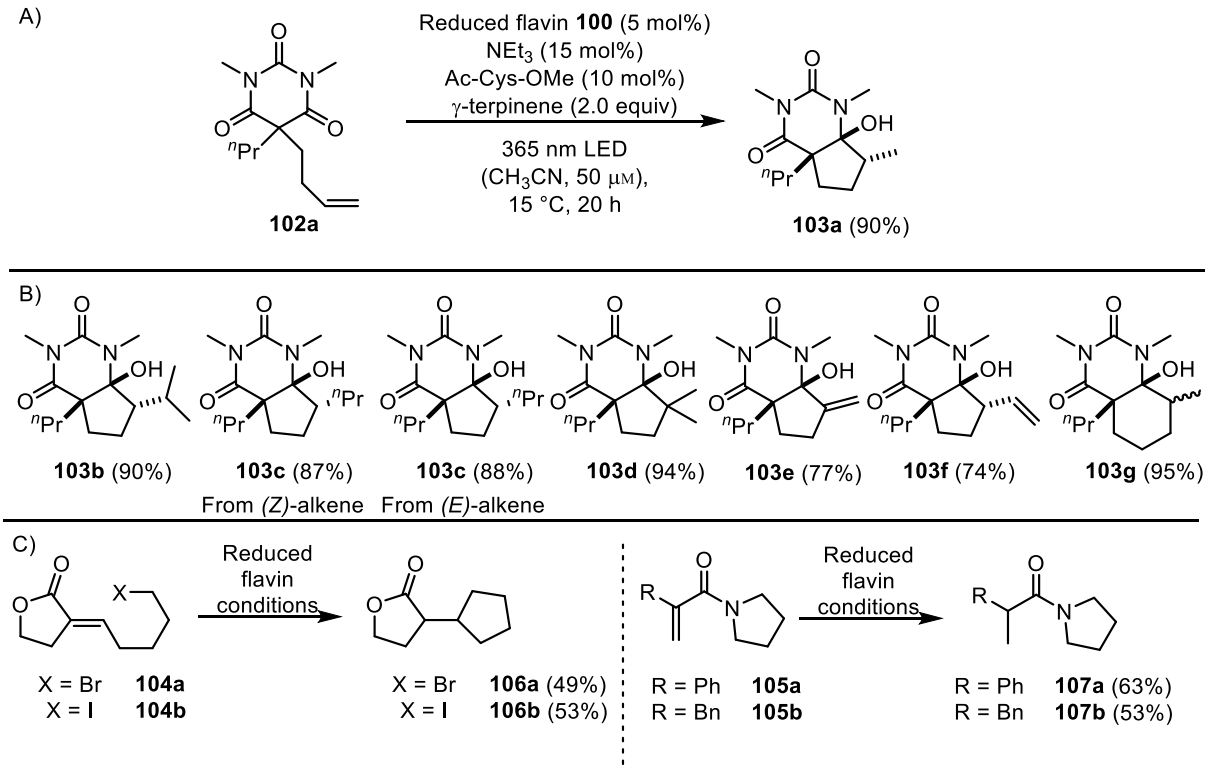

Scheme 26: A) Reduced flavin **100** as the catalyst for cyclization of barbituric acid **102**. B) Scope of the reaction (NMR yield in parentheses).

The reaction is initiated by excitation of the reduced flavin **100** (Scheme 27). Reduction of a carbonyl group of the barbituric acid **102a** results in the formation of a radical anion and a semiquinoid flavin. The radical anion performs a 5-*exo*-trig cyclization to radical anion **108a** which is reduced by γ-terpinene **109** and protonated, yielding bicyclic compound **103a**. The semiquinoid radical is probably reduced by γ-terpinene to regenerate reduced flavin **100**. However, an alternative pathway with another reduction by the semiquinoid radical resulting in the oxidized flavin cannot be ruled out. The reaction quantum yield is very low ($\Phi = 1.8 \times 10^{-3}$) possibly due to inefficient electron transfer and speaks against a radical chain process.

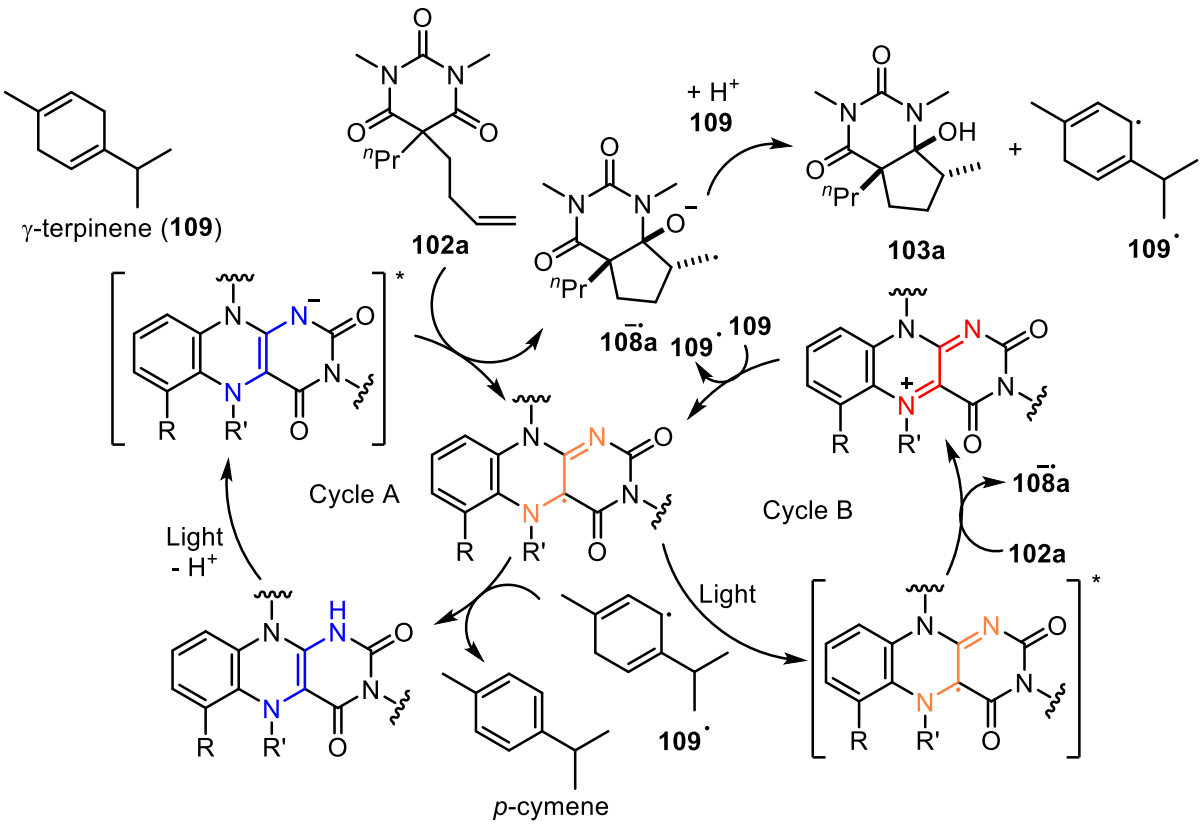

Scheme 27: Putative reaction mechanism. Cycle A describes reduced flavin as a photoexcited SET reagent, while cycle B uses semiquinoid flavin as an active species.

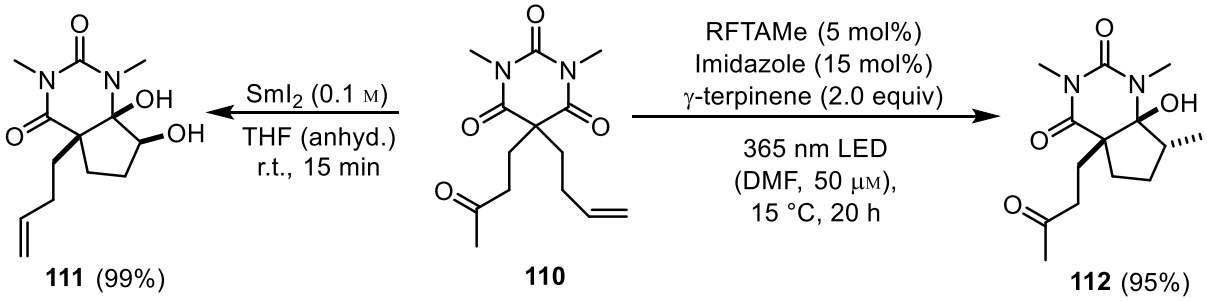

Scheme 28: Divergent reactivity of hybrid substrate **110**.

The reduction of ketone-appended barbituric acids was further investigated to elucidate differences in the mechanism of flavin-mediated reduction and SmI_2. Divergent reactivity for ketone-substituted barbituric acid **102** inspired the synthesis of hybrid barbituric acid **110** with a ketone and an alkene as appended linkers. Theoretically, both pinacol formation as well as alicycle formation are possible upon the formation of a ketyl radical in the barbituric acid core (Scheme 28). Treatment of ketone **110** with SmI_2 exclusively led to the formation of pinacol

111 with no formation of the alicycle **112** observed albeit cyclization with the alkene is possible in principle.

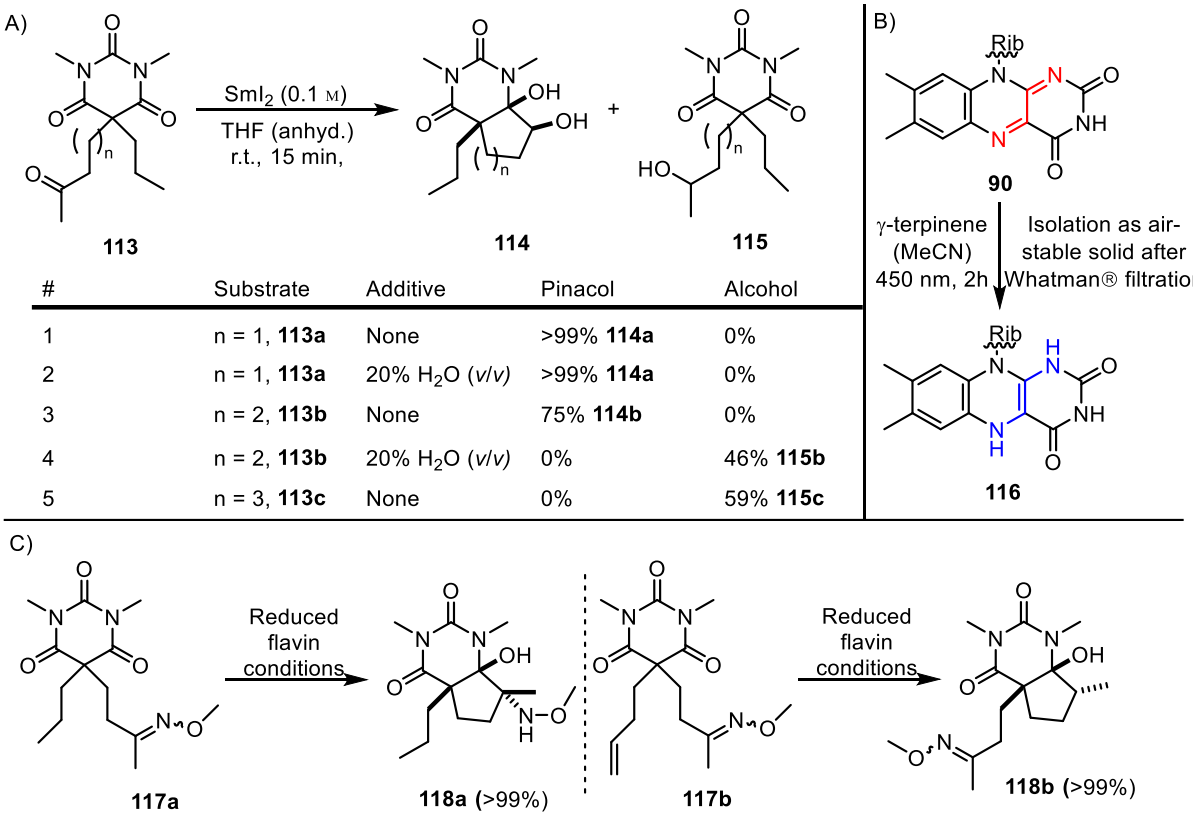

#	Substrate	Additive	Pinacol	Alcohol
1	n = 1, **113a**	None	>99% **114a**	0%
2	n = 1, **113a**	20% H_2O (*v/v*)	>99% **114a**	0%
3	n = 2, **113b**	None	75% **114b**	0%
4	n = 2, **113b**	20% H_2O (*v/v*)	0%	46% **115b**
5	n = 3, **113c**	None	0%	59% **115c**

Scheme 29: A) Spacer length variation supports ketone-first mechanism with SmI_2. B) Stoichiometric reduced flavin. C) *O*-methyl oximes demonstrate reduced flavin utility.

To elucidate the difference in reactivity, barbituric acids with different spacer lengths and no appended alkene were synthesized (Scheme 29A). Substrate **113a** cyclized to 5-membered pinacol **114a** under dry and aqueous conditions. Substrate **113b** is also cyclized to the corresponding 6-membered ring in dry tetrahydrofuran. However, with water formation of the secondary alcohol **115c** was observed and substrate **113c** exclusively formed the alcohol **115c** even without water. This implies that the first site of reduction is at the ketone rather instead of the barbituric acid for SmI_2, presumably due to the coordination of Lewis acidic Sm(II) by oxygen. To investigate flavin reactivity, different methods to use reduced flavin as a stoichiometric reagent have been explored (Scheme 29B). Precipitation of reduced flavin **116** as a solid after photoreduction proved to be successful and furnished reduced flavin as an orange solid. No ketone reduction was observed when using reduced flavin stoichiometrically. Instead, cyclization afforded product **112** which supports a barbiturate-first mechanism. Cyclic

voltammetry suggests that this site should be preferentially reduced ($E_{red} \approx -1.8$ V vs SCE) over the aliphatic ketone.

Under modified flavin conditions (no HAT reagent, imidazole as base, dimethylformamide as solvent), the formation of alicycle **112** was observed with catalytic use of flavin. Reduction of the ketone to the secondary alcohol as a side reaction was suppressed by optimization of reaction conditions. To further demonstrate the utility of flavin as a reductant in comparison to SmI_2, *O*-methyl oximes **117a** and **117b** were prepared (Scheme 29C). No conversion was observed with SmI_2 as a reductant. Gratifyingly, the reduced flavin protocol resulted in the formation of α,β-aminoalcohol **118a** and alicycle **118b** in excellent yields. These transformations demonstrate the utility of the newly developed method and call for further research on reduced molecular flavins to find new unique and useful reactivities.

7. Licenses

Reduced Molecular Flavins as Single-Electron Reductants after Photoexcitation

DOI: 10.1021/jacs.1c13285

Chemoselective Reduction of Barbiturates by Photochemically Excited Flavin Catalysts

DOI: 10.1055/a-2201-7141

Literature

[1] P. Scheipers, V. Biese, U. Bleyer, M. Bosse, in *Chemie: Grundlagen, Anwendungen, Versuche* (Eds.: P. Scheipers, V. Biese, U. Bleyer, M. Bosse), Vieweg+Teubner Verlag, Wiesbaden, **1990**, pp. 138-151.

[2] M. W. G. de Bolster, *Pure Appl. Chem.* **1997**, *69*, 6, 1251-1304.

[3] C. T. Walsh, T. A. Wencewicz, *Nat. Prod. Rep.* **2013**, *30*, 1, 175-200.

[4] W. D. Lienhart, V. Gudipati, P. Macheroux, *Arch. Biochem. Biophys.* **2013**, *535*, 2, 150-162.

[5] C. A. Northrop-Clewes, D. I. Thurnham, *Ann. Nutr. Metab.* **2012**, *61*, 3, 224-230.

[6] C. Walsh, *Acc. Chem. Res.* **1980**, *13*, 5, 148-155.

[7] B. N. Ames, I. Elson-Schwab, E. A. Silver, *Am. J. Clin. Nutr.* **2002**, *75*, 4, 616-658.

[8] T. Kumar Roy, R. Sreedharan, P. Ghosh, T. Gandhi, D. Maiti, *Chem. Eur. J.* **2022**, *28*, 21, e202103949.

[9] A. Sancar, *Chem. Rev.* **2003**, *103*, 6, 2203-2238.

[10] S. Ghisla, C. Thorpe, *Eur. J. Biochem.* **2004**, *271*, 3, 494-508.

[11] E. Mason, C. C. T. Hindmarch, K. J. Dunham-Snary, *Endocrinol. Diabetes Metab.* **2023**, *6*, 1, e385.

[12] K. M. Peterson, K. V. Gopalan, D. K. Srivastava, *Biochem.* **2000**, *39*, 41, 12659-12670.

[13] R. P. Massengo-Tiasse, J. E. Cronan, *Cell. Mol. Life Sci.* **2009**, *66*, 9, 1507-1517.

[14] H. S. Toogood, J. M. Gardiner, N. S. Scrutton, *ChemCatChem* **2010**, *2*, 8, 892-914.

[15] D. J. Opperman, B. T. Sewell, D. Litthauer, M. N. Isupov, J. A. Littlechild, E. van Heerden, *Biochem. Biophys. Res. Commun.* **2010**, *393*, 3, 426-431.

[16] D. Ramirez-Gamboa, A. L. Diaz-Zamorano, E. R. Melendez-Sanchez, H. Reyes-Pardo, K. R. Villasenor-Zepeda, M. E. Lopez-Arellanes, J. E. Sosa-Hernandez, K. G. Coronado-Apodaca, A. Gamez-Mendez, S. Afewerki, H. M. N. Iqbal, R. Parra-Saldivar, M. Martinez-Ruiz, *Mol.* **2022**, *27*, 18, 5998.

[17] K. Schwinn, N. Ferre, M. Huix-Rotllant, *Phys. Chem. Chem. Phys.* **2020**, *22*, 22, 12447-12455.

[18] S. T. Kim, P. F. Heelis, T. Okamura, Y. Hirata, N. Mataga, A. Sancar, *Biochem.* **1991**, *30*, 47, 11262-11270.

[19] S. T. Kim, P. F. Heelis, A. Sancar, *Biochem.* **1992**, *31*, 45, 11244-11248.

[20] T. Carell, L. T. Burgdorf, L. M. Kundu, M. Cichon, *Curr. Opin. Chem. Biol.* **2001**, *5*, 5, 491-498.

[21] T. Langenbacher, X. Zhao, G. Bieser, P. F. Heelis, A. Sancar, M. E. Michel-Beyerle, *J. Am. Chem. Soc.* **1997**, *119*, 43, 10532-10536.

[22] R. A. S. McMordie, T. P. Begley, *J. Am. Chem. Soc.* **1992**, *114*, 5, 1886-1887.

[23] P. F. Heelis, R. F. Hartman, S. D. Rose, *Chem. Soc. Rev.* **1995**, *24*, 4, 289-297.

[24] Y. T. Kao, C. Saxena, T. F. He, L. Guo, L. Wang, A. Sancar, D. Zhong, *J. Am. Chem. Soc.* **2008**, *130*, 39, 13132-13139.

[25] C. Reichhardt, *Wiley-VCH: Weinheim,* **2003**, *3rd ed*.

[26] G. Weber, *Biochem. J.* **1950**, *47*, 1, 114-121.

[27] T. Shiga, L. H. Piette, *Photochem. Photobiol.* **1965**, *4*, 4, 769-781.

[28] J. Baier, T. Maisch, M. Maier, E. Engel, M. Landthaler, W. Baumler, *Biophys. J.* **2006**, *91*, 4, 1452-1459.

[29] E. J. Land, A. J. Swallow, *Biochem.* **1969**, *8*, 5, 2117-2125.

[30] C. T. Moonen, J. Vervoort, F. Muller, *Biochem.* **1984**, *23*, 21, 4868-4872.

[31] R. A. McBride, D. T. Barnard, K. Jacoby-Morris, M. Harun-Or-Rashid, R. J. Stanley, *Biochem.* **2023**, *62*, 3, 759-769.
[32] S. Ghisla, V. Massey, J. M. Lhoste, S. G. Mayhew, *Biochemistry* **1974**, *13*, 3, 589-597.
[33] O. S. Ksenzhek, S. A. Petrova, *J. Electroanal. Chem. Interf. Electrochem.* **1983**, *156*, 105-127.
[34] S. L. Christgen, S. M. Becker, D. F. Becker, *Methods Enzymol.* **2019**, *620*, 1-25.
[35] M. P. Scannell, D. J. Fenick, S.-R. Yeh, D. E. Falvey, *J. Am. Chem. Soc.* **1997**, *119*, 8, 1971-1977.
[36] R. F. Anderson, *Biochim. Biophys. Acta* **1983**, *722*, 1, 158-162.
[37] I. A. MacKenzie, L. Wang, N. P. R. Onuska, O. F. Williams, K. Begam, A. M. Moran, B. D. Dunietz, D. A. Nicewicz, *Nature* **2020**, *580*, 7801, 76-80.
[38] T. Koike, M. Akita, *Trends Chem.* **2021**, *3*, 5, 416-427.
[39] A. J. Birch, *J. Chem. Soc.* **1944**.
[40] J. Broggi, T. Terme, P. Vanelle, *Angew. Chem. Int. Ed. Engl.* **2014**, *53*, 2, 384-413.
[41] P. Girard, J. L. Namy, H. B. Kagan, *J. Am. Chem. Soc.* **1980**, *102*, 8, 2693-2698.
[42] M. Szostak, M. Spain, D. J. Procter, *J. Org. Chem.* **2014**, *79*, 6, 2522-2537.
[43] L. A. Duffy, H. Matsubara, D. J. Procter, *J. Am. Chem. Soc.* **2008**, *130*, 4, 1136-1137.
[44] G. A. Molander, M. S. Quirmbach, L. F. Silva, Jr., K. C. Spencer, J. Balsells, *Org. Lett.* **2001**, *3*, 15, 2257-2260.
[45] K. C. Nicolaou, S. P. Ellery, J. S. Chen, *Angew. Chem. Int. Ed. Engl.* **2009**, *48*, 39, 7140-7165.
[46] W. G. Skene, J. C. Scaiano, F. L. Cozens, *J. Org. Chem.* **196**, *61*, 22, 77918-77921.
[47] M. Szostak, B. Sautier, M. Spain, M. Behlendorf, D. J. Procter, *Angew. Chem. Int. Ed. Engl.* **2013**, *52*, 48, 12559-12563.
[48] P. R. Chopade, E. Prasad, R. A. Flowers, *J. Am. Chem. Soc.* **2004**, *126*, 1, 44-45.
[49] G. A. Molander, C. Kenny, *J. Org. Chem.* **1988**, *53*, 9, 2132-2134.
[50] N. L. Holy, *Chem. Rev.* **1974**, *74*, 2, 243-277.
[51] G. Levin, S. Claesson, M. Szwarc, *J. Am. Chem. Soc.* **1972**, *94*, 25, 8672-8676.
[52] S. Bank, J. F. Bank, *Tetrahedron Lett.* **1969**, *10*, 52, 4533-4536.
[53] J. Jacobus, D. Pensak, *J. Chem. Soc. D* **1969**, 8, 400-401.
[54] W. Adam, J. Arce, *J. Org. Chem.* **1972**, *37*, 3, 507-508.
[55] E. Alonso, D. J. Ramón, M. Yus, *Tetrahedron* **1997**, *53*, 42, 14355-14368.
[56] X. Liu, J. Liu, J. Wu, C. C. Li, *J. Org. Chem.* **2021**, *86*, 16, 11125-11139.
[57] G. Asensio, A. Cuenca, P. Gaviña, M. Medio-Simón, *Tetrahedron Lett.* **1999**, *40*, 20, 3939-3940.
[58] P. K. Freeman, L. L. Hutchinson, *Tetrahedron Lett.* **1976**, *17*, 22, 1849-1852.
[59] T. J. Donohoe, D. House, *J. Org. Chem.* **2002**, *67*, 14, 5015-5018.
[60] J. A. Murphy, *J. Org. Chem.* **2014**, *79*, 9, 3731-3746.
[61] C. Burkholder, W. R. Dolbier, M. Médebielle, *J. Org. Chem.* **1998**, *63*, 16, 5385-5394.
[62] H. S. Farwaha, G. Bucher, J. A. Murphy, *Org. Biomol. Chem.* **2013**, *11*, 46, 8073-8081.
[63] M. H. Shaw, J. Twilton, D. W. MacMillan, *J. Org. Chem.* **2016**, *81*, 16, 6898-6926.
[64] A. G. Condie, J. C. Gonzalez-Gomez, C. R. Stephenson, *J. Am. Chem. Soc.* **2010**, *132*, 5, 1464-1465.
[65] G. Jiang, J. Chen, J. S. Huang, C. M. Che, *Org. Lett.* **2009**, *11*, 20, 4568-4571.
[66] A. McNally, C. K. Prier, D. W. MacMillan, *Science* **2011**, *334*, 6059, 1114-1117.
[67] J. J. Murphy, D. Bastida, S. Paria, M. Fagnoni, P. Melchiorre, *Nature* **2016**, *532*, 7598, 218-222.
[68] N. A. Romero, D. A. Nicewicz, *Chem. Rev.* **2016**, *116*, 17, 10075-10166.

[69] N. P. Ramirez, B. König, J. C. Gonzalez-Gomez, *Org. Lett.* **2019**, *21*, 5, 1368-1373.
[70] B. A. Sandoval, P. D. Clayman, D. G. Oblinsky, S. Oh, Y. Nakano, M. Bird, G. D. Scholes, T. K. Hyster, *J. Am. Chem. Soc.* **2021**, *143*, 4, 1735-1739.
[71] R. Foja, A. Walter, C. Jandl, E. Thyrhaug, J. Hauer, G. Storch, *J. Am. Chem. Soc.* **2022**, *144*, 11, 4721-4726.
[72] R. Foja, A. Walter, G. Storch, *Synlett* **2023**, *35*, 09, 952-956.